UNIVERSITY OF TURIN

DEPARTMENT OF AGRICULTURAL, FOREST AND FOOD SCIENCES

PHD PROGRAM IN AGRICULTURAL, FOREST AND FOOD SCIENCES

Cycle XXXVI

Rhizosphere processes driving phosphorus cycling in rice systems

PhD. Candidate Sara Martinengo

Tutors: Prof. Luisella Celi

PhD coordinator: Prof. Domenico Bosco

a.y. 2020-2023

Academic field code AGR/13 panel ERC PE10_9

LIST OF CONTENTS

CHAPTER 1

Introduction

At global level rice paddy agroecosystems encompass over 150 million hectares, making these peculiar anthropogenic environments the largest wetland areas of the world. Indeed, paddy soils are traditionally flooded for most of the year, thus creating a unique soil-plant environment (Kögel-Knabner et al., 2010). The biogeochemistry of this environment is controlled by a gradient of redox couples formed by an electron donor and an electron acceptor (Borch et al., 2010), and the sequence by which these couples are depleted by the soil processes is determined by thermodynamics (Kögel-Knabner et al., 2010). Iron (Fe), in particular is the most abundant redox-sensitive element on the Earth's surface, and hence it plays a pivotal role in reduced environment biogeochemistry, particularly because its redox wheels affect the cycle of other important not redox-active elements (Borch et al., 2010; Marschner, 2021).

Among the not redox-active elements in soil there is phosphorus (P), a macronutrient for plants, as it plays both structural and energetical functions in their tissues (Rose et al., 2013). Plants take up P from the soil solution mostly in the form of inorganic orthophosphate, however a large variety of inorganic and organic forms P forms are present in the soil system (Turner et al., 2005). All these P forms are characterized by a strong affinity to Fe oxides (Frossard et al 1995), and hence indirectly coupled to their redox transformations (Borch et al., 2010; Marschner, 2021; Wei et al., 2019), which make P a largely dynamic nutrient in paddy soils. Notwithstanding the current knowledge regarding P cycling in reduced soils, the consequence of reduction and oxidation cycles on the processes by which P is released into solution and then take up by plants are still largely debated, particularly regarding the role of organic P forms.

Rice (*Oryza sativa* L.) is one of the main staple foods for the growing world population (Seck et al., 2012). This plant derived from a semi-aquatic ancestor, with unique characteristics in its root anatomy and physiology making it suitable for wetland conditions (Fukai and Inthapan, 1988), albeit, at the same time, it can adapt to grow under aerobic conditions (Gowda et al., 2011). In particular, the formation of root aerenchymatic tissues allows for the aerobic metabolism of the root cells (Colmer, 2003). Furthermore, a thin oxic layer is established around the root surface, and the subsequent increased rhizospheric redox potential (Eh) mediates the detoxification of aqueous Fe(II) by oxidation and results in the precipitation of a Fe coating on rice roots called Fe plaque (Chen et al., 1980; Sahrawat, 2005). The plaque is formed by Fe (hydr)oxides, and thus highly reactive in trapping P from the solution (Zhang et al., 1999). Despite it is well acknowledged that rice plants can mobilize P from soil surfaces, including Fe (hydr)oxides (Rose et al., 2013), the contribution of root Fe plaque to plant P nutrition is still debated, and its role in rhizospheric P cycling largely unknown, especially regarding organic P forms.

The claim for agroecosystem sustainability raised by the ongoing climate change resulted in the need to decrease the water consumption in rice cultivation, thus

recently new water management techniques are been proposed to decrease the freshwater consumption (Datta et al., 2017). Considering the profound impact that soil flooding has on paddy biogeochemistry and nutrient cycles, the introduction of aerobic periods during rice cultivation might completely change Fe and P cycling and consequently affect P availability (Marschner, 2021; Zhang et al., 2003), although the specific effects on Fe plaque are poorly understood.

1.1 Phosphorus in paddy agroecosystems

In plant tissues P serves to structural and energetic functions, as it is an important constituent of phospholipids, which are the main components of the cell membrane, and adenosine triphosphate (ATP), the main form of energy storage in plant cells (Plaxton and Tran, 2011). Despite plants take up only inorganic P, in the soil system P exists as a large variety of inorganic and organic P molecules (Rose et al. 2013). Inorganic P molecules encompass orthophosphate and polyphosphate, which consists in chains of orthophosphate ranging in length from two groups (properly named pyrophosphate), or more. The organic P is instead divided in orthophosphate monoesters, orthophosphate diesters, and phosphonates, based on the bond of P to carbon (C). The orthophosphate monoesters and diesters present an ester bond with one or two C moieties for monoesters and diesters, respectively. The former group includes sugar phosphates (i.e. glucose 6-phosphate), mononucleotides, and inositol hexakisphosphates (Ins6P), while diesters include nucleic acids, phospholipids, and lipoteichoic acid. Conversely, phosphonates are characterized by a direct C-P bond, and include antibiotics and some agricultural chemicals such as the herbicide glyphosate (Cade-Menun and Liu, 2014; Turner et al., 2005). The complexity that characterizes P speciation in soil makes the investigation of its dynamics challenging. Indeed, to gain a further understanding of P dynamics in soil systems, the quantification of the total, inorganic, and organic P supply in soil is of primary importance, however also the identification of the molecules of inorganic and organic P included in the total P supply, the investigation of the processes and reactions, and the role of these processes in governing P bioavailability are crucially important (Kruse et al., 2015).

1.1.1 Soil P cycling

Soil total P supply ranges between 0.1 and 1.5 g P kg^{-1} soil, however most of the macronutrient is in unavailable forms for plant uptake (Frossard et al., 2000). The most common soil P forms include inorganic P salt of calcium (Ca), aluminum (Al) and/or Fe, and the P included in organic structures. Among inorganic P forms, calcium phosphate salts are predominant in alkaline soils, as they become progressively less soluble as soil pH increases. In near-neutral soils monocalcium, dicalcium, and tricalcium phosphates are the most soluble and bioavailable Ca-P forms, which are normally supplied to the soil through mineral fertilizers. However, the immobilization processes which characterize P behavior in soil systems lead to the formation of less soluble and more stable phases like hydroxyapatite [$3Ca_3(PO_4)_2\ Ca(OH)_2$], and fluorapatite [$3Ca_3(PO_4)_2\ CaF_2$].

Oppositely, Fe- and/or Al-phosphates are the most common ones in acidic soils, as their solubility increases at higher soil pH, variscite ($AlPO_4$ H_2O) and strengite ($FePO_4$ $2H_2O$) being the most common forms. Another important source of P in soil are the Fe and Al oxyhydroxides, highly reactive surfaces which are normally very abundant in soils. According to their surface characteristics (i.e. surface area and surface charge) Fe and Al oxides can retain a large amount of P, and they represent a crucial point of P cycle in flooded and submerged environments like sediments and paddy soils (Borch et al., 2010).

Organic P molecules account for an estimated 30 to 65% of the total soil P content, and they are mostly represented by stereoisomers of inositol hexakisphosphate (Ins6P). Among the stereoisomers, *myo*-inositol hexakisphosphate (*myo*-Ins6P) is considered the primary form of P storage in the seeds, while *neo*- and *scyllo*-stereoisomers are only observed in soils and not in plants, and for this reason it is generally assumed that these stereoisomers derive from microbial structures, albeit is still not clear if they represent an end-products of microbial activity rather a than degradation product of microbial structures (Jørgensen et al., 2011; Turner et al., 2005). In the soil system, Ins6P shows a strong affinity with soil constituents (Celi et al., 2003; Prietzel et al., 2016), and thus is generally considered largely stabilized and sparingly available (Cade-Menun et al., 2015; Santoro et al., 2019a). Conversely, the other organic P forms, like orthophosphate diesters, labile orthophosphate monoesters and organic polyphosphates represent less stable forms, which can be readily degraded by biological processes (Santoro et al., 2023).

In agroecosystems, soil P cycling is mostly controlled by the plant demand from the solution. As a result, all the other P pools are in equilibrium with the solution through specific processes of P replenishment from the solid to the solution phase (Frossard et al., 2000; Santoro et al., 2023). As represented in Fig. 1.1, the soil P cycling can thus be conceptualized in P inputs to the soil, P pools, processes of P retention/release, and P losses from the soil. In natural environments P inputs are represented by the weathering of soil parent materials, and the return of plants and animals residues, while in agroecosystems a further P input is represented by inorganic and organic P fertilization (Kruse et al., 2015). Regarding the definition of soil P pools, notwithstanding the current knowledge in P speciation in soil, most of the literature concerning soil P cycling is referred to context-based soil P pools, which in turn may encompass several inorganic and organic P forms. Thus, referring to agroecosystems, soil P pools can be conceptualized according to their decreased availability for plant uptake in i) soluble, represented by P in soil solution; ii) labile, and iii) stable P, both of which referred to the solid phase P (Moody et al., 2013).

Stable-P encompasses all inorganic P forms that are sparingly available to plants, due to strong adsorption processes and physical entrapment of inorganic and organic P molecules (McDowell et al., 2008; Moody et al., 2013). The solid phase in which occluded P is trapped undergo transformation processes that can cause

P release to the labile and soluble pools. Organic P forms are instead released to plants via hydrolysis, a slow process than can be enhanced by enzymatic activity, mediated by either plants or microorganisms (McDowell et al., 2008; Santoro et al., 2023). On the other hand, soluble inorganic P can be immobilized into microbial structures, creating competition between plants and microorganisms (Wang et al., 2022a).

The labile P pool refers to the P forms that are promptly released into the solution to replenish the P taken up by biota from soluble the P pool (Moody et al. 2013). The soil P buffer capacity is supported by abiotic and biotic dissolution reactions, which are governed by soil pH and Eh (Santoro et al. 2023 and references therein). Soluble P can be, in turn, retained by soil surfaces, thus decreasing plant availability via adsorption and precipitation reactions. Adsorption process involves weak and reversible electrostatic bonds, forming binuclear and bidentate or mononuclear monodentate complexes with a decreasing degree of stability. The degree of P adsorption depends on chemical and physical properties of the sorbent phase, like mineral composition, functional group, particle size, and specific surface area (Ciavatta et al. 2017). Among the soil constituents, Fe (hydr)oxides are considered the most efficient P-retaining surfaces, especially poorly crystalline phases like ferrihydrite, in view of its large specific surface area (Celi et al., 2020; Prietzel et al., 2016; Santoro et al., 2023). These structures can be rapidly dissolved by both biotic and abiotic reductive reactions, thus releasing large amounts of P into solution (Borch et al., 2010). The crystallization processes, which naturally occur in soil, lead to the release of P trapped within the evolving structures (Chen et al., 2020; Senn et al., 2017), albeit the P retained in more crystalline Fe minerals, as goethite, is generally considered less available because of the high stability of these surfaces (Santoro et al., 2023 and references therein).

For long time adsorption was considered the dominant mechanism of P stabilization, however the occurrence of precipitation reactions and the consequent variation of P behavior has been recently underlined (Santoro et al., 2019; Voegelin et al., 2013). Indeed, when solution P concentration increases, the coexistence of P and Ca, Al or Fe ions in solution drives the precipitation of metal phosphates subsequently to the formation of Fe-phosphate nuclei which promotes the rapid aggregation of amorphous structures (Santoro et al., 2019). Compared to sorbed P, Fe-phosphate precipitates result in a greater P release during abiotic dissolution, thus apparently improving P availability for plant (Kraal et al., 2019; Santoro et al., 2023).

Soluble P represents the far lowest share of soil total P content (<1%), and must be continuously replenished by the more loosely retain P forms (Frossard et al., 2000). Generally, the main concern is the availability of an adequate inorganic P concentration to continuously sustain plant P uptake; however, the most labile and soluble organic P forms are also present in the soil solution, in a variable percentage up to 50% of the total P in solution (Kruse et al., 2015). In addition,

an increasing percentage of soluble organic P was reported with decreasing total P content, suggesting a possible relationship between P speciation and total P content (Kruse et al., 2015). However, little is known regarding the composition of P speciation as a function of the total P content. Considering that total P conent controls the major abiotic (i.e. adsorption vs precipitation) and biotic (i.e. microorganisms and plant activity) reactions which regulate soil P cycling, a greater focus should be placed also on its role in determining soil P speciation.

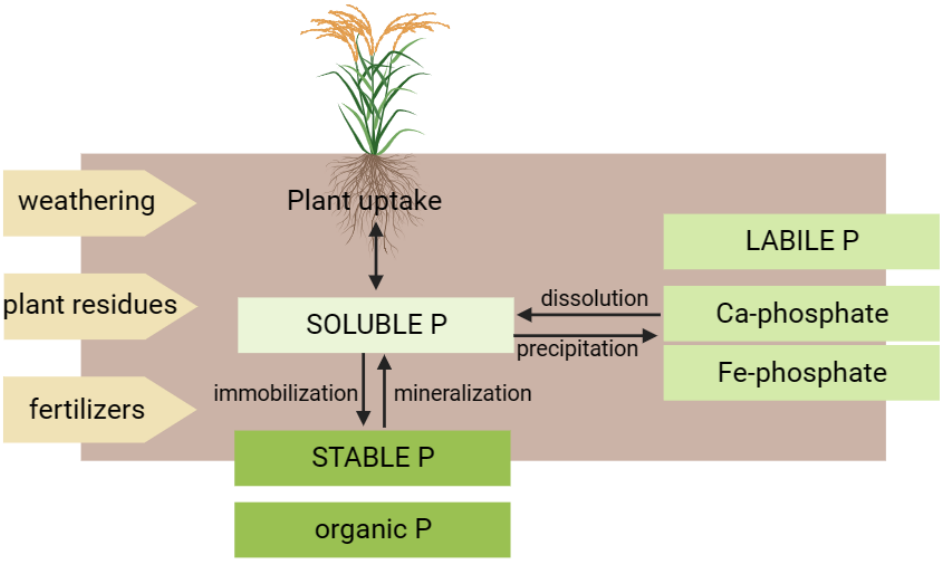

Figure 1.1 Soil P cycle representing the main inputs (yellow arrows), processes (black double arrows) and pools (green boxes). The figure is based on Kruse et al. 2015

1.1.2 Redox-driven processes

Most of the biogeochemical cycles in soils are driven by oxidation-reduction (redox) reactions (Borch et al., 2010). Redox reactions require an electron donor and an electron acceptor as recently reviewed by Marschner (2021). In aerobic soils most of these reactions involve O_2 as the main electron acceptor and organic matter as electron donor (Ajmone-Marsan et al., 2006; Marschner, 2021). However, in paddy soils, the occurrence of flooding periods leads to peculiar changes in the soil chemistry with specific effects on redox cycling and microbial metabolisms. In particular, the decreased rate of O_2 diffusion causes its complete depletion in the top-soil within 24 h, resulting in a shift of the microbial community from aerobic to anaerobic species. Alternative electron acceptors are therefore used, instead of O_2, whose sequence is determined by thermodynamics: nitrate, manganese, iron, sulfur and carbon (Kögel-Knabner et al., 2010). The involvement of Fe in these soil redox reactions is notably relevant for environmental biogeochemistry (Borch et al., 2010). In particular, Fe

(hydr)oxides are by far the most important substrate for both biotic and abiotic reductive dissolution reactions, in which the structural Fe(III) serves as terminal electron acceptor, leading to the production of aqueous Fe(II) (Kappler et al., 2021). The critical Eh-value for Fe reduction and consequent dissolution is +100 mV at pH 7 (Borch et al., 2010; Kappler et al., 2021; Kögel-Knabner et al., 2010). The highly reactive aqueous Fe(II) can be oxidized by both chemical and microbial reactions, however considering that the chemical oxidation of Fe(II) is quite fast, the reaction is microbially catalyzed only at low pH, which disadvantages the chemical reactions (Borch et al. 2009). The occurrence of reducing rather than oxidized reactions is therefore controlled by the soil Eh/pH, which present a surprisingly wide local variability in the soil-rice plant system. Indeed, as a consequence of the plant adaptation strategies to anoxic conditions, the rhizospheric environment is characterized by more oxidizing conditions, compared to the reduced bulk soils (Khan et al., 2016). Thus, despite the reduction of Fe(III) to aqueous Fe(II) is highly favored in the reduced bulk soil, the opposite pattern of Fe(II) oxidation to solid Fe(III) is dominant in rice rhizosphere. Thus, the oxidized and the reduced forms of Fe normally coexist, causing the instauration of mineral phase transition reactions which end in the growth and dissolution of crystalline Fe oxides (Boland et al., 2014; Hinkle et al., 2015).

The high complexity of redox reactions which characterize the transition from the reduced bulk soil to the oxic rhizosphere strongly impacts also the not redox-sensitive elements like P, according to its strong affinity with Fe oxide surfaces. Indeed, after the reduction of solid Fe(III) to aqueous Fe(II), the P retained by these surfaces is released into solution (Ponnamperuma, 1972; Scalenghe et al., 2002). The concomitant presence of Fe(II) and P in solution may lead to further co-precipitation of both Fe and P (Wei et al., 2019), when or where oxidizing conditions are created (Khan et al., 2016a). As a consequence, the amount of P in the solution or promptly available for plant nutrition may spatially and temporally change very differently with respect to aerobic soils, requiring specific methods for assessing P availability.

1.1.3 *Methods of soil P availability assessment*

A wide number of chemical methods had always been applied to identify the optimum soil P concentration required for plant growth (Pierzynski, 2000). Besides, soil P testing was primarily related to the amount of P fertilizer required to maximize yield, and only in the latter years, the increasing pressure regarding environmental pollution pointed out the necessity to apply soil P testing to better manage the nutrient supply in order to prevent unnecessary nutrient losses. For all these reasons, during the time several methods have been developed to address the evolving scope of a sustainable nutrient management (Kruse et al., 2015; Pierzynski, 2000).

Regardless the scope, soil P testing normally refers to the application of single or sequential extraction able to selectively dissolve various forms of P (Condron and

Newman, 2011). Theoretically, the soil test should extract all or a proportion of the amount of plant-available P, however all these methods are empirical, and their predictive usefulness should be calibrated against crop responses in field experiments (Moody et al., 2013; Pierzynski, 2000). Indeed, considering the wide range of processes that regulates P release from soil and its plant uptake, it is clear that there is no a universal soil P test that is useful predictor in all situations (Moody et al., 2013). Besides, the application of other techniques, like spectroscopic techniques to address soil P availability is still limited compared to the application of wet chemical extraction methods. However a recent debate pointed out the necessity to apply a wide range of techniques to investigate soil processes, as the traditionally applied wet-chemical extractions may provide only limited information (Barrow et al., 2021; Gu and Margenot, 2021). Thus, few studies recently compared the feasibility of nuclear magnetic resonance spectroscopy (NMR), or x-ray based synchrotron techniques in investigating soil processes (Cade-Menun et al., 2015; Liu et al., 2019; Lombi et al., 2006). Despite the latter could provide very useful information, their application is still limited due to the low nutrients' concentration which normally characterizes soil samples (Colocho Hurtarte et al., 2020).

Chemical methods

The chemical methods applied to test soil P availability were generally divided in three categories: i) extraction with water or diluted salt, ii) application of infinite sink, and iii) extraction with acid or alkali solution (Pierzynski, 2000). The former category (i.e. extraction with dilute salt, like calcium chloride) refers to the P already present in soil solution (Soltanpour et al., 1974), which represents the driving force of plant P uptake because of its direct link with diffusion processes (Moody et al., 2013). For this reason, soluble P has been proposed as a valuable representation of P availability to plants, however the diffusion process is dependent on many factors including the P concentration gradient between the root surface and the bulk soil solution, and the rate of P mobilization into the solution (Moody et al., 2013). Thus, the application of an infinite sink of P from the soil surface, like anion exchanging resins, was proposed as a better representation of plant available P (Amer et al., 1955; Saggar et al., 1990). Nonetheless, plants can access sparingly available P by several strategies and anion exchange resins are not able to operate P dissolution from soil surfaces, thus representing a possible limitation in addressing plant P uptake (McDowell et al., 2008). Conversely, acid and alkali extractants are able to dissolve P compounds based mainly in the nature and strength of interaction between P moieties and other mineral and/or organic components (Moody et al., 2013), and they possibly are able to better mimic the effects of plant strategies to acquire P. In this category, sodium-bicarbonate extraction, generally referred as Olsen method (Olsen, 1954), is largely applied to solubilize P from Ca-P precipitates, and partially from Fe-P complexes.

Specifically, regarding paddy soils, several methods are being used for estimating P availability in different pedoenvironmental contexts, including diluted salt,

Olsen, and anion exchanging resins. As P release in paddy soils solution is known to be associated to changes in Fe mineralogy, particularly poorly crystalline Fe (hydro)oxides (De Mello et al., 1998; Ponnamperuma, 1972; Wang et al., 2022b), redox-driven changes in Fe (hyr)oxide forms could strongly impact P availability for rice plants. Thus, along with the traditional chemical methods developed to estimate P availability in upland soils, other methods have been proposed to consider and include the contribution of Fe oxide-associated P to available P pools in temporarily flooded soils (De Mello et al., 1998; Reyes and Torrent, 1997). Despite acid oxalate-extractable P is reported to correlate with P availability (Shahandeh, 1995), there is evidence that this pool includes some P forms associated with crystalline Fe phases, potentially overestimating the amount of P available for plants. Reyes and Torrent (1997) thus proposed the citrate-ascorbate extraction as a more specific method to extract poorly crystalline Fe (hydro)oxides. Despite the evaluation of P availability in paddy soils being extensively investigated, all the studies pointed to very conflicting results, and the reason of this contrast remains a matter for debate. It could be hypothesized that the identification of the mechanisms controlling P retention and release under flooding conditions are still far from being completely understood.

Soil P fractionation procedures

The above mentioned chemical methods were also adapted and used in sequence to carry out P sequential fractionation for investigating the dynamic evolution of soil P pools in different natural environments and agroecosystems (Gatiboni and Condron, 2021). Among the different techniques reported in the literature, the Hedley procedure developed in 1982 has been the most largely applied technique to quantify the different inorganic and organic P forms (Hedley et al., 1982). Such a procedure is based on the identification of: i) biologically available inorganic P, removed by anion exchanging resins; followed by ii) 0.5 M sodium bicarbonate to extract labile inorganic and organic P sorbed onto soil surfaces; iii) 0.1 M sodium hydroxide extraction to remove inorganic and organic P chemosorbed to Fe and Al surfaces, iv) occluded P removed by 1 M hydrochloric acid, and v) residual P, extracted by acid digestion, which include a variety of chemically stable organic P forms, and insoluble inorganic P forms. The amount of P which is not specifically extracted by the previous steps is generally referred as residual P (Condron and Newman, 2011).

It is worthy to mention that, regardless the fractionation procedures applied, the quantity and the nature of P extracted by each step is only dependent on the fractionation scheme employed, thus it is not possible to clearly identify specific P forms but only operationally defined P pools (Pierzynski, 2000). Despite these procedures allowed to gain important understanding on the soil P dynamics in the last 60 years, they are recently being widely criticized by Barrow and co-authors (2021) who pointed out that “chemical fractionation are fallacious and should be abandoned”. The discussion opened by this bold statement concluded that, despite the soil P does not occur in discrete pools, but in several forms, and no fractionation procedures is able to distinguish among P forms, the careful

interpretation of the data obtained by these procedures can anyway get useful information regarding soil P dynamics (Gatiboni and Condron, 2021; Gu and Margenot, 2021).

The challenge of organic P

As recently reviewed by Santoro et al. (2023), organic P represents an important pool of P in soils and can replenish inorganic P with time via mineralization processes (Marschner, 2021; Wei et al., 2019). Thus, despite plants take up P only as orthophosphate, organic P forms may contribute to P availability, and in the case of crops grown in aerobic soils, this relationship was already demonstrated (Santoro et al., 2022). Conversely, for paddy rice, less studies have been carried out and mostly regard the lower mineralization rate of organic matter (Kögel-Knabner et al., 2010), and the implication of redox processes related to Fe oxides in enzyme retention (Giaveno et al., 2010; Tang et al., 2006) and organic P stabilization (Celi et al., 2020; Santoro et al., 2019). Little is known on the plant availability of soil organic P pools, possibly because the majority of the soil P testing procedures commonly applied neglect the importance of organic P (McDowell et al., 2008). This gap may also explain the limited capability of soil P testing to predict yield response for a wide range of soil P concentrations, as in low-P soils the importance of organic P for plant nutrition might be greater than supply of P from inorganic P alone (McDowell et al., 2008).

^{31}P Nuclear magnetic resonance spectroscopy

The wide variability of P compounds occurring in soil systems matches with different behaviors during their interactions with soil components, possibly affecting the final P availability for plants. For these reasons, the studies addressing the investigation of the processes of P availability should be focused on P speciation rather than the P pools (Barrow et al., 2021). The ^{31}P nuclear magnetic resonance (P-NMR) spectroscopy was firstly applied in environmental sciences in 1980 by Newman and Tate, and from this point onward the technique substantially contributed to advance the knowledge of organic P in the environment (Cade-Menun, 2005). Because ^{31}P is the only naturally occurring P isotope, all P species within a sample can potentially be detected by NMR spectroscopy (Cade-Menun, 2005; Kruse et al., 2015). The whole of the signal composes a ^{31}P-NMR spectrum, as the exemplificative reported in Fig. 1.2, and the quantity of individual P species in the samples can be assessed by the integrals of each specific signal (Cade-Menun, 2005). The correct quantification of P species by ^{31}P-NMR is limited by the signal-to-noise-ratio of the spectra, particularly in soil and environmental samples. Indeed, this kind of samples is normally characterized by low P concentration, a complex range of P species, and a natural association of P with paramagnetic ions, such as Fe and Mn. Different approaches were developed to face these challenges, and the implementation of liquid-state ^{31}P-NMR has been method of choice to speciate P in soil, rather than the solid-state spectroscopy (Cade-Menun, 2005). Indeed, the liquid-state

spectroscopy requires the extraction of soil samples, allowing higher P concentration, and the application of samples pre- and post-extraction treatments can decrease the concentration of paramagnetic ions (Cade-Menun and Liu, 2014). Despite these challenges, the application of ^{31}P-NMR spectroscopy in studying soil P dynamics is successful increasing in recent years (Cade-Menun et al., 2015; Colocho Hurtarte et al., 2020; Liu et al., 2018, 2015). The main application refers to the investigation of the transformation of the relative proportions of P forms, especially organic P, with respect to soil properties, climate, or disturbance (Cade-Menun, 2005 and reference therein). Despite ^{31}P-NMR spectroscopy been largely applied to study P speciation in reduced environments (i.e. lake sediments and marine water), limited information is available on paddy soils, likely because of the high concentration of paramagnetic iron associated with P.

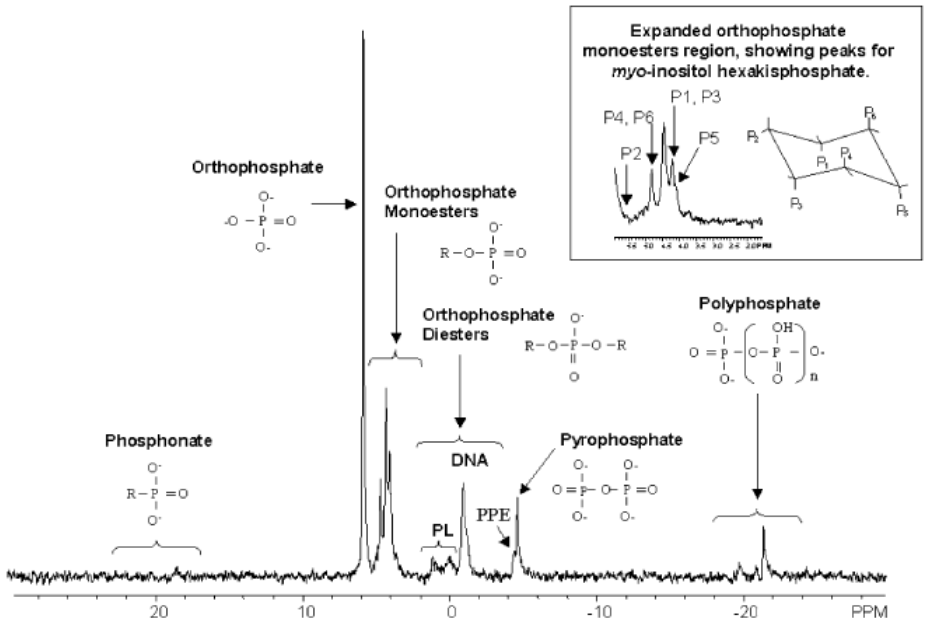

Figure 1.2 An examples of a ^{31}P-nuclear magnetic resonance (NMR) spectrum of forest soil sample, which represent the diversity of P species in natural samples. The insert shows the expanded orthophosphate monoester region, indicating the peaks and structures of myo-inositol hexakisphosphate (taken from Cade-Menum, 2005)

1.2 Rhizosphere modifications related to reducing conditions

The instauration of anaerobic conditions subsequent to flooding negatively affects rice plant physiology mostly because of the lack of O_2 (Barber et al., 1962) and the high concentration of aqueous Fe(II) in the porewater (Kirk, 2004;

Ponnamperuma, 1972). Indeed, under aerobic conditions, the O_2 required by root aerobic metabolisms is directly supplied by the soil pore air, while in flooded soils, the depletion of dissolved O_2 requires specific adaptation mechanisms by rice plants to transport O_2 to the root system (Bedford et al., 1991). Thus, root aerenchyma is formed to enable rice plants to survive to anoxic conditions (Colmer, 2003).

Furthermore, the ferrous Fe released by reductive dissolution has a greater solubility than Fe(III) found under aerobic conditions, and it can be readily taken up by plants causing Fe(II) toxicity (Sahrawat, 2005). There is a general agreement that Fe(II) concentration higher than 5 mM generates Fe toxicity symptoms, as reviewed by Das and co-authors (2017), and Sahrawat (2005). Considering that about 80% of Fe is localized in chloroplast, Fe toxicity strongly affects photosynthesis. Typical Fe toxicity symptoms are manifested as tiny brown spots starting from the tips and spreading towards the bases of the lower leaves (Das et al., 2017; Sahrawat, 2005), and in the most severe cases, Fe toxicity was reported to cause a 12-100% yield reduction (Das et al., 2017). Plant mechanisms to counteract Fe toxicity can involve three types of tolerance mechanisms referred respectively to: the exclusion of Fe(II) uptake (type I), the avoidance via internal distribution and storage of Fe(II) in a less reactive form (type II), and the increasing anti-oxidants activity (type III). These strategies can be further divided in shoot-based or root-based strategy. The former include type II by which Fe is retained in less photosynthetically active tissues, and type III (Briat et al., 2010; Fang et al., 2001). Root-based strategies are instead primarily focused on type I, and thus on avoiding Fe uptake, done by the oxidation of the rhizosphere (Sahrawat, 2005; Tanaka et al., 1966). Such a process is termed as Fe plaque formation, and it is related to the development of aerenchymatic tissues at root levels, as further detailed in section 1.2.2.

1.2.1 Root aerenchyma

Plants do not have active dispersal mechanisms to transport the O_2 required for root aerobic metabolism (Armstrong and Armstrong, 2014), so wetland plants are characterized by the presence of aerenchymatic tissues which contain enlarged gas spaces to convey atmospheric or photosynthetic O_2 from the shoots to the roots (Colmer, 2003; Evans, 2004). In contrast with other cereal crops, rice plants form aerenchyma either constitutively or because of abiotic stress (Evans, 2004; Yamauchi et al., 2013). This means that its constitutive formation is commonly observed in rice roots developed under aerobic conditions, although it can be further induced under O_2-deficient conditions or by nutrient deficiency (Evans, 2004; Fu et al, 2014; Yamauchi et al, 2013). Regardless of the reason of its formation, aerenchyma in rice roots occurs after lysigeny, thus the cells formed during the early development die and are removed leaving gas spaces (Evans, 2004). In the past, aerenchyma formation was attributed to necrosis, a passive process which is caused by the variation from physiological conditions, as the acidification of the cell cytoplasm related to O_2 starvation within the cells (Vartapetian and Jackson, 1997). However, recently it was underlined that the process by which constitutive aerenchyma forms may be different than inductive

aerenchyma formation, as its formation is controlled by ethylene signaling (Yamauchi et al., 2016, 2013; Yamauchi and Nakazono, 2022).
Furthermore, wetland plants form a specific barrier tissue in the outpart of the basal root zone to physically trap the O_2 in the root cells, and facilitate the longitudinal diffusion of O_2 toward root tips (Colmer, 2003; Kotula et al., 2009). However, a portion of the O_2 supplied via the root aerenchyma is being lost to the soil (Colmer, 2003; Mendelssohn and Postek, 1982), causing the oxygenation of the surrounding rhizosphere. Such a process is called radial oxygen loss (ROL), and it creates a millimeter-scale Eh gradient around rice roots ranging from approximately values of 500 mV to about -250 mV moving from the root surface to the bulk soil (Kögel-Knabner et al., 2010; Maisch et al., 2019). This redox gradient is related to the instauration of different processes that can profoundly affect the rhizosphere biogeochemistry of the main elements (i.e. carbon, Fe and P) as reviewed by Khan et al. (2016), and as further discussed in the next section.

1.2.2 Root Fe plaque

Process of formation
Root Fe plaque coating was firstly described by Bacha and Hossner (1977) who related the orange reddish color of the root surface with Fe(II) concentration in solution. Subsequently, Chen and co-authors (1980) explained the formation of root Fe plaque as a measure adopted by the plants to prevent Fe toxicity. As summarized in Fig. 1.3, Fe plaque formation results from the oxidative precipitation of the aqueous Fe(II) by O_2 leaked through the plant ROL, following the reaction:

$$4Fe^{2+} + O_2 + 10H_2O \rightarrow 4Fe(OH)_3 + 8H^+$$

As such, all the abiotic or biotic factors that may affect Fe(II) release into the solution and plant ROL, potentially lead to Fe plaque formation (Chen et al., 1980; Khan et al., 2016). Among the abiotic factors, it should be worth to mention the physicochemical properties of the soil, such as Eh, texture, and contents of poorly crystalline Fe (Mendelssohn et al., 1995). Soil Eh can be considered the master variable controlling the behavior of Fe in soil, as already described in Section 1.1.1, albeit other parameters including soil texture (Ariani et al., 2022 and references therein), may be implicated in the diffusion of atmospheric O_2 into the pore solution. Poorly crystalline Fe (oxyhydr)oxides experience faster and greater dissolution compared to more crystalline structures (Munch and Ottow, 1980). The release of Fe(II) into porewater is also controlled by the microbial community, particularly Fe-reducing bacteria (FeRB), which may favor Fe (hydr)oxide reductive dissolution (Weiss et al., 2004), and Fe-oxidizing bacteria (FeOB), that by contrast favor the precipitation of Fe(III) by mediating Fe(II) oxidation (Weiss et al., 2007), and contribute to Fe plaque precipitation (Khan et al., 2016; Maisch et al., 2019). However, ROL remains the main biotic factor controlling Fe plaque formation, and several factors can affect the plant capacity to oxygenate the rhizosphere. Indeed, Wu and co-authors (2012) reported that different rice genotypes differ in ROL and in the correlated Fe plaque deposit.

Furthermore, stronger tolerance to high Fe(II) concentration was reported in the mid development stages of rice plants, also implicating a temporal variation in ROL (Sahrawat, 2005). The formation of root aerenchyma and the subsequent ROL are generally ascribed to the onset of stress conditions, consistently nutrient deficiency was related to greater oxidizing capacity (Fu et al., 2014; Kirk and Van Du, 1997), albeit its relationship with Fe plaque formation remains unclear (Kirk, 2003).

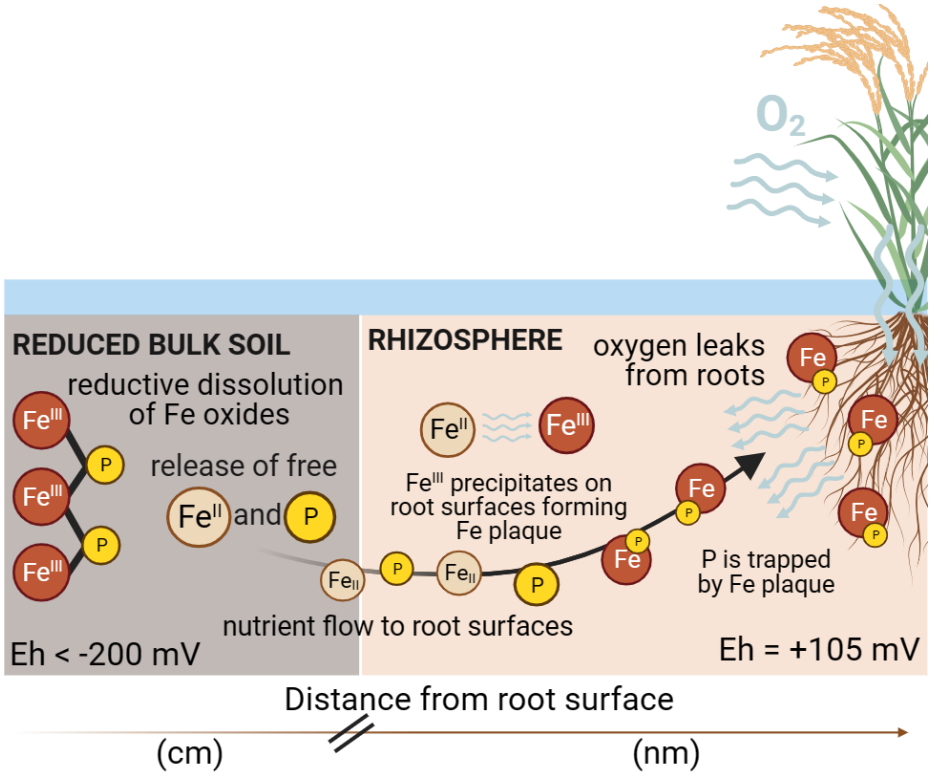

Figure 1.3 Model of the soil-plant processes related to Fe plaque formation and P retention in flooded paddy soils (based on Khan et al. 2016).

Plaque composition and characteristics

Iron plaque occurred on rice roots as a discontinuous coating, with differences in spatial (Liu et al., 2006; Seyfferth et al., 2010), and temporal distribution (Limmer et al., 2021; Zhou et al., 2018). Indeed, preferential Fe plaque formation was observed on thick mature roots near the water-air interface (Seyfferth et al., 2010), and despite limited Fe plaque deposit was related to young and fine roots, its formation was reported to rise exponentially during the vegetative growing phase, matching the exponential growth of the root systems (Limmer et al., 2022). However, several discrepancies in the obtained results are also reported (Liu et al., 2006; Zhou et al., 2018), possibly due to genotypic differences with respect to oxidizing power of rice roots (Mei et al., 2009), but only limited information are available regarding the spatial-temporal variability in root oxidizing capacity,

and the importance of root type (i.e. young, fine roots versus mature, thick roots) on Fe plaque distribution.

Furthermore, the root Fe coating can vary in its mineral composition. Several studies reported the presence of various Fe (hydr)oxides (Amaral et al., 2017; Frommer et al., 2011; Hansel et al., 2001), mainly represented by poorly crystalline ferrihydrite ($5Fe^{III}_2O_3 \cdot 9H_2O$), and lower amounts of more crystalline goethite (α-$Fe^{III}OOH$), and lepidocrocite (β-$Fe^{III}OOH$).

The mineral composition of Fe plaque can be explained considering that the primary product of Fe(III) oxidative precipitation in complex solution at near-neutral pH, is ferrihydrite (Voegelin et al., 2013), which is consistently reported as the main component of root Fe plaque (Amaral et al., 2017 and reference therein). The reaction between ferrihydrite surfaces and aqueous Fe(II) catalyzed recrystallization (Boland et al., 2014; Hansel et al., 2005; Yee et al., 2006), possibly explaining the presence of more crystalline phases, like goethite and lepidocrocite, observed in plaque at the end of rice development. Recent studies attributed to the porewater chemistry a further role in determining Fe plaque dynamics variation, indeed the presence of silicon (Si) was related to earlier deposit of Fe plaque (Linam et al., 2022), and to a higher proportion of poorly crystalline Fe (oxyhydr)oxides (Linam et al., 2022; Seyfferth, 2015). This thesis mostly focusses on P dynamics in paddy soils, however, despite the presence of P being largely reported in paddy porewater, and its effects were related to Fe (oxyhydr)oxide crystallization processes (Section 1.2.3), the role of P in governing Fe plaque formation and transformation kinetics received scant attention.

The debated role of Fe plaque in P nutrition

Because of its composition, Fe plaque coating contains various amounts of nutrients and contaminants, which may be trapped from the solution through adsorption and/or coprecipitation mechanisms as reviewed by Khan and co-authors (2016). The main reason of element adsorption from the solution by Fe plaque can be related to the high percentage of ferrihydrite which is characterized by a high surface area and high adsorption efficiency (Schwertmann et al., 2008). Oppositely, during coprecipitation the elements in solution are physically trapped in Fe crystal structure resulting from Fe(III) oxidative precipitation (Senn et al., 2015). According to the availability of the element retained in plaque, these surfaces can be classified as source, sink, or barrier. In the first case, the presence of Fe plaque facilitates the uptake; by acting as a sink, Fe plaque does not change the uptake; and in the latter case it limits the availability representing a barrier to plant uptake. All these processes can involve both nutrients and contaminants which may be present in the porewater, and are reported in Fe plaque (Limmer et al., 2022 and reference therein). Iron plaque can thus be defined as a complex pool of nutrients and contaminants in paddy soils, which could be characterized by a trade-off between nutrient availability and the limitation of contaminants uptake (Khan et al., 2016). The role of Fe plaque on P nutrition is largely debated, as higher Fe plaque formation was positively related with the retention of P from the nutrient solution, according to the large surface area and strong adsorption

capacity ascribed to Fe oxides by which Fe plaque are composed (Kuo, 1986), albeit excessive Fe plaque deposit decreased P uptake by rice plants (Liang et al., 2006; Zhang et al., 1999). Conversely, a recent study reported that the greater Fe plaque formation related to strong P uptake in plaque may favor the dissolution of these surfaces, positively impacting plant P uptake (Jiaofeng et al., 2022).
The controversial role of Fe plaque in P nutrition could thus be related to the complex interaction between P and Fe (oxyhydr)oxides, however limited information are available regarding the P retention/release mechanisms by root plaque, and most of them are derived from batch experiment on pure Fe(III) oxy(hydr)oxides and with inorganic P only. It is likely that a deeper understanding on the interplays between Fe plaque dynamics and P availability may result in the clarification of its role in rhizospheric P cycling.

Interaction between P and Fe (oxyhydr)oxides
The process of Fe(III)-oxidative precipitation – by which Fe plaque is formed - can be strongly modified by the presence of inorganic and organic P forms in the solution (Santoro et al., 2019; Voegelin et al., 2013). Generally, the presence of P causes a limited Fe polymerization as its incorporation into the newly formed Fe(III)-precipitates interfere with Fe mineral crystallization and spatial organization resulting in different morphology and surface characteristics (Senn et al., 2015; Voegelin et al., 2013). A pivotal role in determining the structure of the Fe(III) precipitation end products was attributed to the solution P:Fe molar ratio (Senn et al., 2015; Voegelin et al., 2013). Indeed, the oxidation of pure Fe(II) resulted in lepidocrocite followed by goethite formation through short-term crystallization processes (Schwertmann et al., 2008; Senn et al., 2015). Conversely, with the introduction of P in the solution at P:Fe higher than 0.2 , the formation of lepidocrocite was superseded by poorly crystalline ferrihydrite, which was in turn hindered at P:Fe higher than 0.5 by the formation of amorphous Fe(III)-phosphate (Châtellier et al., 2013; Senn et al., 2017; Voegelin et al., 2013).
The characterization of the Fe(III) oxidative precipitation end-products underlined that the solution P:Fe molar ratio does not only affect the mineral structure of the precipitates, but also their P retention mechanisms. Indeed, at P:Fe < 0.5 the formation of Fe structures resulted in P sorption by their surfaces, while at greater P:Fe the rapid formation of Fe(III)-phosphate nuclei resulted mostly in P retention by precipitation (Santoro et al., 2019). Such a process can be emphasized by the presence of background electrolytes in the porewater, as the presence of calcium (Ca) favors a faster and greater P uptake from the solution, following the formation of Ca-Fe(III)-phosphate complexes by electrostatic interactions (Senn et al., 2015). Conversely, at P:Fe < 0.5 the presence of other ligands, like Si, can modify Fe(III)-precipitate structure according to the greater affinity of P compared to Si for retention by Fe (oxyhydr)oxides surfaces (Voegelin et al., 2013). The precipitation of ferrihydrite with the subsequent P retention by adsorption was followed by the formation of poorly crystalline phases like Fe(III)-silicate in the external layer of the precipitates (Nenonen et al., 2023; Senn et al., 2017). Besides, different P

forms (i.e. inorganic orthophosphate *versus* inositol hexakisphosphate or phosphatidylcholine) resulted in different behavior during Fe(III) oxidative precipitation (Santoro et al., 2019). Indeed, it was observed that orthophosphate remained in the external layers of the coprecipitate, while Ins6P acted as a nucleus of crystallization and was strongly retained in the crystal. Conversely the P diesters interacted with Fe (hydr)oxides only through physical mechanisms, without affecting the Fe precipitation. Fig. 1.4 reports the mechanism of co-precipitation for the different inorganic and organic P forms described by Santoro and co-authors (2019).

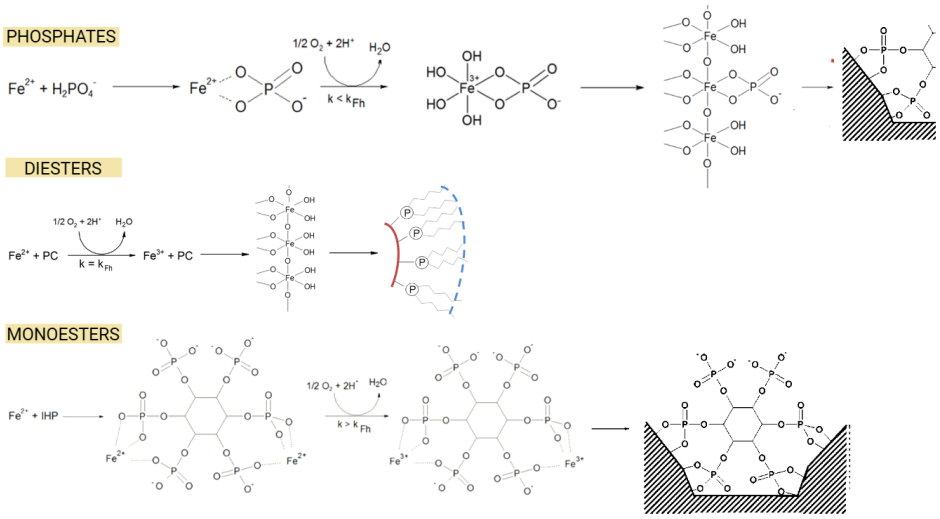

Figure 1.4 Mechanisms of inorganic and organic P co-precipitation with aqueous Fe(II). Based on Santoro et al. 2019

In natural environments, once formed, Fe(III)-precipitates continuously undergo structural transformation and re-arrangements which strongly affect their characteristics, especially concerning nutrient and contaminant retention. The differences in Fe(III)-precipitate structures and P retention mechanisms were related to different behaviors during Fe(III)-precipitate aging and transformation (Kraal et al., 2019; Nenonen et al., 2023; Senn et al., 2017). The Fe(III)-precipitates transformation processes mainly result in an increased crystallization and subsequent decrease in P retention capacity (Chen et al., 2020; Senn et al., 2017). Therefore, the transformation of poorly crystalline Fe(III)-phosphate and/or ferrihydrite, to more crystalline lepidocrocite or goethite resulted in the release of the retained inorganic and organic P in solution (Chen et al., 2020; Senn et al., 2017). Such a process resulted in faster and greater P release when P was coprecipitated in Fe (oxyhydr)oxide structure rather than adsorbed (Kraal et al., 2019; Santoro 2023, personal communication). Despite limited information is available on the fate of organic P forms trapped by Fe (oxyhydr)oxides structures (Chen et al., 2020; Santoro et al., 2019), a lower and slower organic P release was reported compared to inorganic-P (Chen et al., 2020), thus implicating that the greater affinity between organic-P forms and Fe(III) precipitates (Celi et al.,

2020; Santoro et al., 2019) may contribute to different retention/release processes during Fe (oxyhydr)oxides aging and transformation.
Based on the information available for P retention in Fe (oxyhydr)oxides, the dynamic reaction which might be implicated in P release from Fe plaque surfaces to plant uptake, could be profoundly affected by: i) the chemistry of the porewater during Fe plaque formation and transformation, ii) the mineral composition of Fe plaque, and iii) the forms and the mechanisms of P retention by plaque. However, Fe plaque is known to be a highly heterogeneous media, and specific techniques may be required to investigate their formation and composition.

Assessment of Fe plaque mineral composition
The wet chemical methods, as those commonly used in soils, are being extensively applied to assess the total Fe deposit on wetland plant roots. For instance, dithionite-citrate-bicarbonate (DCB) extraction is the most commonly reported procedure (Khan et al., 2016 and reference therein). Moreover, Yang and co-authors (2018) proposed the implementation of DCB extraction in combination with acid ammonium oxalate (AAO), to discriminate between crystalline and poorly crystalline Fe forms in plaque, respectively. Such an approach can provide information regarding the whole root system, and thus it is able to reflect the heterogeneity which characterizes Fe plaque (Khan et al., 2016 and reference therein). Moreover, it could provide useful information on the availability of nutrients and contaminants in the plaque, as it is well known that poorly crystalline Fe (oxyhydr)oxides can be more easily dissolved by chemical and microbial reactions (Schwertmann et al., 2008). However, wet chemical extractions are not able to capture the structural differences in Fe mineral composition, as each operationally defined pool (i.e. AAO- and DCB-extractable Fe) might include several types of Fe mineral structures, and the investigation of whether porewater chemistry might affect the processes of Fe plaque formation and transformation is crucially important to understand its role in the soil-plant interactions (Amaral et al., 2017). For these reasons, synchrotron-based X-ray techniques have been implemented in investigations of Fe plaque mineral composition (Khan et al., 2016; Seyfferth et al., 2010, 2021). From the late 1980s' techniques such as micro-X-ray fluorescence imaging, micro-X-ray absorption spectroscopy, and micro-X-ray diffraction were applied to small portions of root plaque to investigate their composition and the relative co-localization of nutrients/contaminants and Fe mineral structures (Blute et al., 2004; Hansel et al., 2001; Seyfferth et al., 2010). However considering the spatial heterogeneity which characterizes Fe plaque, the results presented in the earlier works were of limited relevance to investigate the relationship among porewater chemistry, Fe plaque structures and nutrient/contaminant uptake (Kuzyakov and Razavi, 2019; Seyfferth et al., 2021). Recently, a new procedure to sample intact Fe plaque through gentle sonication was proposed to allow the application of bulk x-ray diffraction and/or extended X-ray absorption fine structure (EXAFS) spectroscopy on the whole root system (Amaral et al., 2017). The implementation

of this protocol on the Fe plaque investigation enables to gain further insights in the role of porewater chemistry on Fe plaque mineral structure, and on its effect on contaminant availability to rice plants (Linam et al., 2022)

Assessment of the P forms retained by plaque

As for Fe, wet chemical extraction mostly considers P bound to Fe minerals, differentiating between AAO-extractable and DCB-extractable P. However, the presence of oxalate and sulfate in the reagent can create artifacts during the colorimetric determination of P in the extracts (Guedes et al., 2015; Wolf and Baker, 1990), as well as the amount of P extracted from the root cells may overestimate P in the plaque (Khan et al., 2016 and reference therein). Moreover, different inorganic and organic P forms can be present in the plaque and show a different behavior during their interactions with Fe (oxyhydr)oxides (Celi et al., 2020; Santoro et al., 2019), thus making the identification of P forms in the plaque a crucial point to understand rhizosphere P cycling; and such information cannot be addressed by wet chemical extractions (Kruse et al., 2015). Unlike soils, in root plaque the co-occurrence of P with a high Fe concentrations, makes the application of specific spectroscopic techniques, like NMR spectroscopy, unfeasible (Khan et al., 2016a; Lombi and Susini, 2009). This further methodological challenge could partially explain the lack of information on the forms and the mechanisms of P retention in plaque. Fourier Transformed Infra Red (FTIR) spectroscopy might represent a valuable technique to investigate P dynamics in plaque, as it furnishes useful information in the investigation with pure Fe (oxyhydr)oxides (Celi et al., 2003; Santoro et al., 2019; Zhang et al., 2021). Besides, synchrotron-based x-ray techniques were proposed as the most powerful solution to solve the spatial-temporal complexity of the rhizospheric environments (Lombi and Susini, 2009), albeit their application on Fe plaque are limited to the above mentioned investigation of Fe mineral structures, and their co-occurrence with heavy contaminants, like arsenic (Khan et al., 2016; Linam et al., 2022; Seyfferth et al., 2010). The latest development of x-ray sources, coupled with advances in manufacturing technologies of focusing optics has led to the access to the K-absorption edge of medium-light elements, like P (Lombi and Susini, 2009). Among these techniques, x-ray absorption near edge structure (XANES) is sensitive to the P oxidation state and local environment of the P atoms (Kruse et al., 2015). The P-XANES spectra are thus composed of the weighted sum of the local bonding environments of all P atoms within a sample, and its deconvolution allows the identification and quantification of the P forms present in the sample (Kruse et al., 2015; Lombi and Susini, 2009). The most commonly applied deconvolution technique is the linear combination fitting (LCF), which is a mathematical procedure based on the inclusion of a number of reference compounds (Calvin and Furst, 2013). The main challenge of P-XANES application on environmental samples is represented by the huge complexity of P forms in the samples, which in turn corresponds to a little differentiation of their relative spectra (Kruse et al., 2015; Lombi and Susini, 2009). Recent studies successfully demonstrate the capability of P-XANES to differentiate among the major soil P components (Prietzel et al., 2016). The authors also introduced the

question whether the LCF is capable to investigate different P forms retained by different Fe (oxyhydr)oxides (Prietzel and Klysubun, 2018). Despite P-XANES has been introduced to analyze the complexity of soil P cycling (Cade-Menun et al., 2015; Colocho Hurtarte et al., 2020; Liu et al., 2019, 2018), we are not aware of its application in Fe plaque investigations.

1.3 Rice plant responses to P supply in flooded soils

The uptake of P is particularly important in the early growth stages, as it is implicated in tillering and root development (Dobermann and Fairhurst, 2000). The subsequent reproductive stages involve the translocation of the P stored in the vegetative tissues to the grains, resulting in an accumulation of 60-85% of

aboveground P in seeds as Ins6P (Wang et al., 2016). Mild P deficiency in soil does not affect plant growth, while severe P deficiency mostly cause limited tillering, delayed development of thin and spindly stems and narrow and "dirty" dark green leaves (Dobermann and Fairhurst, 2000).

Soils generally contain a large amount of total P, but only a small proportion of it is immediately available for plant uptake with an average porewater P concentration lower than 10 μM, as recently reviewed by Santoro et al. (2023). The primary source of P uptake by plants is orthophosphate and it is absorbed via root phosphate transporters to overcome the steep P concentration gradient between the soil solution and cytoplasm of root cells (Rose et al., 2013 and reference therein). A threshold P concentration of 5 μM is generally considered to be sufficient for rice plant P acquisition (Frossard et al., 2000; Shahandeh et al., 1995), but below this soil P concentration a range of strategies are normally adopted by plants to overcome P limitation (Hinsinger, 2001). The primary plant response to limited P concentrations is the over-expression of the genes encoding for P root transporter (Rose et al., 2013 and refences therein). This family of genes is divided into low-affinity P root transporters, which operate when the P concentration in solution is in the range of millimolar (mM), and the high-affinity P root transporters, which in turn are over-expressed when P concentration in the solution is in the range of micromolarity (μM). Although the family of P transporters encompasses 13 genes (OsPT1-OsPT13), only few of them have been functionally characterized (Goff et al., 2002; Julia et al., 2018). Particularly, OsPT2 and OsPT6 are generally reported as low-affinity transporter genes, and OsPT1 and OsPT8 as high-affinity P transporters (Julia et al., 2018; Rose et al., 2013).

The several other strategies adopted by rice plants to overcome P limitation can be broadly divided into increase P-utilization *versus* P-acquisition efficiency (Rose and Wissuwa, 2012; Wang et al., 2010). The former is referred to a better internal use efficiency of P attributed to a more efficient re-translocation of the stored P from metabolically-inactive to -active sites, and it could be partially related to soil P supply, as the P translocated within plant tissues results from the amount of P taken up from the soil (Rose and Wissuwa, 2012). Nevertheless, the plant strategies to increase P acquisition are referred to a better uptake of the nutrient from the soil (Das et al., 2017; Wang et al., 2010), and thus directly implicated in the complex soil-plant interplays that govern P availability to rice. These strategies include several mechanisms, which can be further divided in i) increased soil exploration through modification of the root systems, and ii) increased pools of mobile P in the soil (Rose et al., 2013). The low mobility that characterizes P in the soil system is generally considered the key factor in limited P soil, and root exploration into new volumes of soil will be critical to enhance P uptake (Hinsinger, 2001). However, the peculiar soil chemistry which characterizes flooded paddy fields (Kirk, 2004) leads to a substantial increase in P diffusion because of the reduced tortuosity of diffusion paths, and thus the

contribution of root modification in increasing P uptake could be limited in rice plants compared to aerobic soil conditions (Rose et al., 2013). Furthermore, the formation of Fe plaque at root level and the consequent P retention represents a further difference with crops grown in aerobic soils (Khan et al., 2016; Rose et al., 2013), suggesting that rice plants adopt specific strategies to increase P uptake from sparingly available-P pools. A graphical summary of the strategies adopted by rice plants to deal with P limitation is given in Fig. 1.5.

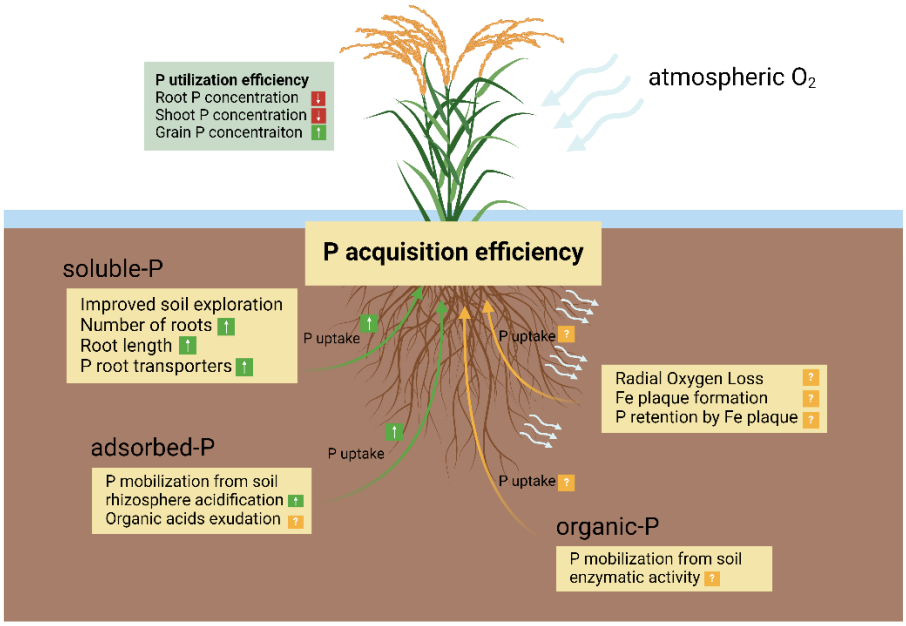

Figure 1.5 Comprehensive summary of the strategies adopted by rice plants to increase P utilization and P acquisition efficiency under P-limiting conditions (based on Rose et al, 2013)

1.3.1 Soil exploration by roots

In the soil system nutrients are mainly taken up by plants via mass flow and diffusion processes. Considering the limited mobility which characterizes P in soil, the contribution of mass flow is relatively small compared to diffusion, which in turn represents the mechanisms by which 95% of the P is taken up by plants (Hinsinger, 2001). Therefore, plant P uptake creates a step decrease in the concentration of P ions in the rhizosphere, generally referred to as P-depletion zone (Hinsinger, 2001; Lynch and Brown, 2008). The formation of a depletion zone is considered the driving force for the diffusion of P ions toward the roots, thus enabling P uptake. However, considering the limited mobility of P in soils, P acquisition is highly dependent on continued root growth and exploration of new soil domains that have not yet been depleted of P (Lynch and Brown, 2008). For this reason, increased root growth and modification of root architecture are generally considered the best-documented responses of plants to P starvation

(Lynch, 2007; Santoro et al., 2023). It is however worth to mention that the development of root biomass represents a cost for the plants in terms of both carbon and P (Lynch and Brown, 2008). Thus in the most severe cases of P deficiency, a net decrease of the root biomass was observed (Rose et al., 2013; Wissuwa, 2003). More precisely, P deficiency causes an increase in the root:shoot ratio, which is related to an absolute increase in root biomass under mild P deficiency, and to a proportionally larger decline in shoot biomass under more severe P deficient conditions (Rose et al., 2013). Indeed, as P uptake is mostly related to the root surface area rather the root biomass, rice plants develop a series of adaptation strategies to increase soil exploration without increasing its metabolic cost (Rose et al., 2013). Low P availability was thus related to changes in the distribution of root growth among various root types (Lynch, 2007), with a greater proportion of root length occurred as fine roots (Kirk and Van Du, 1997), formation of cluster roots, and increased density of root hairs (Ming et al., 2002).

Although the modification of root architecture observed in P-deficient rice plants could be ascribed to the same mechanisms adopted by aerobic crops, it should be noticed that the structure of rice roots is dominated by the need for internal gas transport which results in aerenchyma formation (Colmer, 2003). Such an effect was controversially attributed to a decreased nutrient efficiency, as the modification of the root structure consequent to aerenchyma formation was related to a limited nutrient uptake and transport from the roots to the photosynthetically active tissues (Kirk, 2003). Regarding P, however the hypothesis of an apparent trade-off between internal aeration and nutrient use efficiency was inconsistent with the increased root porosity (Kirk and Van Du, 1997), and aerenchyma formation (Evans, 2004) observed in P-deficient rice plants. The latest studies come together to the conclusion that P limiting conditions induce the formation of root aerenchyma (Fu et al., 2014; Pujol and Wissuwa, 2018), and such an effect was proposed as a comprehensive response with various functions, such as the decrease of the metabolic cost to increase soil exploration (Lynch and Brown, 2008a), and the nutrient remobilization consequent to the decomposition of the cell wall to form aerenchymatic lacunes (Fu et al., 2014).

1.3.2 Increasing the pool of mobile P

Among the strategies adopted by rice plants to increase the mobility of P in soil, rhizosphere acidification is generally considered the most important one (Begg et al., 1994; Rose et al., 2013a). Indeed, since the latter 1960s the pH changes of the rhizosphere related to root development were well reported (Hinsinger et al., 2003; Rose et al., 2013). Such an effect can be ascribed to different processes that increase accessibility of sparingly available P pools to plants (Rose et al., 2013), as also corroborated by the findings of Kirk and Van Du (1997) who demonstrated that rice roots depleted various P fractions in soil, and most remarkably the acid soluble fraction in the rhizosphere.

Although rhizosphere acidification is well known also for aerobic crops (Santoro et al., 2023), the peculiar chemistry of flooded soils can further create modifications in the rhizosphere pH (Hinsinger et al., 2003; Khan et al., 2016). Begg et al. (1994) firstly related the formation of the Fe(III)-accumulation zone in proximity of the root surface to a strong acidification. The redox-coupled rhizospheric acidification was further described by Kirk and Van Du (1997) who stated that the process of Fe plaque formation is accompanied by a decrease in soil pH, as a consequence of the reaction described in Section 1.2.2. Although the effects of rhizosphere acidification were positively related to increased P availability in aerobic crops (Hinsinger et al., 2003; Santoro et al., 2023), in rice soils, the complex chemistry makes this argument still a matter of debate as a consequence of the complex interactions between P and Fe plaque at rhizospheric level (Liang et al. 2006; Rose et al., 2013). Whether the mechanisms and the forms of P retained by Fe plaque affect rice P nutrition especially under P-limiting conditions remains largely unknown.

Furthermore, the peculiar chemistry of flooded paddy fields causes the modification of the biogeochemical cycles of all the major nutrients (Marschner, 2021; Wei et al., 2019). In the case of nitrogen (N), this results in a generally low concentration of nitrate (NO_3^-) over ammonium (NH_4^+), which in turn is the main N form taken up by rice plants (Wei et al., 2019). Therefore, the greater concentration of cations over anions present within the cells creates a pH imbalance. The cytosolic cell pH is normally maintained in a narrow range of values around 7.3, through a pH-stat system (Hinsinger, 2001). This comprises both physiological and biochemical reactions, the latter in particular result in the exudation of protons (H^+) to counterbalance the excess of positive charge inside the cells, leading to a further source of rhizosphere acidification (Hinsinger et al., 2003; Kirk and Van Du, 1997). Although the root-induced acidification of the rhizosphere which occurs for plants fed with NH_4^+ was reported to increase bioavailability of soil P, Kirk and Van Du (1997) estimated that the root-induced oxidation contributed to a significant and even major proportion of the measured rhizosphere acidification, and thus such a process could represent the main driving force of P acquisition in rice.

In addition to these mechanisms, the efflux of H^+ as a direct response to P limiting conditions was also proposed by several authors (Rose et al., 2013 and reference therein), however, there is still a lack of specific studies addressing this effect. This gap could be attributed to the complexity of the measurement of net rhizosphere acidification, as the H^+ release by roots could be involved in dissolution reaction and thus consumed without contributing to a measurable pH drops. A further complexity is represented by the dynamic formation and dissolution of Fe plaque on root surfaces, which partially contribute to the variation of rhizosphere pH as previously explained.

In aerobic crops, the mobility of P at limited soil supply is further increased by the exudation of ligands, like low molecular weight organic acids (LMWOAs),

and chelating agents (Rose et al., 2013). Considering that chelating agents like siderophores are commonly exuded by aerobic plants to acquire Fe, when it is limitedly available (Das et al., 2017), in the case of rice such a strategy may result in excessive Fe uptake favored by the greater Fe mobility under flooded soil conditions (Sahrawat, 2005). Consistently, Zhang et al. (1999) reported a limited effectiveness of siderophores in increasing P availability to rice plants, after the formation of Fe plaque, thus suggesting that other strategies may be implicated in increasing P mobility in rice rhizosphere. By contrast, it is well known that a variable percentage (30-60%) of the photosynthesized C is allocated to the roots, resulting in the efflux of LMWOAs (Aulakh et al., 2001; Marschner, 2002; Rose et al., 2013a). The most common components of root exuded LMWOAs are those from Krebs cycle and associated biochemical pathways, like oxalic, malic, and citric acids (Hinsinger et al., 2003). The quantitative and qualitative composition of root exudation is, however, subjected to large variations, both quantitative and qualitative, mostly attributed to phenological stage and genotype variability (Aulakh et al., 2001; Bhattacharyya et al., 2013; Hoffland et al., 2006). Although the information available regarding the role of LMWOAs on P mobilization are still limited, their role increase the accessibility to sparingly available P seems to be limited compared to the general mechanisms of rhizospheric acidification (Aulakh et al., 2001; Hinsinger et al., 2003; Kirk and Van Du, 1997; Rose et al., 2013).

Furthermore, plants can take up organic P after its hydrolysis to orthophosphate through enzymatic activity, and phytases and phosphatases represent the main enzymes involved in soil P cycling (Nannipieri et al., 2011; Santoro et al., 2023 and reference therein). As previously discussed, the important contribution of organic P in total soil P supply is accompanied by a large uncertainty in the understanding of the organic P cycle in paddy soils, including also the role of enzymatic activity. Despite an up-regulation of the genes encoding enzymes involved in organic-P hydrolysis in low P availability conditions, this was not related to a higher activity of enzymes in soil (Rose et al., 2013 and reference therein). Such an effect could be related to the high P retention capacity which characterizes Fe oxides in plaque. Tang et al. (2006) and Giaveno et al. (2010) reported indeed the inactivation of enzymes subsequently to their retention by ferrihydrite and goethite, respectively. It is thus likely that, under reducing conditions, the enzyme activity may be limited due to the interaction with highly reactive Fe oxides, in agreement with an observed increase of phosphatase activity in aerobic soils compared to anoxic conditions (Parsons et al., 2017). The soil microbial community could represent a further source of enzymes to hydrolyze organic P, however a recent study demonstrated that the competitive utilization of P between rice plants and soil microbial community under P deficient conditions resulted in a limited development of the latter (Wang et al., 2022a). All these information taken together suggested that enzymatic activity could not be the most effective strategy to increase P acquisition in rice plants.

1.4 The introduction of water saving techniques in rice cultivation

Increased competition for fresh-water consumption between the growing population and agricultural activity is one of the main concerns regarding the sustainability of rice systems (Datta et al., 2017; Pennisi, 2008). Indeed, the peculiar irrigation practices adopted in paddy fields make rice the most water-consuming cereal crop (Bouman, 2007; Mekonnen and Hoekstra, 2011). Considering the increasing frequency of drought events related to the ongoing

climate change, since the late 2000s, dry periods during rice growing cycle have been proposed to save water (Carrijo et al., 2017). In temperate paddy agroecosystems, rice is normally direct seeding, as rice crop is established from seeds directly sown in the field rather than by transplanting seedling (Datta et al., 2017). Following this practice, rice is traditionally sown in flooded soil, however between the onset of soil flooding and the full development of rice canopy causes large water losses due to direct evaporation of the water table (Dunn and Gaydon, 2011). Thus, the practice of dry seeding in which rice seeds are directly sown into dry soil, followed by a delayed soil flooding at tillering stage (DFL) has been introduced. This practice was reported to reduce the water requirements by 20% without affecting rice yields (Miniotti et al., 2016; Zampieri et al., 2019). However, water scarcity is not only referred to rainfall reduction, but also to technical unavailability of water over the territory (Datta et al., 2017). This happens for instance in mixed agroecosystems when dry-seeded rice co-exists with other spring cereals like maize. Indeed, the delay in maximum water requirements for completely flooding paddies to further development stage (i.e. tillering) may increase competition for water with other crops, making the adoption of DFL irrigation barely feasible in temperate paddy agroecosystems characterized by a complex pattern of crops in the same area (Miniotti et al., 2016; Zampieri et al., 2019). As a result, current efforts are focused on the potential application of alternating wetting and drying (AWD) irrigation, which is characterized by the intermitted flooding cycles and the subsequent instauration of oxidizing conditions in soil (Fischer et al., 2007). In AWD, the irrigation is interrupted, and the water allowed to decrease via drainage and/or crop evapotranspiration until it reaches a predetermined value of soil water potential. It can be applied in the form of "safe" irrigation, when the soil water potential is maintained above -20kPa, or "severe" AWD in the case the soil water potential dropped below -20 kPa (Gilardi et al., 2023 and reference therein). This technique may save up to 50% of water, based on the level of water saving rigorousness (Miniotti et al 2016).

The introduction of dry periods in the rice life cycle further affects P forms and availability for plants, although limited or no information is available on the consequences of the adoption of DFL and AWD techniques on P cycling.

1.4.1 *Implication for soil P availability*

The application of intermittent irrigation in aerobic soils normally results in increased nutrient availability, as theorized by the so-called "Birch effect" (Birch, 1958; Dodd et al., 2015). This suggests a positive implication of AWD on soil P availability in aerobic soil (Dodd et al., 2015 and reference therein). However, as stressed in section 1.1, paddy soils are generally characterized by a more complex chemistry related to the onset of long-term anoxic conditions, which in turn has an impact on P and Fe cycles. If oxic conditions are re-established, the aqueous Fe(II) released by reductive dissolution is rapidly oxidized to solid Fe(III), characterized by a high P sorption capacity, thus resulting in decreased P

availability in solution (Kirk, 2004). Besides, when Fe(II) and P coexist in the same solution, the instauration of coprecipitation phenomena may increase the P retention during Fe(III)-oxidative precipitation (Santoro et al., 2019a; Senn et al., 2017), possibly further decreasing P availability to rice plants (Zhang et al., 2003). Regarding the Fe mineral structures, the application of alternating redox conditions, similarly to those established during AWD irrigation, resulted in increased Fe oxide crystallinity attributed to the transformation of poorly crystalline Fe oxides to more crystalline phases (Thompson et al., 2006). Considering that poorly crystalline Fe oxides are widely reported as a preferential substrate for microbial reductive dissolution, this finding may explain a decrease in P release by the application of AWD. However, such an effect was barely reported by addressing P dynamics during redox oscillations in flooded soils (Parsons et al., 2017), and a general increase of P release in solution and of easily extractable-P concentration in soil was instead observed (Scalenghe et al., 2012; Schärer et al., 2009). Furthermore, recent studies pointed out that the original Fe mineral composition of the soil, and the leaching rate of aqueous Fe(II) had contrasting effects on the trajectory of Fe oxide evolution under alternating redox conditions, which may result in both increased and decreased Fe oxide crystallinity (Schulz et al., 2023; Winkler et al., 2018). Differences in soil characteristics might explain the contrasting reports on P availability under redox oscillations, and further suggested potential implication of root Fe plaque formation in regulating P availability to rice plants with the adoption of water saving techniques.

1.4.2 Plant responses to aerobic soil

Although rice is generally grown in submerged soils, it can adapt to aerobic conditions, even maintaining its yield capacity (Song et al., 2018). This ability has been mainly attributed to the root architecture plasticity under dry conditions, which led to an increasing number of branching points and lateral roots compared to rice developed in anoxic soils (Kato and Okami, 2011). Vallino et al. (2014) related the modification of root architecture to the great plasticity characterizing rice roots, as changes from dry to wet conditions caused an increasing number of lateral roots. The opposite (i.e. from wet to dry conditions) led to a decrease in lateral roots and branching points. Such an effect was however observed only on the short-time frame, while longer periods may exceed the root cell reprogramming capacity resulting in longer time frame for modification of the root architecture (Vallino et al., 2014). In addition, variations in root morphology were also related to a greater P acquisition efficiency observed under AWD (Xu et al., 2020), suggesting that the plasticity to adapt the root morphology (and physiology) might play a greater role in regulating P availability in AWD compared to continuously flooded conditions.

Nonetheless, although intermittent irrigation was reported to increase soil P availability, whether these fluctuations can be actively managed to enhance soil nutrient provision to plants has received little attention (Dodd et al., 2015), and

most of the focus was on the variation in root morphology related to root-to-shoot phytohormone signaling (Dodd et al., 2015 and reference therein; Song et al., 2018; Xu et al., 2020), albeit the results were in contrast. Indeed, some studies reported that the increased soil P availability was only barely correlated with an increased P uptake in plants (Acosta-Motos et al., 2020), or even to a decreasing P uptake in the case of most severe P-limitation (Song et al., 2018), despite a concomitant modification of root morphology was observed.

Aerobic rice cultivation slightly modifies the strategies adopted to increase P acquisition from soil. Conversely in flooded soils where increased P solubilization was mostly attributed to rhizosphere acidification processes (Begg et al., 1994), a greater citrate exudation was reported in aerobic rice compared to flooded paddies, which facilitate the solubilization of P inaccessible forms (Kirk et al., 1999). Furthermore, root architecture varied showing differences in the aerenchyma development and a discontinued formation of inducible aerenchyma (Vallino et al., 2014). All these processes might affect temporal Fe plaque formation/dissolution, as root aerenchyma plays a pivotal role in radial oxygen loss from rice roots, and citrate is highly effective in dissolving Fe (hydr)oxides (Kraal et al., 2019; Wu et al., 2012).

The introduction of dry periods during rice cultivation is well known to decrease the amount of Fe plaque deposited on root surface (Liang et al., 2006; Limmer et al., 2022; Linam et al., 2022), with contrasting evolution of Fe plaque mineral composition, as both poorly crystalline Fe mineral (Linam et al., 2022), and an increased crystallinity (Yang et al., 2018) were reported. These contrasting findings may be related to the complex soil-plant interplays and to the interconnected equilibrium between redox reactions. Despite this, the kinetics of Fe plaque formation during plant growth and transformation under alternating redox conditions are poorly investigated, and the consequent variation on P retention and release processes limitedly available.

1.5 Aims and highlights of the PhD thesis

Beyond its invaluable importance as a staple crop, rice paddies represent the most widely investigated wetland agroecosystems in view of the peculiarity which characterizes their nutrient cycling. The step-up gradient of redox conditions from the anoxic bulk soil to the oxygenated rhizosphere creates a unique environment in terms of soil-plant interactions. However, notwithstanding the current knowledge regarding P cycling in reduced environment (Marschner, 2021; Wei et al., 2019), still little is known on the temporal dynamics which

regulate P availability along this step-up redox gradient as well as on most appropriate methods to evaluate soil P availability, especially in temperate agroecosystems.

The establishment of reducing conditions causes an increased P supply in solution (Marschner, 2021; Scalenghe et al., 2002), counteracted by the peculiar oxidizing environment around the rice roots, which lead to the coprecipitation of Fe and P, forming the so called Fe plaque. However, the effects of Fe plaque on P availability are still debated, particularly regarding its relationship with soil total P supply and on strategies adopted by plants to acquire P from the rhizospheric Fe plaque. Indeed, under limited soil P supply, plants can adopt several strategies to overcome P starvation. An increased formation of root aerenchyma has been observed and related to a greater P uptake from root Fe plaque (Fu et al., 2014; Liang et al., 2006; Zhang et al., 1999), however the extent by which the P trapped by Fe plaque surfaces represents a source and/or a sink to the rice plant uptake remains largely unknown.

Furthermore, the interaction between P and Fe oxyhydroxides encompasses several mechanisms, mostly ascribed to P adsorption and co-precipitation. The extent by which one mechanism is predominant over the others has been mainly attributed to the involved P forms (Santoro et al., 2019). Indeed, the different molecules that characterize the soil P pools further increase the complex interaction between P and Fe cycling, since organic P forms are characterized by a greater affinity toward Fe (hydr)oxides compared to inorganic forms (Chen et al., 2020; Santoro et al., 2019a; Wang et al., 2017). Notwithstanding the importance of these processes, further studies are required to understand the role of organic P cycling on P availability, as a function of total P supply.

Rice agroecosystems are widely required to reduce water consumption and find new saving water technologies to face the dramatic effects of climate change (Datta et al., 2017; Zampieri et al., 2019). Considering the effect of continuous flooding on the soil processes which regulate nutrient cycling, the adoption of water saving techniques can strongly impact all the abovementioned processes, thus changing the interplays between reducing conditions and rhizospheric oxygenation that control P availability. With the introduction of dry periods we indeed expect changes in the solution P:Fe ratio, as a function of soil total P supply, which can have a key role on determination of coprecipitation mechanisms on root surfaces and, in turn, on the capacity of plants to acquire P. Although the needs to find saving water techniques seem to require a trade-off with an efficient use of P fertilizers, the investigation of rhizosphere mechanisms could provide novel insights on the P fluxes from reducing/oxidizing bulk soil to aerobic rhizosphere that allow to design more sustainable rice agroecosystems.

Within this framework, this thesis aimed to investigate i) the role of Fe redox cycling in regulating the availability of P in rice-soil systems as a function of P supply, ii) the influence of P availability on Fe plaque formation, iii) the availability of inorganic and organic P to rice plants as a function of their affinity

during Fe(II) oxidative precipitation, and ultimately iv) the role of Fe plaque as a temporal dynamic P pool in rice grown under different water management. A summary of the objectives of this thesis is presented in Fig. 1.6.

To address these objectives, this thesis encompasses four different experiments. In the first study – described in chapter 2 - P availability was investigated in 12 different paddy soils, ranging from high to low total soil P supply, to estimate easily desorbable P (Olsen, anion exchanging resins) and Fe-bound P (citrate-ascorbate, and oxalate). In the same soils, rice plants were cultivated for 60 days under continuously flooded conditions to evaluate total plant P uptake, matched by the investigation of plant responses to P deprived conditions (i.e. phosphate root transporter gene-encoding expression, enzymatic activity, and roots oxygenation capacity). The results showed that continuous flooded conditions decrease the availability of redox-sensitive P to rice plants more than what was supposed until now, because of a temporal decoupling between P release from reductive dissolution and plant uptake. Nonetheless, the plant responses to limited P availability profoundly shape the rhizosphere environment resulting in a preferential depletion of loosely sorbed inorganic P, matched with an increased rhizosphere oxidation.

Based on the results presented in chapter 2, a second study was carried out to evaluate the effects of two levels of P supply on Fe plaque formation and the subsequent uptake of the P retained by root plaque. As further detailed in chapter 3, rice plants were grown hydroponically under two different levels of P, representative of the average porewater P concentration observed in low and high-P soils described in chapter 2. The greater rhizosphere oxygenation, observed in soils with limited P supply, led to a higher Fe plaque deposit and to a larger plant P uptake. It can be inferred that rice plants can favor a prompt dissolution of Fe plaque to utilize the sparingly accessible P and counteract limited P supply. Conversely, at higher P supply, we observed a limited release of P from plaque, suggesting that these surfaces can act both as a sink or source of P as a function of the overall P availability in the system.

The results described both in chapter 2 and 3 pointed out the importance of soil-plant interactions to overcome P limitation in submerged paddies. Chapter 4 further investigated the role of total soil P supply in driving the evolution of inorganic and organic P forms during rice cultivation. The soils, derived from the experiment detailed in chapter 2, were further analyzed by wet chemical P fractionation and ^{31}P nuclear magnetic resonance spectroscopy before and after rice cultivation. Consistently to the higher availability of easily exchangeable P to rice plants observed in chapter 2, the exchangeable P pool resulted in the greatest depletion within rice cultivation, while the redox-sensitive P pool increased during rice cultivation likely because of the co-precipitation processes with aqueous Fe(II) released by reductive dissolution. Particularly in the case of organic P forms, the interplays between soil processes and plant responses to P supply resulted in a specific accumulation of organic P forms as a function of

total P supply. The results obtained in chapter 4, also further support the hypothesis that the mechanisms which regulate P release from the soil for plant uptake are different in the reduced bulk soil with respect to the oxidized rhizosphere. Indeed, the dissolution of Fe plaque and the subsequent P uptake should result in a depletion of the redox-sensitive P pool. By contrast, the mechanisms of P stabilization established in the reduced bulk resulted in an increase of inorganic and organic P co-precipitation with the free Fe(II) released in solution after reductive dissolution.

Ultimately, Chapter 5 provides novel insights on the role of Fe plaque in governing P availability to rice plants grown under different water management techniques. In this experiment, rice plants were cultivated under continuously flooded conditions (WFL), delayed flooding (DFL), and alternating wetting and drying (AWD) irrigation, with two levels of P. The kinetics of Fe plaque formation, dissolution, and P retention were followed during the entire rice growing season. The findings demonstrated that porewater chemistry influenced Fe plaque formation and crystallization processes as a function of Fe(II) concentrations and P:Fe molar ratio. In particular, the higher P:Fe ratio observed during dry periods resulted in lower Fe plaque crystallization and greater P retention through co-precipitation. Thus water-saving techniques determined a different P availability to rice plants over time, in line with the increased dissolution rate of Fe-phosphate precipitates compared to sorbed P. Consistently to the results observed in Chapter 4, organic P was more available when the total soil P supply was lower, resulting in a greater accumulation on Fe plaque surfaces.

All the experiments presented in this thesis were financially supported by the Regione Lombardia research project “Fosforo in risaia: equilibrio tra produttività e ambiente nell’ottica delle nuove pratiche agronomiche” d.d.s. March 28th 2020—n. 4403 and by the Fondazione Cassa di Risparmio Torinese research project “Enhanced biological N fixation through improved P acquisition by leguminous plants” (FOS4FIX).

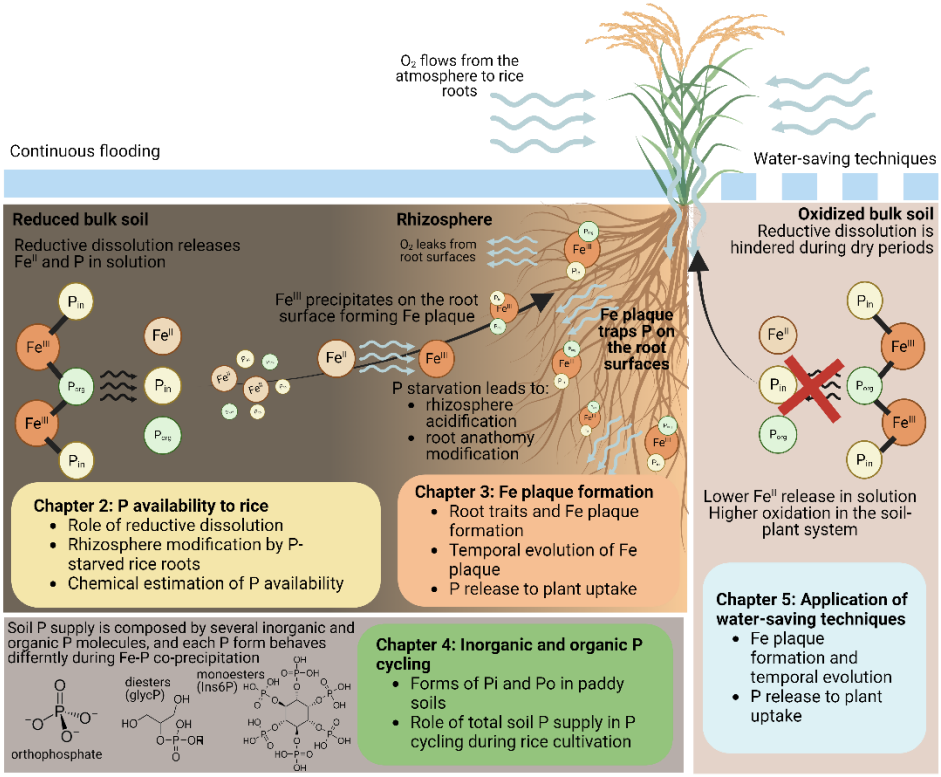

Figure 1.6 The general aims of this thesis were to clarify the mechanisms governing Fe and P interaction in paddy soils, and in particular the effects on: i) P availability to rice plants grown in flooded soils, ii) processes of P release after Fe plaque formation and dissolution, iii) evolution of inorganic and organic P forms in paddy soils, and iv) the modification of these processes with the introduction of water saving techniques.

The data presented in Chapter 2 and 3 have been published in:

- **Martinengo**, S., Schiavon, M., Santoro, V., Said-Pullicino, D., Romani, M., Miniotti, E.F., Celi, L., Martin, M., 2023. Assessing phosphorus availability in paddy soils: the importance of integrating soil tests and plant responses. Biol. Fertil. Soils 59, 391–405. https://doi.org/10.1007/s00374-023-01714-8
- **Martinengo**, S., Santoro, V., Schiavon, M., Martin M., Celi L. Said-Pullicino D., 2023. The influence of phosphorus availability on rice root traits driving iron plaque formation and dissolution, and implications for phosphorus uptake. Plant Soil. https://doi.org/10.1007/s11104-023-06306-x

Chapter 4 and 5 present the main materials and methods, results and discussions which allow for the best interconnection among chapters and overall comprehension of the whole work. The manuscripts discussing the data presented in Chapters 4 and 5 are currently under preparation.

CHAPTER 2

The role of Fe redox cycling in regulating P availability in rice-soil system

2.1 Introduction

For long time, P availability in paddy agroecosystem has been considered not yield-limiting. However, protracted flooding conditions resulted in a limited P release in solution (Santoro et al. 2019; Zhang et al. 2003), likely reducing P availability for crops more than supposed until now.

A number of methods has been used for estimating P availability to paddy rice in different pedoenvironmental contexts (Pierzynski, 2000), and, for each chemical method, the amount of P extracted as a proxy for plant available P reflects the soil P pool(s) and process(es) for which the soil P test is designed (Moody et al., 2013). Considering the information available in literature up to present, there is not agreement on the most suitable method to estimate P availability to rice plants grown in flooded soils. This implies that the mechanisms by which P is released from the soil surfaces to the plant uptake, are still debated. Indeed, the acknowledged relationship between the reductive dissolution of Fe oxy(hydr)oxides and P mobilization would well explain the results of those papers that identified extractants targeting Fe pools (e.g., citrate-ascorbate, De Mello et al., 1998; oxalate, Rabeharisoa et al., 2012; citric acid, Hernández et al., 2013) as good predictors of P availability to rice, however a number of other works point to methods related to P desorption (e.g., Olsen, Maftoun et al., 2003; anion extracting resins, Teo et al., 1995; DGT, Six et al., 2013), possibly indicating that P release from reductive dissolution is not the only mechanism of P availability to rice plants. Besides, most of the cited studies focused mainly on tropical soils, thus, their results are poorly adaptable to temperate paddy systems because of the differences in soil parent materials and soil-forming processes that possibly affect P release for plant uptake (Kögel-Knabner et al., 2010; Moodly et al., 2013). In subtropical and tropical regions where soils are highly weathered, the porewater P concentration could be very low compared to the plant P demand, due to the high content of stable Fe and aluminum oxides and to their lower reducibility (Hinsinger, 2001).

Furthermore, as already introduced, rice plants respond both to anoxic conditions (Colmer, 2003; Sahrawat, 2005), and to the soil P supply (Rose et al., 2013) by creating a peculiar rhizospheric environment characterized by a step-up gradients of redox conditions from the reduced bulk soil to the oxidized rhizosphere, and by the presence of root and the relative exudation products to access low available P forms. The interaction between plant P acquisition strategies and soil redox dynamics could drive changes in the different soil P forms and their availability, thus justifying the large variability of mechanisms proposed to explain rice P nutrition in paddies and the involved P pools (Hernández et al., 2013; Madurapperuma and Kumaragamage, 2008; Shahandeh et al., 1995).

Based on these considerations we hypothesized that the reductive dissolution process can effectively release P to plant uptake, however the plant adaptation

mechanisms to continuously flooded soil conditions and P limitation further shape the rhizospheric environment resulting in a not-linear relationship between reductive dissolution and P availability to rice plants. Therefore, this chapter aims to assess the involvement of different P pool(s) in rice P nutrition, as a function of soil P content, while combining the changes in Fe and P dynamics with the response of rice plants to soil flooding and P supply. We hypothesized that P bound to reducible Fe pools could play a major role in paddy soils from temperate regions, as recently reported for tropical soils (Wang et al., 2022a, b), and that plant adaptation mechanisms could enhance P uptake under P deficiency by acquiring P from soil pools generally considered sparingly available under flooding conditions. To test these hypotheses soil P availability was assessed with four different chemical methods - mainly divided in easily desorbable P pools and Fe-bound P pools - in 12 paddy soils, representative of a large range of total P contents. The estimated P availability was compared to the effective P uptake by rice plants cultivated in mesocosms under continuous flooding and related to plant responses.

2.2 Material and methods

2.2.1 Determination of the most suitable method for assessing soil P availability under reducing conditions

Study sites, soil sampling and chemical analyses

The North-West Italy rice cropping area was chosen as study site, representative of temperate paddy soils. In this area, 100 paddy top-soils were randomly collected from different sites represented in Figure 2.1.

The soils were sampled at 0-20 cm, air dried and sieved < 2 mm. The pH was determined potentiometrically in a 1:2.5 soil:H_2O suspension. Total carbon (C) and nitrogen (N) contents were determined by dry combustion (UNICUBE, Elementar Analyses System GmbH, Langensbold, Germany). When present, the $CaCO_3$ content was calculated from the difference between total and organic C determined by dry combustion after carbonate dissolution with 0.1 M HCl. Total P (P_{tot}) was determined after sulfuric-perchloric digestion (Olsen & Sommers, 1982) and the concentration of molybdate-reactive P (MRP) in the extracts was determined according to Ohno and Zibilske (1991). Iron (Fe) and aluminum (Al) were extracted with ammonium oxalate (Schwertmann et al., 2008), and the total Fe and Al concentration in the extracts was determined by atomic absorption spectroscopy (AAS, PerkinElmer AAnalyst 400, Norwalk, CT, USA). Particle-size distribution was assessed by the pipette method after sample dispersion with Na-hexametaphosphate (Gee and Bauder, 1986). The soil cation exchange capacity was determined in 10% $BaCl_2$ (Burt, 2004), and the concentration of exchangeable cations in the extracts was determined by AAS.

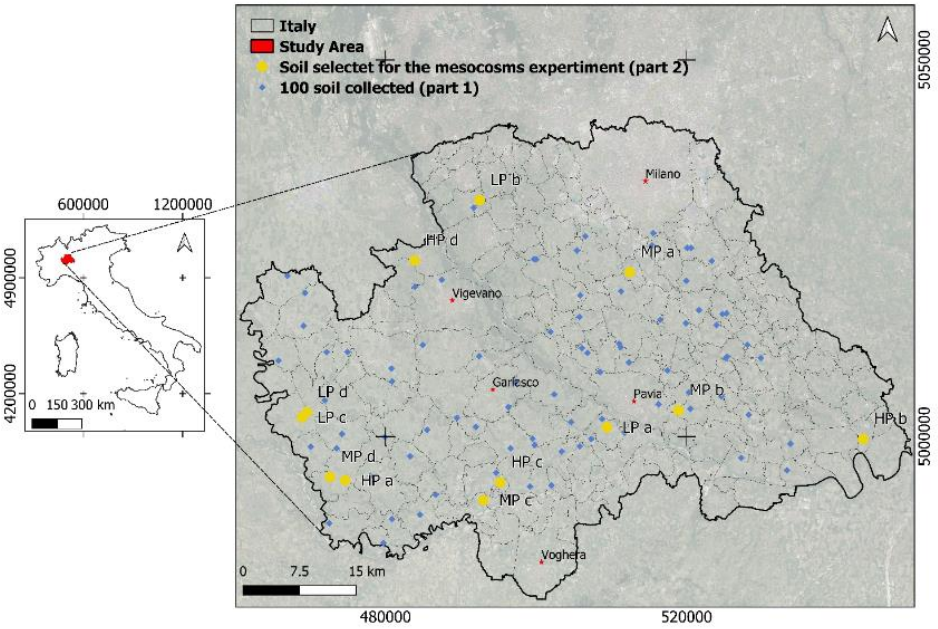

Figure 2.1 Localization of the study area, in red, in North-Western Italy; and localization of the 100 sampling points (in blue) and localization of the 12 representative paddy soils (in yellow) used in the pot experiment. The abbreviation used to label yellow points refer to the soil ID listed in Table 2.3. Reference frame: WGS84

Soil P availability assessment

The soils were subsequently grouped in 12 classes based on their total P content, pH and particle size distribution (Table 2.1). One soil per class, totally 12 representative soils, were further selected as the most representative and grouped based on total P content as "low", "medium", and "high".

Table 2.1 List of criteria used for soil classification in the twelve groups

Soil group		Total P (mg kg^{-1})	pH	Sand (%)
High P				
	#1	> 800	> 6	> 50
	#2		< 6	< 50
	#3		< 6	> 50
	#4		> 6	< 50
Medium P				
	#5	> 500 < 800	> 6	> 50
	#6		> 6	< 50
	#7		< 6	< 50
	#8		< 6	> 50
Low P				
	#9	< 500	> 6	< 50
	#10		> 6	> 50
	#11		< 6	< 50
	#12		< 6	> 50

These soils were analyzed for P availability using four extraction methods according to the target P pool, as listed in Table 2.2. The selected extraction methods were divided in: (i) methods assessing easily desorbable pools, including the extraction in $NaHCO_3$ (Olsen et al., 1954), and anionic resins (Saggar et al., 1990), and (ii) methods targeting Fe-bound P pools, as citrate-ascorbate (Reyes and Torrent, 1997) and oxalate (Schwertmann et al., 2008) methods. The phosphate in the extracts was determined colorimetrically according to Murphy and Riley (1962) using excess molybdate when necessary (Weaver, 1974).

Table 2.2 Short description of the extraction methods used in this study and related mechanisms of P release from soil

Extractant	Process	Extraction procedure	References
Olsen	Exchange	1 g of soil with 20 ml of 0.5 M $NaHCO_3$, pH 8.5; 30 min	Olsen 1954
anion exhange resins	infinite sink	2 g of soil with 0.5 g of DOWEX resins in 40 ml H_2O; overnight	Saggar et al.1990
citrate ascorbate	Fe-ox(hydro) complexation and reduction	1 g of soil with 40 ml of 0.2 M Na-citrate, 0.05 M ascorbate, pH 6.0; 16 h	Ruiz et al.1997
acid NH_4 oxalate	Fe-ox(hydro) complexation and dissolution	0.5 g of soil with 20 ml of 0.2 M $(NH_4)_2C_2O_4$, pH 3.0; 2 h	Schwertmann 1964

2.2.2 Evaluation of plant responses to different soil P supply

Mesocosm experiment set up

Rice cultivation was performed in the 12 selected soils (four replicates) for 60 days under continuous flooding, shown in Fig. 2.2. 2.5 kg of fresh soil were carefully inserted in each mesocosm by reproducing the original bulk density. The soils were then flooded by maintaining 5 cm of water above the soil surface and the Eh measured potentiometrically and monitored to confirm the establishment of soil reducing conditions (7 days after flooding, DAF). Rice seeds (cv *Selenio*) were pre-germinated for 3 days at 25°C in the dark and transferred to the mesocosms at 5 DAF. The mesocosms were then transferred inside a climatic chamber at a constant temperature of 20°C and 12 h light per day, with a light intensity of 600 μmol m^{-2} s^{-1}. At 20 DAF plants were fertilized with 40 kg N ha^{-1}, considering a mesocosm volume of 0.02 m^3. One Rhizon sampler (Rhizon MOM 19.21.21F, Rhizosphere, Wageningen, The Netherlands) was installed vertically in the proximity of the root system, and the soil solution was collected weekly and analyzed for Fe(II) and dissolved phosphate. Dissolved Fe(II) concentration was measured colorimetrically immediately after porewater

sampling, using the 1,10-orthophenanthroline method (Loeppert and Inskeep, 1996), and dissolved P was measured as previously described for soil extracts. Additionally, for each soil P level, unplanted soil mesocosms were also setup and soil solution was weekly collected and analyzed for Fe(II) concentration. The difference in porewater Fe(II) concentration between non-planted and planted samples was used as a proxy to monitor radial O_2 loss (ROL) from plant roots. Indeed, the extent of Fe mineral reduction could be used as an indicator of the ability of rice plants to control rhizospheric soil redox conditions under flooding (Doran et al. 2006).

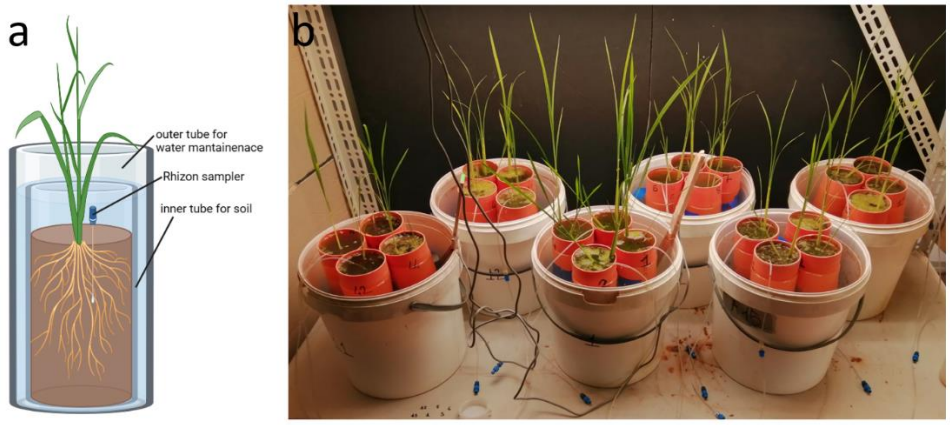

Figure 2.2 a) schematic representation of the mesocosm set up, and b) picture of the rice plants cultivated in the mesocosm system for 60 days under continuous soil flooding.

Plant sampling and analysis

Plant shoots and roots were harvested separately at 60 DAF, when plants were at the maximum number of tiller detectable stage. Thus, plants were at the end of the vegetative stage when the concentration of P in plants was reported to be mainly dependent on plant uptake rather than internal redistribution (Wissuwa, 2003). Roots were carefully washed with deionized water and a subsample (200 mg) was rapidly frozen with liquid N_2 and stored at -80 °C for enzymatic and gene expression analyses. The remaining root and shoot material was dried at 40°C for determining dry biomass and elemental composition. Total C, N and P content (P_{plant}) was determined according to the methods previously described for soil samples. Phosphorus-acquisition efficiency (PAE) was calculated as the ratio of P accumulated in tissues to soil total P, P-utilization efficiency (PUE) was calculated as the ratio of dry biomass to P concentration in the plant tissues (Neto et al., 2016), and P-translocation efficiency (PTE) as the ratio of P concentration in the shoot to the P concentration in the root (Santoro et al., 2021).

Phosphate transporters gene transcript quantification

Aliquots (100 mg) of the frozen roots were ground using a Qiagen TissueLyzer II (Retsch MM300, Germany). Total RNA was extracted using the Trizol Reagent (ThermoScientific) according to manufacturing instructions and treated with DNase I (ThermoScientific) at 37°C for 30 min to remove residual genomic DNA. First-strand cDNA was synthesized from 500 ng of purified total RNA

using SuperScript® IV Reverse Transcriptase (ThermoScientific) according to the manufacturer's instructions. For transcript quantification of target genes, the quantitative reverse-transcriptase PCR (qRT-PCR) reactions were carried out by Chromo4TM Real Time PCR Detection System (Bio-Rad Laboratories) using the SYBR Green (Applied Biosystems) methods. Thermal conditions were: 95 °C for 3 min as the first denaturing step, followed by 95 °C for 10 s, 55 °C for 30 s, for 39 cycles. The CT values were analyzed with the Q-gene software by averaging three independently calculated normalized expression values for each sample. Expression values are given as the mean of the normalized expression values of the triplicates, calculated according to Eq. 2 of the Q-gene software (Muller et al., 2002). Three independent biological replicates (= 3 plants) were analyzed per soil, and each qRT-PCR reaction was run in technical duplicates.

Enzyme activity in root tissues

Root enzymatic activity was assayed following the method of Hayes et al (1999). Briefly, the root material (0.5 g) was ground in 15 mM 2-(N-morpholino)ethanesulfonic acid (MES) buffer (pH 5.5) containing 0.5 mM $CaCl_2$ and 1 mM EDTA. After centrifugation, the extract was subjected to gel filtration on Sephadex G-25 columns. The activity of acid phosphatase and phytase enzymes was measured on the same root extracts using the substrates 10 mM p-nitrophenyl phosphate (pNPP) and 2 mM potassium myo-inositol hexaphosphate (IHP), respectively. Assays were conducted for 60 min and the reactions stopped by addition of ice-cold 10% trichloroacetic acid (TCA). Solutions were subsequently centrifuged to remove precipitated material and p-nitrophenol and phosphate concentration, respectively, determined spectrophotometrically.

Statistical analyses

The statistical analyses were performed using the R version 4.1.1. Normality and data homoscedasticity were checked with Shapiro-Wilk and Levene tests, respectively. When necessary, data were transformed according to the data distribution. Correlation analyses were used to relate P content in the plant tissues (P_{plant}) to the amount of P extracted by the different extractants in order to determine the best method to estimate P availability in flooded paddy soils. All the variables were tested for the analysis of variance (two-way ANOVA), followed by pair-wise post hoc analyses (Student-Newman-Keuls test) to determine the difference among the mean value at $p < 0.05$.

2.3 Results

2.3.1 *Chemical methods for assessing soil P availability to rice*

Soil chemical and physical properties

The majority of the 100 analyzed soils had a sandy loam texture, the pH close to neutrality, and the total P content ranged from 200 to 1000 mg P kg^{-1}. Fig. 2.3 reports the average characteristics of the 100 collected soils, while Table 2.3 details the properties of the 12 representative soils selected for the mesocosm experiment.

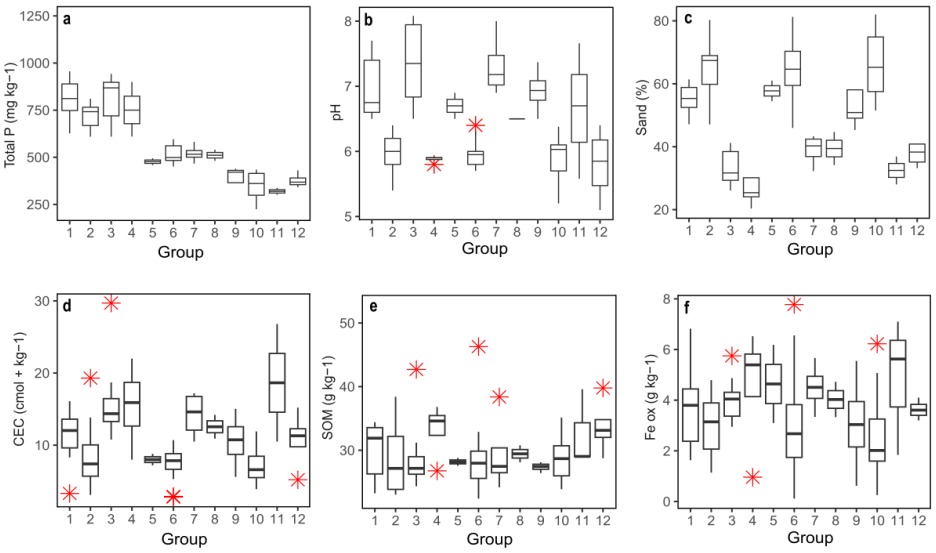

Figure 2.3 Average values of soil total P (a), pH (b), sand content (c), cation exchange capacity (d), soil organic matter (e), and Fe extractable in oxalate (f), of the 100 soils collected in the study area and divided in the 12 classes. Red asterisks represent outliers.

In the representative 12 soils, total P values were over 800 mg kg^{-1} in high P soils, around 500-550 mg kg^{-1} in medium P soils, and below 420 mg kg^{-1} in low P soils, consistently with the soil grouping criteria (Table 2.2). Conversely, the 12 representative soils showed low and comparable values of total organic C, being on average 11.3±0.98 g kg^{-1}. The average value of oxalate-extractable Fe was 3.04±0.58 g kg^{-1}, with the lower values associated to higher sand content.

Table 2.3 Selected physicochemical properties of the 12 soils used to assess P availability to rice plants, divided in three groups based on their P content

	Soil ID	Total P (mg kg^{-1})	pH	Sand (g kg^{-1})	Organic C (g kg^{-1})	CEC ($cmol_{(+)}$ kg^{-1})	Fe_{ox} (g kg^{-1})
HIGH P	HP a	893	6.1	770	13	5.2	1.47
	HP b	899	5.8	250	20	22	6.53
	HP c	877	5.7	780	9	5.6	0.62
	HP d	810	5.9	570	10	7.4	4.7
MEDIUM P	MP a	549	6.4	840	10	7.6	0.74
	MP b	512	6.9	420	10	11	3.34
	MP c	541	7.9	290	10	15	3.41
	MP d	534	6.6	620	6	5.4	0.53
LOW P	LP a	420	6.5	440	12	9.4	5.63
	LP b	414	6.5	550	14	14	3.33
	LP c	377	5.6	330	12	5.2	4.1
	LP d	287	5.7	510	10	6	2.06

Soil available P assessment with different chemical methods

The amounts of P extracted by the different chemical methods were grouped and averaged based on the three total P levels, as reported in Figure 2.4. In all the cases, the amount of P extracted was well related to the total soil P supply, albeit differences between high and medium P soils were much higher than between medium and low P soils, and largely varied according to the extraction strength of each chemical method. On average, Olsen (29.5 ± 19.2 mg kg^{-1}) and anion exchanging resins (45.3 ± 38.2 mg kg^{-1}) resulted in lower values that the methods commonly used to determine Fe-associated P forms, which were respectively 222 ± 132 mg kg^{-1}, 331 ± 167 mg kg^{-1} in citrate-ascorbate and oxalate extractions. Not all the chemical methods resulted in the same statistical differences among soil P levels, as citrate-ascorbate and oxalate resulted in the best separation among the levels.

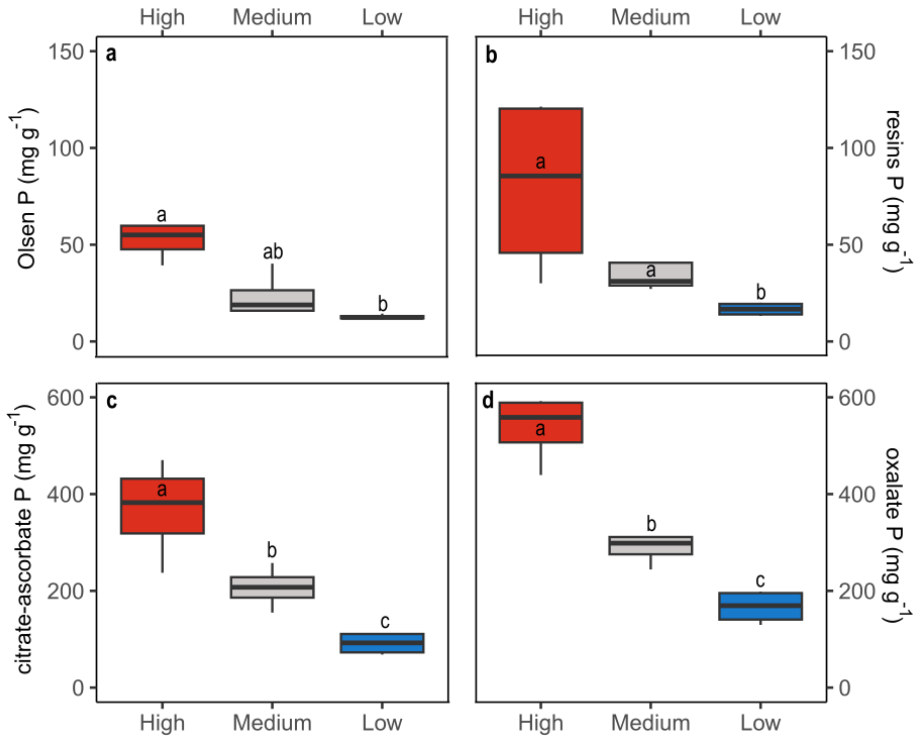

Figure 2.4 Average concentration of inorganic P extracted with Olsen (a), anion exchange resins (b), citrate-ascorbate (c), and oxalate (d), for each of the three soil P levels. Different letters represent significant differences among soil P levels. Note the different y axes between the first (a-b) and the second (c-d) row.

2.3.2 Kinetics of Fe(II), P, and DOC in porewater during plant development

In the soil-rice mesocosms, after the beginning of the submersion, soil redox potential passed from values well above +300 mV to nearly zero mV within one week, indicating the instauration of reducing conditions. The temporal trends in porewater Fe(II), and P were similar, but at different extent, for the three soil P levels over the plant growing period (Figure 2.5). Three major phases could be

identified: (i) a Fe(II), and P increase to the maximum values during the first 14 days, (ii) a decreasing phase within the subsequent 10 days, and (iii) a last time span characterized by a steady increase of Fe(II), and P. Additionally, the porewater P concentration during rice growth was first related to soil total P with higher mean values in high P soils with respect to medium and low P soils. The kinetics of P in porewaters followed a similar trend to that of Fe(II), with a more pronounced relationship in high than low P soils. After the initial peak at 14 DAS, a minimum concentration was reached in the subsequent 20 days, followed by a slight increase until a final concentration of 1.75 ± 0.77 mg L^{-1} in high P, 0.40± 0.39 mg L^{-1} in medium P and 0.12 ± 0.08 mg L^{-1} in low P soils.

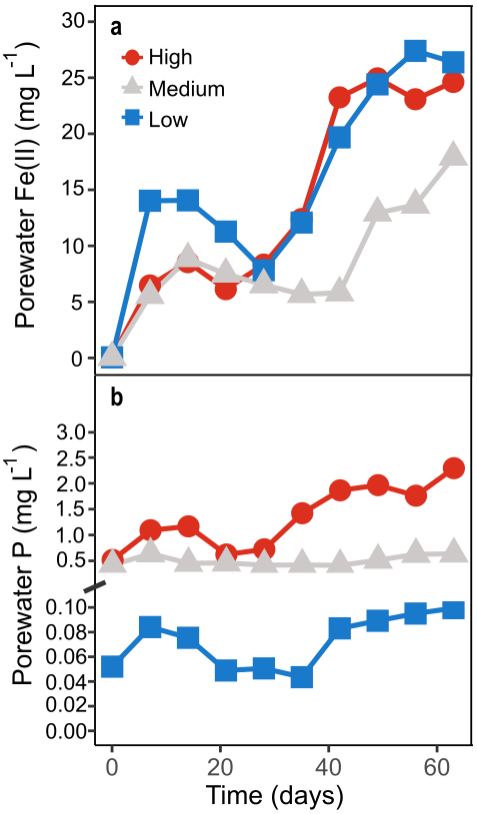

Figure 2.5 Average concentration of reduced iron [Fe(II)] (a), and phosphorus (b) in the porewater of three soil P levels in planted mesocosms. For the sake of graph readability SEs are not reported.

2.3.3 *Plant responses to soil P supply*

Plant biomass and elemental composition

Notwithstanding the similar total (shoot plus root) dry biomass of rice plants grown in soils with different P availability, significantly larger root biomass was observed in plants grown in low P soils ($p < 0.01$). All plants showed no significant differences in total C and N concentrations, whereas P concentrations in total biomass decreased in the order high P > medium P > low P (Table 2.4),

with a stronger effect in the roots than in the shoots. Plants grown in high P soils accumulated indeed two times more P than those grown in low P soils.

Table 2.4 Dry biomass, total carbon (C), phosphorus (P) and nitrogen (N) in total plant biomass, shoots and roots at 60 days after flooding (DAF). Each value represents the mean of four replicates (± SD). Different letters indicate significant differences among the three soil levels.

Treatment	Dry biomass (g)	Total C (mg g^{-1})	Total N (mg g^{-1})	Total P (mg g^{-1})	P content (mg)
Total					
High P	1.7 ± 0.5	366.8 ± 22.3	10.2 ± 1.8	3.29 ± 0.76 a	5.59 ± 0.38 a
Medium	1.7 ± 0.6	370.5 ± 19.9	9.2 ± 1.3	2.75 ± 0.38 ab	4.66 ± 0.23 ab
Low P	1.7 ± 0.6	349.2 ± 64.8	9.8 ± 2.6	2.32 ± 0.31 b	3.94 ± 0.19 b
Shoot					
High P	0.9 ± 0.3	378.8 ± 15.3	11.5 ± 2.6	3.42 ± 0.41 a	3.08 ± 0.12 a
Medium	1.1 ± 0.6	738.5 ± 15.3	10.2 ± 1.5	1.92 ± 1.85 b	2.11 ± 1.11 b
Low P	1.0 ± 0.3	387.5 ± 11.9	12.5 ± 2.8	2.22 ± 0.34 b	2.22 ± 0.10 b
Root					
High P	0.6 ± 0.3 b	353.9 ± 45.2	8.2±1.0	3.04 ± 1.35 a	1.82 ± 0.41 b
Medium	0.8 ± 0.3 b	361.7 ± 34.3	7.6 ± 1.2	1.99 ± 0.92 b	1.59 ± 0.28 b
Low P	1.9 ± 0.5 a	335.7 ± 52.2	7.6 ± 1.2	1.23 ± 0.22 c	2.34 ± 0.11 a

Plant responses to P-limiting conditions

When plant have reached a significant root development (20 DAF), the release of Fe(II) in the soil solution was different in mesocosms with plants compared to mesocosms without plants (Fig. 2.6). In all cases the Fe(II) porewater concentrations tended to be lower in planted mesocosm. Although in high-P soils the differences between planted and un-planted mesocosms were not significant, in medium and low P soil the Fe(II) porewater concentration was significantly higher in mesocosms without rice plants ($p < 0.05$). Particularly, in medium P soil the Fe(II) porewater concentration was doubled in un-planted mesocosms compared to the planted, and in low P soil the Fe(II) porewater concentration was three-time higher in the former compared to the mesocosm with rice development.

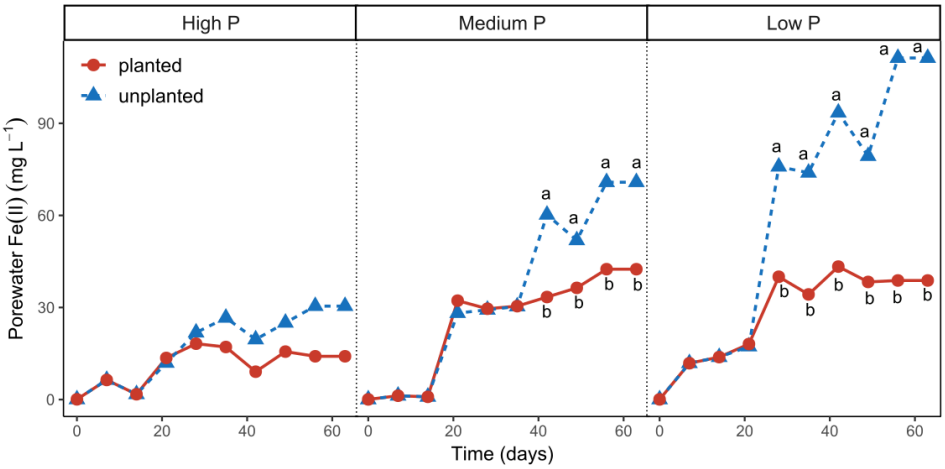

Figure 2.6 Average concentration of reduced iron [Fe(II)] in the porewater of planted and unplanted pots in high, medium and low P soil groups. Different letters represent significant differences between planted and unplanted pots in the same soil P level.

The genes encoding the root high affinity P transporters OsPt1 and OsPt8 were more expressed in plants grown in low than high P soils. The transcript abundance of the low affinity P transporters OsPt2 and OsPt6 was generally lower compared to OsPt1 and OsPt8, but an increase in gene expression of OsPt2 was observed in roots of plants grown in low P soils (Fig. 2.7).

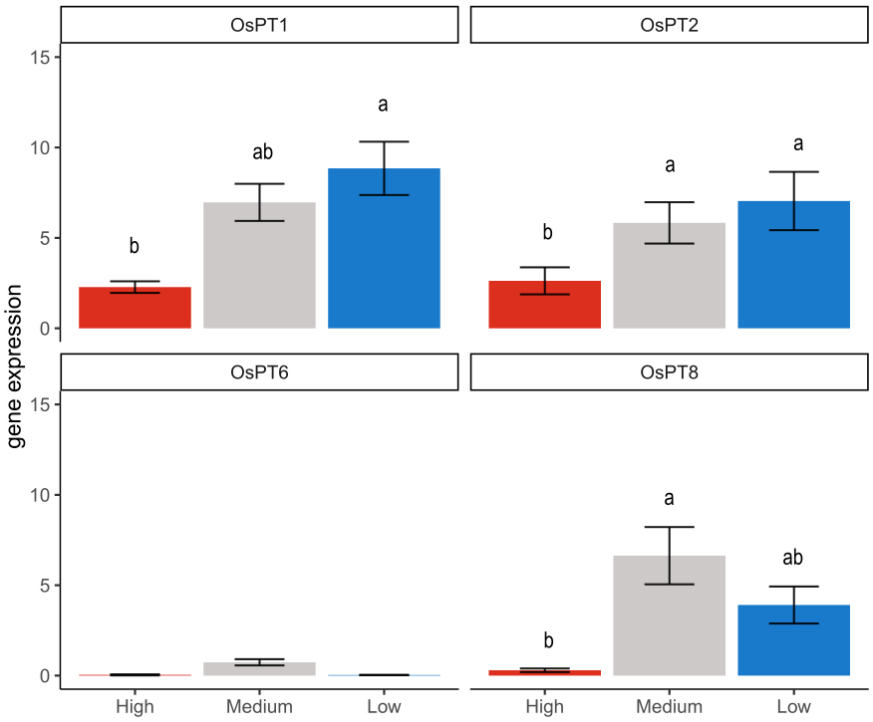

Figure 2.7 Average normalized gene expression values for high-affinity P root transportes OsPT1, OsPT8, and low-affinity P root transportes OsPT2 and OsPT6 of rice plants grown in soil with high, medium, and low P availability for 60 days. Different letters indicate significant differences among soil P levels.

The average activity of acid phosphatase (6.2 mM P s^{-1} g^{-1} root FW) was generally higher than that of phytase (0.18 mM P s^{-1} g^{-1} root FW) and, in the former, no significant differences were observed among plants grown at different soil P levels, while low P plants showed a slight increase in phytase activity.
The calculation of efficiency indexes resulted in plant phosphate acquisition efficiency (PAE) was 2-fold higher for plants grown in low P than in high P soils. Similarly, phosphorus utilization efficiency (PUE) and translocation efficiency (PTE) were greater in low P plants (PUE = 0.96; PTE =2.5) than medium and high P plants (PUE = 0.5; PTE = 1.4), which in contrast did not result in significant differences for all parameters.

2.3.4 Correlations between soil P forms and plant responses

In all the extracts, the resulted soil P positively correlated with plant P uptake (Fig. 2.8), however anion exchange resins resulted in the best performance followed by Olsen, oxalate and citrate-ascorbate respectively.
When discriminating between the three classes of soils, the correlation among P_{plant} and the P extracted by the different methods were different in low P soil compared to high and medium P. Particularly in the former the correlations were in all the cases weaker, and even negative in the case of Fe-associated P methods.

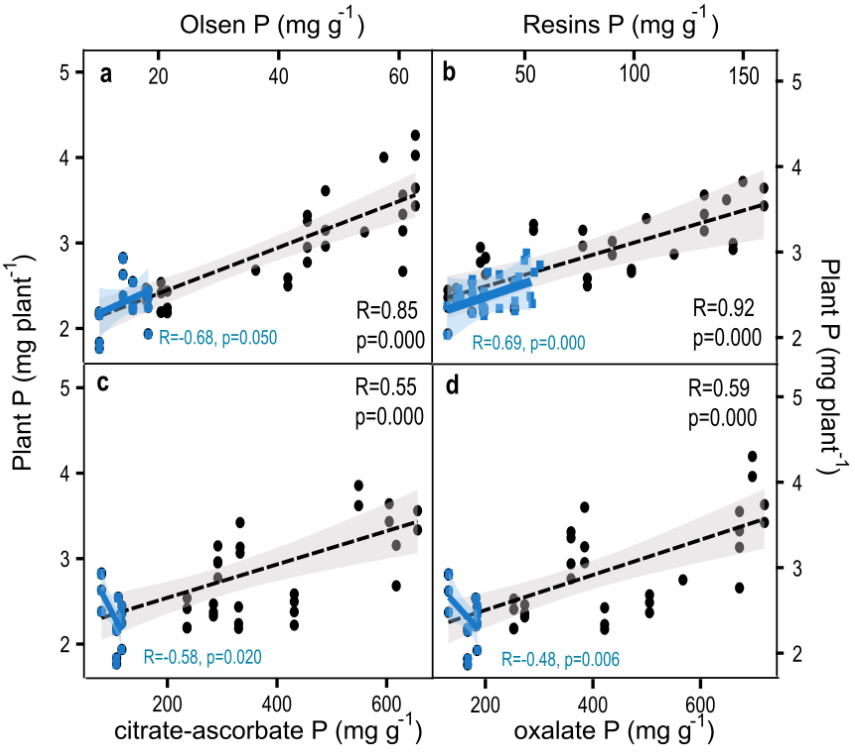

Figure 2.8 Correlation between soil P extracted by Olsen method (a), anion exchanging resins (b), citrate-ascorbate (c), and oxalate (d), and plant P uptake. Blue points and blue correlation lines represent the correlation between the same parameters in low P soils.

Regarding the plant strategies to overcome P limitation in soil, and particularly the expression of P root transporters encoding genes, within each class of affinity for phosphate (high and low), the transcripts positively correlated. In addition, OsPT8 and OsPT2 showed a positive correlation (Fig. 2.9). OsPT1, OsPT2 and OsPT8 positively correlated with the root biomass, PUE, PAE and PTE, while OsPT6 showed positive correlation only with PUE. Other positive correlations were found between the root biomass and PUE, whereas negative correlations existed between root biomass and P_{plant} and resin-extractable P, a further positive correlation was observed between phytase and P_{plant} (Fig. 2.9).

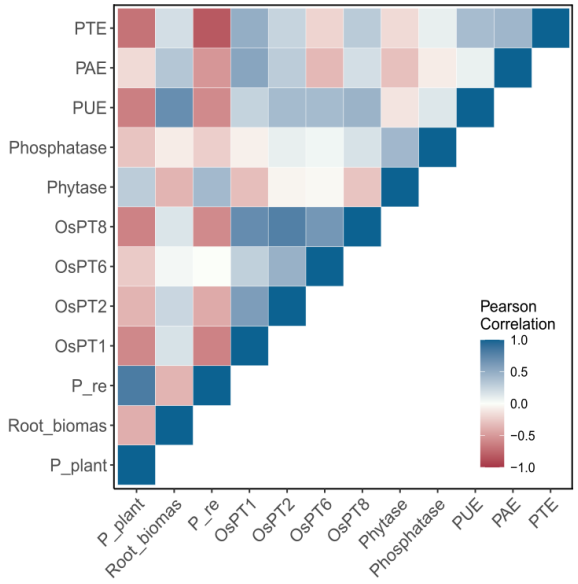

Figure 2.9 Correlation heatmap of the plant strategies to overcome P limitation represented by P root transporter encoding gene (OsPT1, OsPT2, OsPT6, OsPT8); enzymatic activity (phytase, phosphatase); root biomass; P use efficiency (PUE), P acquisition efficiency (PAE), and P translocation efficiency (PTE); P concentrations in plant tissues (P_plant), and P extracted by anion exchange resins (P_re).

2.4 Discussion

2.4.1 Desorbable P is the best related pool with rice uptake

Despite the effect of reductive dissolution on the release of the Fe-bound P into paddy soil porewaters is widely acknowledged (Ajmone-Marsan et al., 2006; Ponnamperuma, 1972a; Shahandeh et al., 1995a), the relationship between redox transformations of Fe (hydr)oxides and P availability for rice plants is still debated. Extraction methods involving the release of P from Fe minerals with citrate-ascorbate or oxalate have been proposed as alternative and more appropriate approaches for estimating the P supply capacity of paddy soils, than Olsen and anion exchanging resins. The reason is because the former methods mimic, to different extent, the effect of reductive dissolution of Fe mineral pools on P release in submerged paddies, particularly in highly weathered environments (De Mello et al., 1998; McDowell et al., 2008), whereas the latter methods

estimate P release into soil solution based exclusively on adsorption-desorption mechanisms (Moody et al., 2013). In our study, desorption methods solubilized lower amounts of P, as expected, but the differentiation among the three soil classes was poorly underlined. In contrast, the methods based on P release from Fe minerals extracted higher amounts of P with a clear differentiation between the three soil classes. The positive effect of reductive dissolution on P release in solution was further supported by the positive correlation between Fe(II) and P concentrations in the soil porewaters during the rice growth experiment under continuous soil flooding, which, however did not correspond to a parallel P uptake by plants. This was attributed to a temporal decoupling of P release during the reductive dissolution of Fe (hydr)oxides and plant P requirements. The temporal changes in porewater composition over time evidenced an increasing concentration of Fe(II) and P during the initial phase of plant growth (0-20 DAF) related to the rapid reductive dissolution of the Fe-minerals with the onset of anoxic conditions, driven by anaerobic Fe-reducing microorganisms (Wang et al., 2022; Wei et al., 2019; Zhang et al., 2003). Therefore, inorganic phosphate was readily released in solution in those soils rich in oxalate-extractable Fe, and total P. However, already after 10-20 DAF, the concentration of both porewater Fe(II) and P decreased, possibly for the coprecipitation and P re-adsorption onto less reducible or newly formed mineral active surfaces (Santoro et al., 2019; Wang et al., 2017). These processes have been related to an increase in soil P sorption capacity after soil flooding (Refait et al., 2007; Zhang et al., 2003), thus the subsequent re-adsorption of the P released during the first phase by the formation of Fe-phosphate precipitates (Santoro et al., 2019) would explain the decrease in plant available P during the second higher nutrient-demanding phase. Although we have no direct evidence of the formation of these Fe-P associations, their occurrence could explain both the time course of P and Fe(II) in solution, and the weak estimate of available P offered by citrate-ascorbate and oxalate. Indeed, the increasing demand for available P by the plants after the depletion of seed reserves at about 20 DAS (Wissuwa 2003) could have coincided with the decrease in porewater-P at later stages of plant development. Thus, the initial P release from Fe-minerals under anoxic conditions could be temporally decoupled from the increasing plant P demand, suggesting that other interacting mechanisms could be involved in driving rice P nutrition in paddy soils, possibly with even greater importance. Besides the progressive slowing down of P uptake in the final stages of the plant growing cycle, the late steady-increasing phase of porewater P could be enhanced by the boosting effect of C compounds released after the reductive dissolution (Sodano et al., 2017), which likely act as electron donors to Fe-reducing microorganisms (Scalenghe et al., 2002) and as competitors for the same sorption sites of P, thus replenishing the soil solution after P depletion (McDowell et al., 2008; Moody et al., 2013). This may further explain the more effective estimation of P availability offered by anion exchanging resins, which act as a P-sink.

2.4.2 Plant responses to P deficient soil conditions

The correlation patterns between estimated soil P availability and plant P uptake were different when P was limitedly available. Particularly, the weaker correlations which characterized the low P soils could indicate that the mechanisms underpinning P release into solution and subsequent plant P uptake likely differ as a function of soil P content, since rice plants may adopt specific strategies to cope with P limitation by accessing less readily available pools (Rose et al., 2013a). A first evident effect was the manipulation of rhizosphere redox conditions, indeed although no significant differences were observed among the soil P groups in terms of poorly crystalline Fe content, the low P soils showed a slightly lower Fe(II) concentration in porewater during the last phases of plant development. Furthermore, the significantly lower porewater Fe(II) concentration observed with plants than without suggests a higher degree of Fe oxidation driven by plants, particularly in low P soils and attributed to a larger radial oxygen loss. This process has been reported to be more expressed under low P availability (Fu et al., 2014a; Kirk and Van Du, 1997a) and involves a higher oxidation potential in the rhizosphere compared to the anaerobic bulk soil (Zhang et al., 2004a), likely shaping the redox gradient governing P dynamics in the root surrounding. Rhizosphere oxygenation may contribute to counteract the formation of green-rust like Fe-P coprecipitates that can limit P availability under persisting anaerobic conditions (Huang et al., 2022; Zhang et al., 2004a). It has been demonstrated that anaerobic conditions may limit the rate of P release from green rust-P complexes because the high Fe(II)/Fe(III) ratio which characterizes these minerals retards their transformation to Fe(III) (hydr)oxides with lower P retention capacity (Huang et al., 2022). Conversely, under oxidative conditions, the evolution of green rust-P complexes to Fe(III) (hydr)oxides prompts the release of P (Fang et al., 2021; Huang et al., 2022), thus possibly offering a further explanation for the increase in P porewater concentration observed in the last plant development stage (40-60 DAS). The observation that P release from the Fe (hydr)oxides newly formed under oxidative conditions after the transformation of green rust-like materials is governed by anion-exchange mechanisms (Huang et al., 2022) could further corroborate the effectiveness of anion exchanging resins in predicting P availability to rice plants.

Other observed differences involved P uptake and translocation capacity. In our study, P concentration in rice shoots was comparable between medium and low P soils, possibly due to the higher PTE of plants grown in these soils, especially in low P compared to high P soils. In support of this, the gene encoding OsPT8, which has a major role in P translocation, was up-regulated in plants of low and medium P soils. Furthermore, the total biomass produced by rice plants was similar across different soils classes, but plants grown in low P soils had a higher root-to-shoot ratio as a consequence of the larger root biomass, which indicated a differential allocation of C resources to this organ to promote its growth and mining activity (Lynch and Brown, 2008). The trend of PTE was the same as that of PUE, this latter primarily dictated by the regulation of genes encoding P root transporters. We found that the lower the soil P supply, the higher the induction of P transporters that aim to increase plant P uptake. More specifically, the high

affinity P transporter principally involved in the primary P uptake, OsPT1 (Rose et al., 2013), was most expressed in roots of plants grown in low P soils. In the same plants, the transcription of OsPT2 was also increased. OsPT2 is a root low-affinity Pi transporter that mediates the translocation of the stored P in the plant, therefore playing a critical role in the initial stage of plant development for P acquisition (Julia et al., 2018; Rose et al., 2013a). The parallel increase of OsPT1, OsPT2 and OsPT8 transcription suggests a coordination in the response of rice plants to P limitation in terms of acquisition, usage and translocation. The transporter OsPT6, which is reported to have a role in P translocation as OsPT8 (Julia et al. 2018), was however substantially less expressed in plants, regardless of P available in soil. Thus, a minor role in P translocation for OsPT6 can be hypothesized in rice plants under the experimental conditions used in this study.

2.5 Conclusions

The results (Fig. 2.10) point out that combined multifaceted effects contribute to rice P nutrition besides P release from Fe minerals, which might not be the only nor the most relevant mechanism, probably because of the asynchrony between P release into soil solution and plant requirements. Additionally, in moderately weathered soils, where the dominance of Fe minerals on soil chemical properties is not so much expressed as in highly weathered tropical environments, plant responses to P limitations can effectively enhance P uptake. In particular, the capacity of rice root to oxygenate the rhizospheric environment could boost the release of P after its temporary solubility decline. The different P utilization efficiency measured in low P compared to high P soils further confirmed the interplay between plant strategies and soil P pools. The increased root development and up-regulation of phosphate root transporters encoding genes contribute to P uptake in the complex environment of rice paddies.

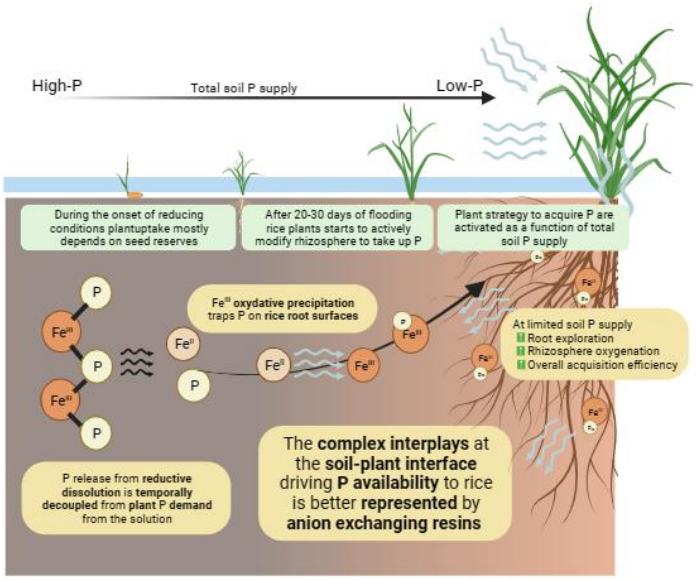

Figure 2.10 Comprehensive conceptual model of the results discussed in Chapter 2.

CHAPTER 3

Influence of P availability on Fe plaque formation and implications for rice P uptake

3.1 Introduction

Although paddy soils are generally characterized by a higher solution P concentration compared to aerobic soils, this does not necessarily result in a higher plant P uptake, as described in the previous chapter. Indeed, the P released by Fe (oxyhydr)oxides reductive dissolution is only partially available to plant uptake, as a consequence of the complex interplays among plant responses to flooding conditions and soil biogeochemical processes. Indeed, the P released after reductive dissolution can be involved in the oxidative precipitation of the aqueous Fe(II), following the reaction with plant ROL, forming a solid Fe(III) coating on the root surfaces, generally referred to as Fe plaque (Khan et al., 2016a). These surfaces show chemical and physical properties similar to those of pedogenic Fe (hydr)oxides present in soil, and therefore have a high capacity to retain various anions in the soil solution, including P (Amaral et al., 2017; Hansel et al., 2001; Seyfferth et al., 2010; Zhang et al., 1999).

The role of Fe plaque in controlling P plant uptake remains controversial (Khan et al., 2016), as previous studies have reported its role as both a barrier/sink (Liang et al., 2006) and a source of plant available P (Zhang et al., 1999). These contrasting observations probably arise from studies overlooking the varying responses of rice plants to different P availabilities, and/or neglecting the interaction between the temporal dynamics in Fe plaque formation/dissolution and plant P acquisition strategies. The dynamics affecting P retention on Fe plaque minerals can be confounded by the ability of rice plants to alter the rhizosphere environment in response to nutrient deficiency (Zhang et al., 2004). Indeed, the increased root development observed under low P availability is related to an increase in root aerenchyma formation to reduce the metabolic cost of this adaptation mechanism (Kirk and Van Du, 1997; Lynch and Brown, 2008), thus increasing the rhizosphere oxygenation capacity (Fu et al., 2014).

Notwithstanding the positive relationship between Fe(III) oxidative precipitation and higher plant O_2 release in the rhizosphere (Wu et al., 2012), the effects of root modifications in response to P availability on Fe plaque formation and the implications for P acquisition in rice plants are however still largely debated. Some studies have observed an increase in Fe plaque formation under low P availability (Jiaofeng et al., 2022; Liang et al., 2006), but mechanisms underlying this phenomenon are not yet clear. Fu et al. (2014) argued that this increase may be due to enhanced ROL. Kirk and Van Du (1997) suggested that it may be related to an increase in root volume, as they did not find a significant difference in O_2 release per unit of root volume. Moreover, it remains unclear whether the high affinity of Fe plaque minerals for P combined with the higher amounts of root-associated Fe might emphasize their role as P sink under P limiting conditions, thereby hindering plant growth by impeding P acquisition.

Nonetheless, rice plants growing under P limited conditions have been reported to activate strategies to access mineral-bound P forms through different rhizospheric mechanisms (Hoffland et al., 2006; Kirk and Van Du, 1997; Rose et al., 2013). Specifically, the exudation of protons (H^+) and low molecular weight organic acids (LMWOAs) from roots may promote the release of sparingly available soil P forms, such as P retained by metal oxides (Hinsinger, 2001; Hoffland et al., 2006; Bhattacharyya et al., 2013; Santoro et al., 2022). Unlike other plant species that rely on organic acids to solubilize P by competing for adsorption sites (Bhattacharyya et al., 2013; Hoffland et al., 2006), proton exudation by rice plants is considered as the primary mechanism by which these lowland plants release P from Fe minerals in response to P deficiency, especially considering their relatively low rates of organic acid exudation (Mori et al., 2016). Given the similarity between Fe plaque and Fe oxides present in soil (Amaral et al., 2017; Hansel et al., 2001; Seyfferth et al., 2010), these strategies could be also effective in enhancing the uptake of P associated with Fe plaque, thereby converting this P pool from a P sink into a P source for the plant. The role of Fe plaque to serve as a sink or a source of available P and consequently regulate plant P uptake could therefore be viewed as a dynamic process influenced by the rates of both Fe plaque formation and dissolution as a function of P availability, although evidence remains lacking.

Based on these considerations, it can be hypothesized that the response of rice plants to P deficiency could (i) induce a greater formation of root-associated Fe plaque as a result of an enhanced root development and ROL, but at the same time (ii) favor Fe plaque dissolution (and the release of plaque-associated P) through increased proton exudation, thereby promoting P uptake. As such, it is therefore further hypothesized that (iii) the capability of Fe plaque to serve as either a P sink or a source of plant available P will be strongly influenced by the dynamic nature of this Fe pool, which is dependent on P availability (i.e., P source under low P availability vs. P sink under high P availability). To test these hypotheses rice plants were grown in a hydroponic system under P-sufficient or P-deficient conditions. Plants were exposed to multiple Fe-plaque induction periods and analyzed for differences in root traits, changes in the rates of Fe plaque formation and contents, and net proton exudation, and differences in P uptake over a 62-d growth period.

3.2 Material and methods

3.2.1 Plants cultivation and Fe plaque formation

To investigate the impact of P availability on the formation and evolution of Fe plaque in rice (cv. Selenio) and, consequently, on P uptake by rice, a hydroponic experiment was performed using a factorial design in which plants were grown under either P-deficient (–P) or P-sufficient (+P) conditions for 62 days. During this period, half of the plants for each treatment were exposed to Fe plaque forming conditions (+Fe) while the other half served as a control group without Fe plaque induction (–Fe). In detail, rice seeds were surface sterilized with H_2O_2 for 10 min, rinsed thoroughly with distilled water and germinated for three days in the dark at 20°C. Afterwards, a total of sixteen seedlings of uniform size per

treatment were transferred to plastic pots containing half-strength modified Yoshida solution (Yoshida, 1967) for the first two weeks and then shifted to full strength nutrient solution (day 0), that was replaced every 4 days. The modified Yoshida solution had the following macronutrients composition (mM): NH_4NO_3, 1.43; K_2SO_4, 0.51; $CaCl_2$, 1.0; $MgSO_4$, 1.65; and micronutrients composition (μM): $MnCl_2$, 9.1; $(NH_4)_6Mo_7O_{24}\cdot 2H_2O$, 0.52; H_3BO_3, 18.5; $ZnSO_4\cdot 7H_2O$, 0.15; $CuSO_4\cdot 5H_2O$, 0.16 and $FeCl_3$(EDTA), 35.8. The nutrient solution used for plants grown under P-deficient conditions contained 10 μM NaH_2PO_4, while that for plants grown under P-sufficient conditions contained 100 μM NaH_2PO_4. The pH of the solution was adjusted to 6.0 by using diluted HCl or NaOH.

Fe plaque induction was carried out twice during the growth period. On the 30th and 45th days after seeding (DAS), half of the plants for each P treatment were removed from the nutrient solution, and their roots were rinsed in deionised water and subsequently transferred to a 0.9 mM (as $FeCl_2\cdot 7H_2O$) solution buffered at pH 5.5 (15 mM 2-(*N*-morpholino)ethanesulfonic acid). Fe plaque induction was carried out in deionized water to avoid any possible formation of Fe precipitates with other elements present in the nutrient solution (Liang et al., 2006; Zhang et al., 1999). Fe plaque on the root surfaces was allowed to form for 48 h. The plants were then transferred back to their respective P-deficient or P-sufficient nutrient solutions, as described above (i.e., +P +Fe and –P +Fe treatments). Plants not exposed to Fe plaque induction (i.e. +P –Fe and –P –Fe treatments) were treated in the same way, by replacing the ferrous solution with deionized water. To limit the oxidation of Fe(II) by external sources of O_2 other than ROL during Fe plaque induction, the Fe(II) solution was previously flushed with N_2 and, after plant root insertion, the containers were wrapped in foil and their mouths sealed with parafilm around the shoots to limit O_2 diffusion. Separate containers with the Fe(II) solution but without plants were also included to account for any possible oxidation of Fe(II) not induced by ROL. The Fe(II) concentration in all the treatment was constantly monitored during the 48 h induction; more detailed information are reported in Section 3.2.2. A graphical summary of the experimental set-up and of the measurements conducted is provided in Fig. 3.1, together with a picture of P-sufficient and P-deficient rice plants after Fe plaque induction.

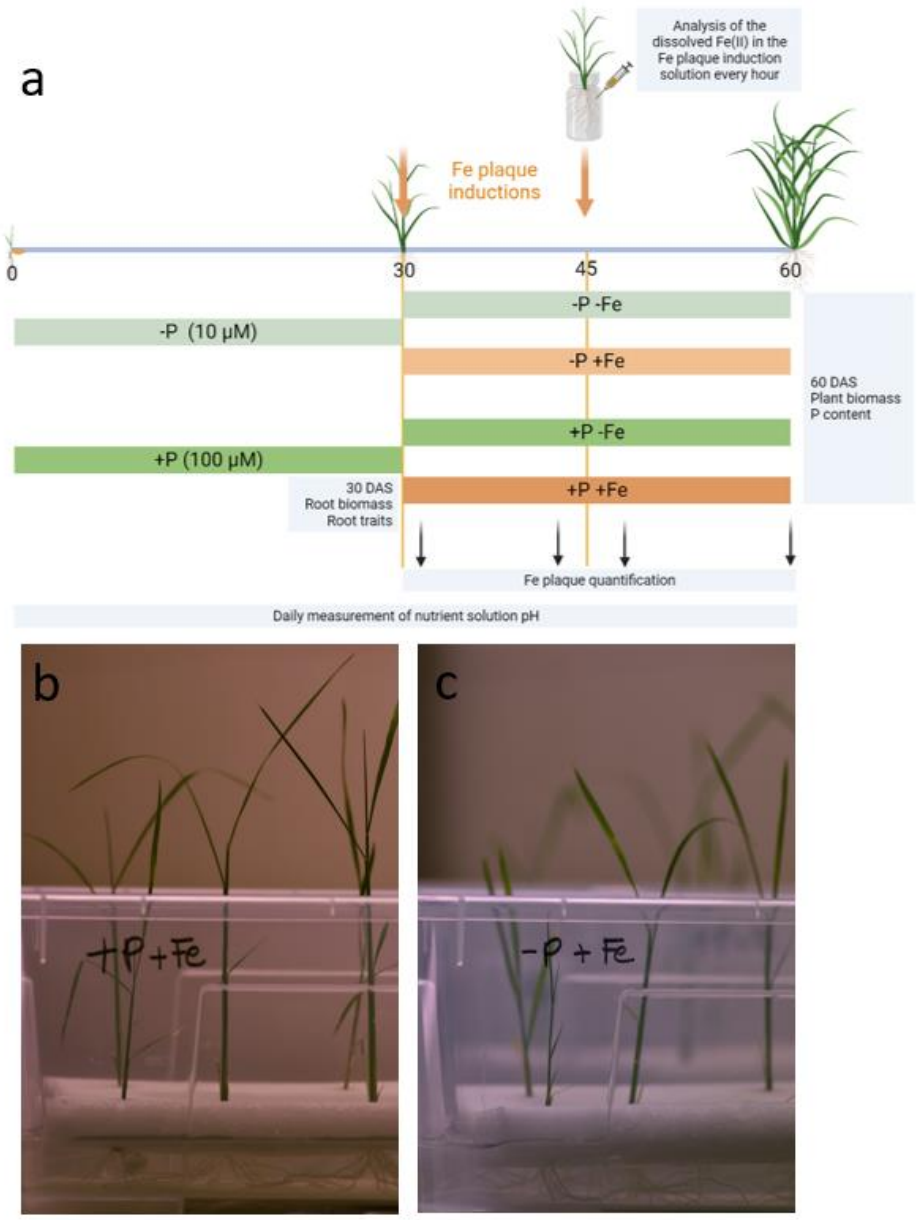

Figure 3.1 a) graphical summary of the experimental set-up and of the conducted measurements on plants and nutrient solution (figure created with BioRender.com), b) picture of phosphorus sufficient plants with iron plaque (+P+Fe), and c) picture of phosphorus limited plants with iron plaque (-P+Fe) after 45 days of hydroponic cultivation.

3.2.2 Plant analysis

Plant samples were collected (four replicates for each treatment) at four different time points throughout the experiment. They were first sampled at 30 DAS in correspondence with the first Fe plaque induction period, then before (45 DAS) and after (48 DAS) the second Fe plaque induction period. The final plants were collected at 62 DAS. Plants that were sampled at 30 DAS were used to evaluate the impact of P availability on root development and morphology. In addition to determining root biomass, three plants from each treatment were imaged using a Nikon D3500 digital camera. Root traits including total root length (cm), surface area (cm^2), total root volume (cm^3), and number of root tips were quantified using saRIA software (Narisetti et al., 2019). The root density (mg cm^{-3}) was estimated as the ratio between the root biomass and the root volume. The development of root aerenchyma was assessed qualitatively on three roots per plant after sectioning 3 cm from the root tip and examined under a light microscope (Leitz Dialux 20 EB) with a 24 MP digital camera (Nikon D3500). At 62 DAS, plants were collected to evaluate the final dry biomass (shoot + root) and P contents in all plant parts. The P concentration in root and shoot tissues was determined on dry plant material (50 mg) after sulfuric-perchloric digestion and colorimetric quantification of P in the extracts using the malachite green method (Ohno and Zibilske, 1991b). To evaluate the changes in Fe plaque contents during the growth period as a function of P availability, all root samples collected before and/or after Fe plaque induction were analyzed for root-associated Fe. For each plant, the entire root system was first rinsed with deionized water and subsequently extracted with 0.1 M acidic ammonium oxalate (Hossain et al., 2009). Fe concentration in the extracts was quantified by atomic absorption spectroscopy (AAS, PerkinElmer AAnalyst 400, Norwalk, CT, USA).

3.2.3 Rate of Fe plaque formation and net proton release

The rate of Fe(II) oxidation for the P-sufficient +Fe and P-deficient +Fe treatments during the second induction period (45 DAS) was determined on four independent replicates for each treatment. During the 48 h-induction period, small aliquots of the ferrous Fe solution were sampled every hour and the residual dissolved Fe(II) concentrations were quantified spectrophotometrically, immediately after sampling using the 1,10-phenanthroline method (Loeppert and Inskeep, 1996). The decrease in the concentration of Fe(II) in the solution over time was related to the kinetics of Fe(II) oxidation that served as a proxy for the rate of Fe plaque formation by ROL, after accounting for the minimal Fe(II) oxidation in the absence of plants and assuming that plant uptake of dissolved Fe over this short period was negligible. Moreover, it was ensured that the precipitation of Fe minerals occurred only on the root surfaces as the solution remained clear and no precipitation of Fe (oxyhydr)oxides was observed on the container walls during the Fe plaque induction period. Under these experimental conditions, the rate of Fe(II) oxidation by O_2 continuously released from the roots and at constant pH was described by a pseudo-first order rate expression with respect to Fe(II) according to the equation

$$[\mathrm{Fe(II)}]_t = [Fe(II)]_0 \cdot e^{-kt}$$

Where $[Fe(II)]_t$ and $[Fe(II)]_0$ where the concentrations of Fe(II) at time *t* and at the beginning of the induction period, respectively, while *k* was the pseudo-first order rate constant (in h^{-1}). Since we expected P availability to influence other root traits (including root surface area) in addition to ROL, the cumulative amount of Fe(III) precipitated on the root surfaces (in mmol Fe) over the first hours of Fe plaque induction, calculated as the difference between $[Fe(II)]_0$ and $[Fe(II)]_t$ was normalized on the basis of root surface area (mmol Fe m^{-2}) and plotted against time, as proposed by Kirk and Van Du (1997). Similarly, rate constants were also normalized for root surface area for comparison between treatments.

To quantify the capacity of rice roots to exude protons as a function of the different treatments, the pH of the growth solutions was monitored every 24 h in the 3 days preceding and succeeding each Fe induction event, by means of a pH-sensitive electrode (inoLab pH 7110, WTW GmbH, Weilheim, Germany). The net H^+ release (mM) over time was calculated from the decrease in pH with respect to the initial pH of the growth solution.

3.2.4 Statistical analysis

The statistical analyses were performed using the R version 4.1.1. Normality and data homoscedasticity were checked with Shapiro-Wilk and Levene tests, respectively. When necessary, data were transformed according to the data distribution. All the variables were tested for the analysis of variance (two-way ANOVA), followed by pair-wise post hoc analyses (Student-Newman-Keuls test) to determine the difference among the mean value at $p < 0.05$. The ggplot2 package was used to plot all the figures.

3.3 Results

3.3.1 Plant growth, root traits and elemental composition

The root dry biomass measured at 30 DAS (Table 3.1) did not show significant differences between P-deficient and P-sufficient plants. However, the root traits were strongly influenced by P treatment ($p < 0.001$), with P-deficient plants showing a 2 to 3-fold higher root volume, surface area, total length, and number of root tips compared to P-sufficient plants (Table 3.1).

Table 3.1 Root dry biomass and root traits after 30 days of growing in P-sufficient (+P) and P-deficient (–P) nutrient solution. Each value represents the mean of four replicates (± SE). Different letters indicate significant differences between treatments ($p < 0.01$).

Treatment	Dry biomass	Volume	Density	Surface area	Total length	Root tips
	mg $plant^{-1}$	cm^3 $plant^{-1}$	mg cm^{-3}	cm^2 $plant^{-1}$	cm $plant^{-1}$	$plant^{-1}$
+ P	20.1 ± 5.0	8.3 ± 2.4 b	2.4 ± 0.3 a	172 ± 56 b	296 ± 23 b	7.8 ± 3.9 b
– P	25.8 ± 4.4	24.3 ± 3.2 a	1.1 ± 0.0 b	432 ± 51 a	632 ± 24 a	13 ± 6.2 a

The root density was lower in the P-deficient plants, which is consistent with the higher development of aerenchyma as evidenced through the microscopic observation of the root sections (Fig. 3.2).

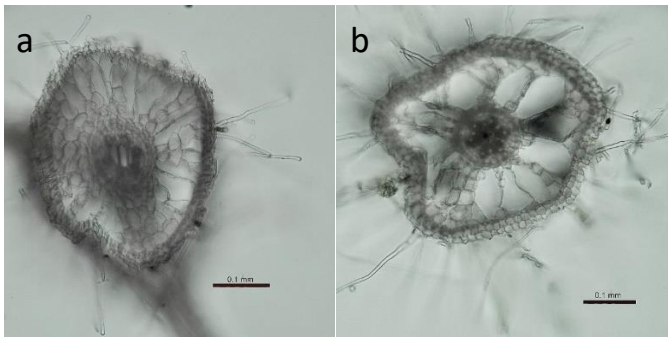

Figure 3.2 Root sections of representative rice plants grown for 30 days in P-sufficient (a) and P-deficient (b) nutrient solutions. Scale bar is 0.1 mm.

Similarly, at the end of the growing period (62 DAS), the differences observed in the total dry biomass, were mainly attributed to differences in shoot biomass, as the root biomass was unaffected by both P and Fe treatments (Table 3.2). The shoot biomass at 62 DAS was highly dependent on P treatment ($p < 0.01$), Fe treatment ($p < 0.01$) and their interaction ($p < 0.05$; Table 3.2). Although P-sufficient plants showed a higher shoot biomass than P-deficient plants in the absence of Fe plaque, shoot growth in the former was strongly hindered when Fe plaque (P-sufficient +Fe) was present, compared to plants grown without Fe plaque (P-sufficient–Fe). On the other hand, no significant differences were observed in P-depleted plants with or without Fe plaque (P-deficient +Fe vs. P-deficient –Fe; Table 3.2). These effects on plant growth resulted in significant differences on the root-to-shoot ratio (R/S), based on P treatment ($p < 0.05$), Fe treatment ($p < 0.05$) and their interaction ($p < 0.05$; Table 3.2). Particularly, P-sufficient plants showed a lower R/S ratio compared to P-deficient plants, and in the latter a decrease R/S in absence of Fe plaque was observed. Conversely, P-sufficient plants did not result in significant alteration of R/S when Fe plaque was induced, but the average R/S ratio was close to P-deficient plants with Fe plaque (Table 3.2).

Table 3.2 Effect of P treatment and Fe plaque induction on root, shoot and total dry biomass, and root-to-shoot ratio (R/S) of P-sufficient (+P) and P-deficient (–P) plants in the presence (+Fe) or absence (–Fe) of Fe plaque, after 62 DAS. Each value represents the mean of four replicates (±SE). Lower-case letters indicate significant differences between Fe treatment within the same P treatment ($p < 0.01$), and upper-case letters indicate significant differences between P treatment within the same Fe treatment ($p < 0.01$)

Treatments		Total DW (g^{-1} plant)	Shoot DW (g^{-1} plant)	Root DW (g^{-1} plant)	R/S
+ P					
	+ Fe	0.72 ± 0.12 b A	0.54 ± 0.08 b A	0.19 ± 0.06	0.35 ± 0.09 a B
	– Fe	1.51 ± 0.03 a A	1.18 ± 0.04 a A	0.33 ± 0.01	0.28 ± 0.01 a B
– P					
	+ Fe	0.53 ± 0.10 a B	0.41 ± 0.01 a B	0.15 ± 0.03	0.38 ± 0.09 a A
	– Fe	0.60 ± 0.11 a B	0.39 ± 0.06 a B	0.20 ± 0.04	0.50 ± 0.02 b A

The root P concentration and total root P content were higher in P-sufficient compared to P-deficient plants ($p < 0.05$), whereas the presence or absence of Fe plaque did not cause any significant differences in root P within the P treatments (Fig. 3.3). Conversely, both shoot P concentration and content showed a significant dependence on the P treatment ($p < 0.001$ and $p < 0.01$, respectively), Fe treatment ($p < 0.01$ and $p < 0.001$, respectively), and their interaction ($p < 0.05$ and $p < 0.001$, respectively). In all cases, P-sufficient plants accumulated more P in the shoot than P-deficient plants (Fig. 3.3). However, whereas under P-sufficient conditions the presence of Fe plaque on the roots strongly limited P uptake in comparison to plants without Fe plaque, the opposite was evident for plants grown under P-deficiency (Fig. 3.3). Consistently with shoot P accumulation, the difference in total P uptake between plants grown under P-sufficient and P-deficient conditions was much more evident in the absence rather than in the presence of Fe plaque (Fig. 3.3; $p < 0.001$).

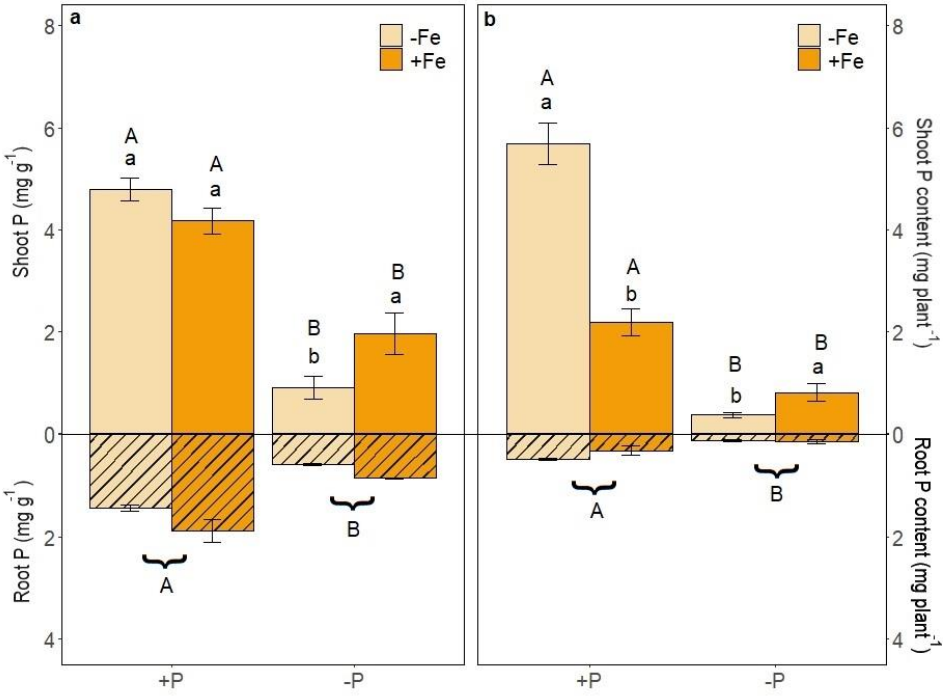

Figure 3.3 P concentrations (a) and contents (b) in the roots and shoots of rice plants grown under P-sufficient (+P) and P-deficient (–P) conditions, in the presence (+Fe) or absence (–Fe) of Fe plaque at 62 DAS. Each value represents the mean of four replicates (±SE). Lowercase letters above bars indicate significant differences between Fe treatment within the same P treatment ($p < 0.01$), uppercase letters above bars indicate significant differences between P treatment within the same Fe treatment ($p < 0.01$). Uppercase letters with brackets represent significant differences between P treatments when no interaction with Fe treatment was observed ($p < 0.05$).

3.3.2 Fe plaque formation and dissolution

The rate of Fe(II) oxidation during Fe plaque induction followed pseudo-first order kinetics with respect to Fe(II). Notably, the rate of Fe(II) oxidation was considerably faster in the presence of plant roots grown under P-deficient conditions and the rate constant (k) was 8 times higher than that observed in the presence of P-sufficient plants (Fig. 3.4a; Table 3.3). Although P-deficient plants had a significantly larger total root surface area (Table 3.1), they still displayed a faster rate of Fe plaque formation when the cumulative amount of Fe(III) precipitated on the root surface was normalized to root surface area (Fig. 3.4b).

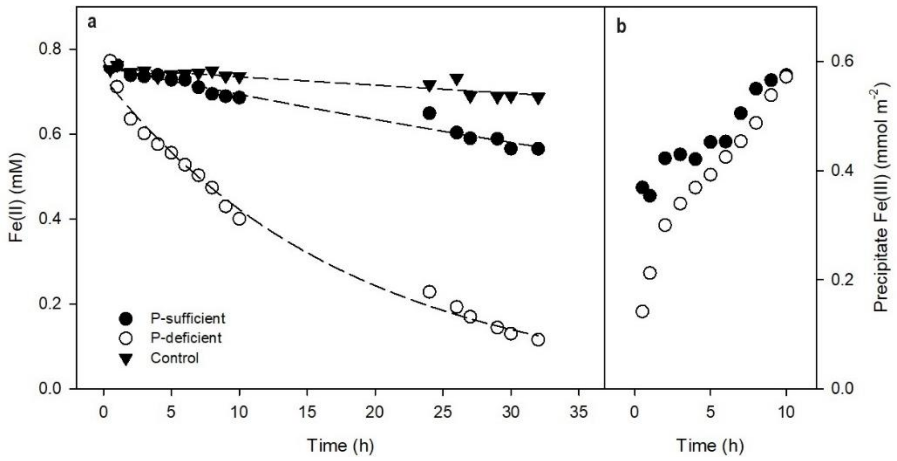

Figure 3.4 Fe(II) oxidation kinetics during the 48 h Fe plaque induction period approximated by a pseudo-first order reaction for plants grown for 45 d under P-sufficient (+P) and P-deficient (–P) conditions, as well as for the control without plants (a), and the amount of precipitated Fe(III) with time over the first 10 h of Fe plaque induction normalized per unit root surface area (b). Values represent the mean of measurements on four independent replicates per treatment. For the sake of graph readability, SEs are not reported.

Similarly, surface area-normalized rate constants were 2.5 times faster for P-deficient with respect to P-sufficient plants (Table 3.3). Although initially P-sufficient plants showed higher amounts of precipitated Fe per unit root surface area compared to P-deficient plants, the differences were merely transient and soon reached similar values within 5 h of Fe plaque induction (Fig. 3.4b).

Table 3.3 Pseudo-first order rate constants (k) and root surface area normalized rate constants (k') for Fe precipitation kinetics during the Fe plaque induction period as a function of P availability (curves are reported in Figure 3). Data represent the means (±SE) of measurements on three independent replicates per treatment, different letters indicate significant differences between treatments ($p \leq 0.05$).

P treatment	k (h^{-1})	R^2	P	k' (h^{-1} m^{-2})
+ P	0.009 ± 0.001 b	0.9716	< 0.0001	0.518 b
– P	0.055 ± 0.002 a	0.9926	< 0.0001	1.280 a
Control	0.003 ± 0.001 b	0.8437	< 0.0001	–

The amount of Fe plaque formed after the first Fe plaque induction period (on 30 DAS) was slightly higher for P-deficient than P-sufficient plants (Fig. 3.5). However, by 45 DAS most of the Fe plaque was redissolved for both treatments, even though P-deficient plants still showed significantly lower root-associated Fe concentrations than P-sufficient plants. After the second Fe plaque induction period (on 48 DAS), the quantity of root-associated Fe was significantly higher in P-deficient compared to P-sufficient plants (in line with the faster rate of Fe(II) oxidation). Over the following 15 d, the amount of Fe plaque on P-sufficient plants remained relatively unchanged, while in P-deficient plants, a substantial dissolution of Fe plaque occurred, resulting in no significant differences in Fe plaque contents between the two P treatments by 62 DAS. In all cases, no root-associated Fe plaque was detected in control roots of both P-deficient –Fe and P-sufficient –Fe plants.

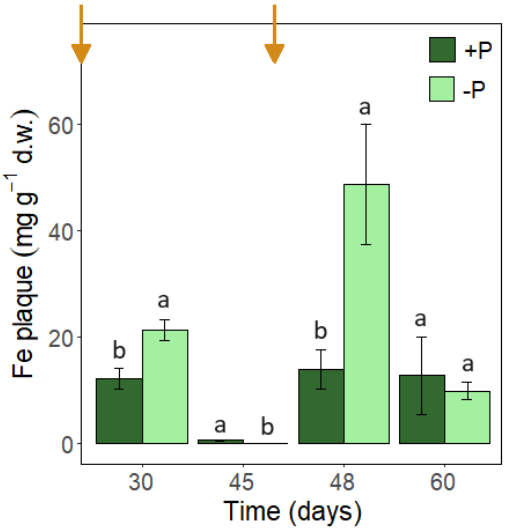

Figure 3.5 Changes in the Fe plaque content over time in P-sufficient (+P) and P-deficient (–P) plants over the growth period (root analysis carried out on 30, 45, 48 and 62 DAS). Yellow arrows in the top bar of the figure indicate the timing of Fe plaque induction. Oxalate-extractable Fe in –Fe control plants were under the detection limits and not included. Values represents the mean of four replicates (±SE). Different letters above bars indicate significant differences between treatment ($p < 0.05$).

3.3.3 Net proton release

The net proton release by rice plants over time differed as a function of P availability, presence of Fe plaque as well as the plant growth stage (Fig. 3.6). In the 72 h before the first Fe plaque induction period, the net proton release was only influenced by the P treatment ($p < 0.001$), as no Fe treatment was yet applied. In particular, P-deficient plants showed significantly higher rates of H^+ exudation than P-sufficient plants throughout the monitoring period (Fig. 3.6a). After the first Fe plaque induction period, the kinetics of net H^+ release was influenced by the combined effects of both P and Fe treatments ($p < 0.001$). In the absence of Fe plaque, P-deficient plants continued to exhibit higher values of H^+ exudation than P-sufficient plants, with rates very similar to those observed earlier. On the other hand, net H^+ release in solution in the presence of Fe plaque on the root surface, which was only observed after 48 h from induction, was not significantly different between P-sufficient and P-deficient plants. Moreover, the rates of H^+ release were much lower compared to those observed in the absence of Fe plaque, regardless of P availability (Fig. 3.6b). During the 72 h before the second Fe plaque induction, H^+ exudation kinetics in the absence of Fe plaque followed similar trends to those described previously, with significantly higher values observed for the P-deficient treatment in comparison to the P-sufficient treatment (Fig. 3.6c). However, in the presence of Fe plaque, the net release of H^+ by the roots was significantly higher in the P-sufficient treatment. Similar results were observed immediately after the second Fe plaque induction period, with P-deficient plants showing the highest values of net H^+ release in the absence of Fe plaque and the lowest values in the presence of Fe plaque (Fig. 3.6d). During this period, the kinetics of H^+ release appeared to be faster compared to the 72 h succeeding the first Fe plaque induction (Fig. 3.6b).

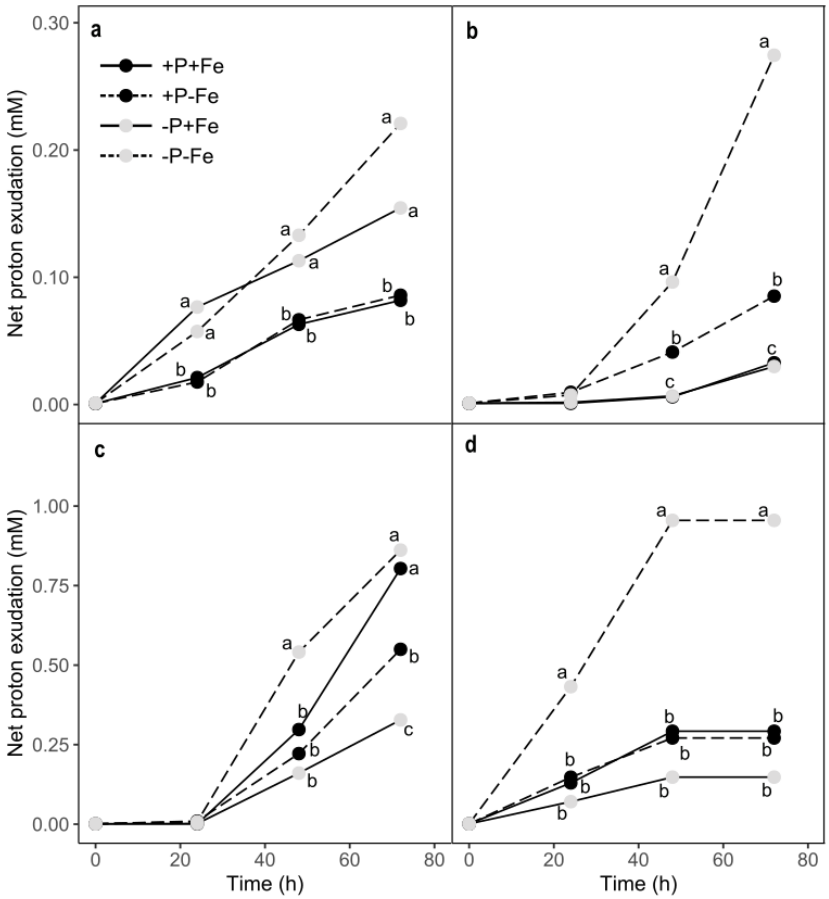

Figure 3.6 Kinetics of net proton exudation over 72 h (a) before and (b) after the first Fe plaque induction (30 DAS), and (c) before and (d) after the second Fe plaque induction (45 DAS) in P-sufficient (+P) and P-deficient (–P) plants, with (+Fe) or without Fe (–Fe) plaque induction. Values represent the mean of measurements on four independent replicates per treatment. For the sake of graph readability, SEs are not reported, while different letters indicate significant differences between treatments for each analysis time ($p \leq 0.001$). Note the different range of values on the y-axis between the two induction periods.

3.4 Discussion

3.4.1 Influence of P availability on Fe plaque formation and dissolution

As expected, P-deficiency induced rice plants to modify their root morphology and traits. Specifically, P-limited plants significantly enhanced their root length, volume, surface area, and tips number compared to plants grown under P-sufficient conditions, without affecting root dry weight. This response was accompanied by a greater development of aerenchyma as previously reported by Fu et al. (2014). Aerenchyma develops in rice plants to facilitate the diffusion of O_2 from the shoot to the submerged roots and, under P limitation, the development of these tissues is further promoted to sustain the higher O_2 requirements associated with a greater soil exploration by the roots, without increasing the C cost of a higher root biomass (Lynch and Brown, 2008). Increased O_2 transport to the root is crucial to support energy-dependent

processes related to plant growth and nutrition under P limitation and indicates a relationship between P availability and O_2 dynamics in the root environment.

Due to enhanced ROL, in the presence of sufficient amounts of dissolved Fe(II) as those typically found in the porewaters of anaerobic rice paddy soils, P-deficient plants showed a faster precipitation of Fe(III) (oxyhydr)oxides on their root surfaces, resulting in significantly higher amounts of Fe plaque immediately following induction, compared to P-sufficient plants. This finding supports our initial hypothesis that changes in rice root traits in response to low P availability led to an increase in Fe plaque formation on the root surface. Despite similar results being reported in other studies, the underlying factors that drive the increase in Fe plaque formation at low P supply remain controversial. In fact, previous research conducted by Kirk and Van Du (1997) investigated the changes in root architecture, porosity and O_2 release in 30 d-old rice plants grown under P concentrations similar to those used in our experiment, and observed a higher apparent rate of O_2 release in P-limited compared to P-sufficient plants. Such an effect was entirely attributed to an increased root volume rather than to higher rates of O_2 release per unit of root volume. On the other hand, in line with our findings, Fu et al. (2014) observed an increase in oxygenation capacity of rice roots under P-deficient conditions, which was associated to enhanced root aerenchyma development. However, it is worth noting that these authors did not evaluate the consequences of this oxygenation on Fe plaque formation. Also, Wu et al. (2012) did not find a significant relationship between root volume and the degree of Fe plaque formation under similar growing conditions, but their study revealed a positive correlation between Fe plaque formation and the ROL when comparing different rice genotypes. Our results indicate that the higher rate of Fe(II) oxidation and Fe plaque formation under P-deficient conditions was not solely attributable to a larger total root surface area but, considering the values of root surface area-normalized rate constants, also to higher ROL. Although we did not measure the rates of root O_2 release directly, our study strongly supports the influence of ROL on the observed phenomena.

Despite the significantly higher amount of Fe precipitated on the root surfaces of P-deficient plants following the Fe plaque induction periods, the subsequent decrease in root-associated Fe over the entire growth period clearly indicated the dynamic nature of this Fe pool, and presumably any associated P. We speculate that the amount of Fe plaque present on the roots is likely determined by the interplay between the rates of formation and dissolution, both of which are notably influenced by P availability. In support of this, albeit the higher rates of Fe mineral precipitation on the root surfaces, P-deficient plants are capable of up-regulating strategies for the dissolution of Fe plaque. This adaptive response enables them to release the required P associated with the Fe plaque to cope with the limited P availability. Indeed, it is well known that P-deficient plants can acidify the rhizosphere via proton exudation to promote the dissolution of sparingly available P forms, as well as the release of P adsorbed onto Fe oxides (Hinsinger, 2001a; Kirk and Van Du, 1997b; Santoro et al., 2022). Given that Fe plaque is composed of Fe (oxy)hydroxide phases similar to those found in soil (Amaral et al., 2017b; Hansel et al., 2001b; Seyfferth et al., 2010b), we expect

similar mechanisms to be more effective at the root surface. This observation would explain the faster decline of root-associated Fe over time in P-deficient compared to P-sufficient plants following Fe plaque induction, albeit differences in root elongation and architecture as a function of P availability could have also been partially responsible for the observed changes in the amount of root-associated Fe with time. Our second hypothesis is nevertheless supported by the higher net H^+ release in P-deficient compared to P-sufficient plants in the absence of Fe plaque, and the significant consumption of these protons during Fe plaque dissolution in the former when Fe plaque was present on the root surfaces. In fact, the dissolution of Fe oxide phases always involves a stoichiometric consumption of protons that explains the lower net H^+ exudation in P-deficient with respect to P-sufficient plants in the presence of Fe plaque. Therefore, assuming that root H^+ exudation was only influenced by P availability but not by the presence or absence of Fe on the root surface, the lowest values of net H^+ release in solution under P-deficient conditions suggest that most of the protons released were used for Fe plaque dissolution. In contrast, the lack of significant differences in net H^+ release between +Fe and –Fe treatments under P-sufficient conditions suggest that Fe plaque dissolution mechanisms were not activated when P supply was sufficient. This finding is further confirmed by the smaller change in Fe plaque contents over time following each induction.

3.4.2 The role of Fe plaque in regulating P uptake by rice plants

The importance of Fe plaque dynamics over time has been recently related to their role in regulating nutrient and/or contaminants availability for rice (Limmer et al., 2022a; Zhou et al., 2018). Nonetheless the majority of the previous hydroponic studies generally focused on a very short time frame (Liang et al., 2006; Liu et al., 2019; Zhang et al., 1999) after a single Fe plaque induction period (Jiaofeng et al., 2022), thus failing to consider the effect of the temporal transformations in Fe plaque in relation to plant development. In this study we finally hypothesized that the different findings reported in literature regarding the role of Fe plaque in serving either as a sink or a source of P for rice acquisition, mainly arise from a lack of consideration of the interdependence and temporal variation of various rhizosphere processes that regulate P availability throughout the rice growth period. For example, the studies by Zhang et al. (1999), Liang et al. (2006), and Jiaofeng et al. (2022) related a higher Fe plaque formation to an inhibitory effect on plant P uptake, however the tested range of P concentrations (> 150 µM) were higher than the threshold (6 µM) above which P availability is considered to be sufficient for rice plants (Frossard et al., 2000a; Shahandeh et al., 1995b). With these experimental designs they were thus not able to appreciate the plant adaptation mechanisms (e.g. rhizosphere acidification) on Fe plaque dissolution and P uptake under low P availability.

The results of our study suggest that the equilibrium between Fe plaque formation and dissolution depends on the availability of P in relation to plant requirements. Whereas the presence of Fe plaque resulted in a limitation of plant P uptake under P-sufficient conditions over a growth period of 60 d, a higher P uptake was observed in the presence rather than in the absence of Fe plaque under P-deficient

conditions. By combining these findings with the enhanced Fe plaque dissolution observed at low P availability, we provide support for our third hypothesis. Indeed, Fe (oxyhydr)oxides on the root surface can strongly bind P (Khan et al., 2016; Liang et al., 2006; Zhang et al., 1999), and their dissolution facilitated by rhizosphere acidification might have promoted the release and uptake of the bound P at rhizosphere level. Our results therefore confirm that Fe plaque can act as a barrier to plant P uptake under high P availability but serve as a P source under low P availability partially attenuating the nutrient deficiency.

3.5 Conclusions

Due to the high affinity of Fe (oxyhydr)oxides for P, Fe plaque, generally associated with rice roots under anoxic soil conditions, can influence P uptake for sustaining growth. In this chapter we show that both Fe plaque formation and dissolution during the early stages of plant growth are influenced by root traits, in turn, regulated by P availability. The overall results (Fig. 3.7) thus contribute to further understanding the complex interactions between modifications in rice root traits and temporal Fe plaque dynamics on root surfaces as a function of P availability, which deeply shape nutrient cycling in the rhizosphere.

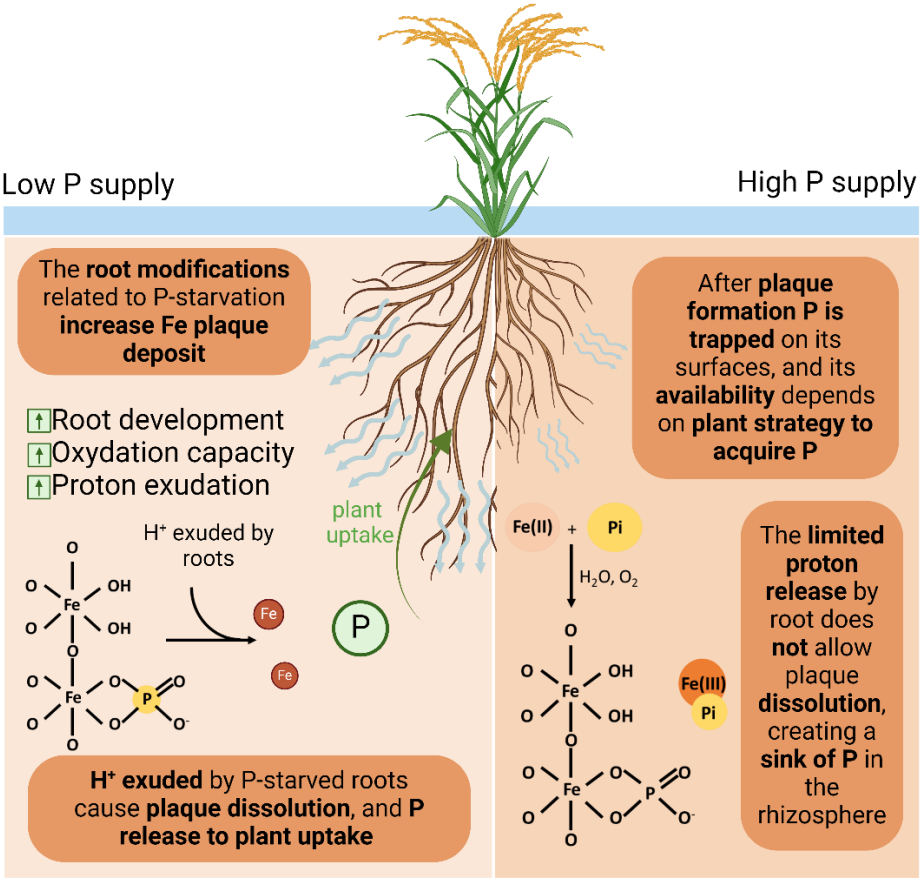

Figure 3.7 Overall conceptual model of the results discussed in Chapter 3

CHAPTER 4

Phosphorus availability to rice plants as a function of inorganic and organic P forms in submerged paddy soils

4.1 Introduction

The formation of Fe(III)-P co-precipitates is characterized by spatial variability due to the differences in redox potential moving from the anoxic bulk soil to the oxic rhizospheric layer (Zhang et al., 2003). As demonstrated in chapter 2 and 3, the occurrence of Fe(III)-P coprecipitates in the bulk soil leads to a decreased availability of the redox-sensitive P pool, because of the temporal decoupling between P coprecipitation and plant P uptake. Nonetheless, plants may adopt specific strategies to acquire P leading to an increased availability of the inorganic P retained by root Fe (hydr)oxides. Co-precipitation processes may involve also organic P forms (Chen et al., 2020; Santoro et al., 2019b; Wang et al., 2017), however little is known about their behavior after co-precipitation and, consequently, their potential to be a source or sink of P for rice plants. In batch experiments, Santoro et al. (2019) showed that the oxidative co-precipitation processes with dissolved Fe(II) led to a faster and greater retention of organic compared to inorganic P forms, and the extent of this process depended on the involved organic P form. Particularly, during co-precipitation, diesters, such as phospholipids, were retained onto the surface through weak physical interactions whereas inositol phosphates were chemically adsorbed and/or precipitated creating more stable complexes. Moreover, similarly to the mechanisms underlined in the previous chapters for inorganic P, also the Fe-organic P co-precipitates might be dissolved by the onset of reducing conditions, albeit the extent and the mechanisms of these processes have been scarcely investigated.

Organic P cycling is further complicated by the strong relationship with soil organic matter (SOM) (Celi et al., 2022; Santoro et al., 2023), since organic P forms are ascribed to the P bound to an organic component (Turner et al., 2005). The abiotic stabilization processes protecting SOM by chemical interaction with mineral surfaces (Chen and Thompson, 2018; Sodano et al., 2017) are effective on organic P compounds, as largely argued by George et al. (2007) and Giaveno et al. (2010). On the other hand, biotic immobilization of soluble P into the microbial biomass may further reduce P availability and can stress the competition between the microbial community and rice plants (Wang et al., 2022a). Plants may activate several strategies to overcome P limitation favoring P release from the microbial biomass by the root exudation of C compounds and enzymes (Rose et al., 2013; Wang et al., 2022b). The interplays between redox-driven co-precipitation and plant strategies to acquire P could thus cause a selective enrichment of specific P forms based on the enzymatic activity (Nannipieri et al., 2011) and affinity between the P forms and Fe oxides (Celi et al., 2020; Prietzel et al., 2016; Santoro et al., 2023). Furthermore, as the activation of plant strategies to acquire P is directly related to soil P supply (McDowell et al., 2008; Rose et al., 2013), the selective enrichment of P compounds can lead

to a different P speciation as a function of soil total P supply. However, scant attention has been posed to the effect of redox processes on organic P characteristics in temperate paddy soils and its availability to rice plants.
Based on these considerations this chapter will focus on the hypotheses that i) the amount and forms of organic P in paddy soils vary as a function of total P; and the composition of soil P species may be driven by both ii) redox-driven processes and iii) the needs of P by rice plants. To test these hypotheses, this work aims to determine the amount and composition of organic P forms and their changes during rice growth under continuously flooded conditions, as a function of the soil total P supply.

4.2 Material and methods

The analyses described in this chapter were carried out on the same soil samples described in chapter 2, whose characteristics are reported in Table 2.3. Besides, the relationship between organic P forms and plant P uptake were investigated considering the plant P uptake measured in the mesocosms experiment described in chapter 2 – section 2.2. Briefly, the total P content in plant tissues was measured after 60 days of cultivation under continuously flooded conditions, and it ranged from 3.94, 4.66 and to 5.59 mg g^{-1} in low-, medium-, and high-P soils, respectively (Table 2.4).

4.2.1 P chemical fractionation

Soils samples were analyzed before the mesocosms filling (Pre), and at the end of the 60 days cultivation period (Post). At each sampling time soil samples were air dried, sieved < 2 mm, and used for the sequential chemical fractionation of the P pools present in each soil. According to the results obtained in Chapter 2 the steps included in the P chemical fraction were: a) soluble-P (sol-P; 0.1 M $CaCl_2$, 1 h reaction time for soluble P); b) exchangeable-P (exchang-P; anion exchanging resins, 2 h contact time for desorbable P), as representation of the plant available P pool; c) redox sensitive-P (Fe-P; acid ammonium oxalate, 2 h reaction time for P bound to amorphous Fe (hydro)oxides), as representation of the P pool involved in redox-driven processes after soil flooding; and e) residual-P (res-P; sulfuric-perchloric digestion, for P in the residual unextracted fractions). Despite also Mn is involved in redox reactions, for the sake of simplicity the redox-sensitive P pool was entirely attributed to Fe as Fe oxides represents the most important sorption site for P. In all extracts derive from step a, b, and c molybdate-reactive phosphate (MRP) and molybdate-unreactive phosphate (MUP) were determined. The MRP was determined colorimetrically according to Murphy and Riley (1962) using excess molybdate when necessary (Weaver, 1974). Aliquots of the extracts were dried in the oven at 105°C and digested with sulfuric-perchloric acid mixture (Martin et al., 1999) to determine the total P concentration in the extracts by the same colorimetric reaction. For residual P, after sulfuric-perchloric digestion all the inorganic and organic P was assumed to be in solution, and thus the colorimetric reaction in this case measured total P in the extracts. In all the other steps (i.e. a, b and c) the MUP concentration was determined as the difference between total P and MRP in the extracts. As

persulfate digestion may underestimate the true value in samples that contain Ins6P due to incomplete digestion of this compound (Denison et al., 1998), the efficiency of persulfate digestion procedure was tested by digestion of an Ins6P standard. As stated by Cade-Menun and Liu (2014), the MUP includes mainly organic P along with some inorganic P forms that do not react with molybdate. In relation to the scope of this study, we assumed that the MUP pool corresponded mainly to organic P forms. Therefore, we will hereafter refer to MRP and MUP in the extract as inorganic P (Pi) as organic P (Po), respectively. The same soils were also extracted by 0.5 M $NaHCO_3$ (Olsen, 1954) as a comparison of soil P availability with former literature reports from aerobic soils.

4.2.2 Soil enzymatic activity

The potential activities of two of the main hydrolytic soil enzymes linked to P cycling, alkaline phosphomoesterase (Alk-PME), and acid phosphomonoesterase (Ac-PME), were determined as described by Eivazi and Tabatabai (1977) using air-dried soil samples (48 samples). In brief, Alk-PME and Ac-PME were assayed with a modified universal buffer of pH 11.0 and 6.5, respectively, using p-nitrophenyl phosphate (pNP) as the substrate. The released p-nitrophenol (pN) was measured spectrophotometrically at 400nm and the activities were expressed as mg pN kg-1 dry soil h-1. Despite the procedure of air-drying could impact the absolute values of enzymatic activities (Lane et al., 2022), this approach could be considered acceptable when treatment comparisons are the interest of the study and all samples have been subjected to the same storage (Peoples and Koide, 2012). Besides, the implementation of enzymatic activity to measure soil processes was often criticized, as specific enzymatic activity is generally considered a best representation of soil dynamics (Raiesi and Beheshti, 2014; Trasar-Cepeda et al., 2008), and it is less affected by sample storage (Peoples and Koide, 2012).The specific enzymatic activity is normally calculated as the ratio between enzyme activity and total organic carbon in soil, or microbial carbon content (Trasar-Cepeda et al. 2008; Raiesi and Beheshti 2014). However, considering that P is the target nutrient for Ac-PME and Alk-PME activity, and the activation of plant and/or microbial enzymatic activity has been related to the P soil content (Rose et al. 2013; Wang et al. 2022c), to the scope of this study the specific enzymatic activity was calculated by the ratio between Ac-PME and Alk-PME activity and the values of soil total Po subtracted by the concentration of monoesters, as these forms do not contribute to phosphomonoesterase activity.

4.2.3 *Liquid-state ^{31}P nuclear magnetic spectroscopy*

Following the method proposed by Cade-Menun and Preston (1996), 1 g of each soil was shaken overnight with 10 mL of 0.25 M NaOH and 50 mM EDTA (NaOH-EDTA). After centrifugation (10 min x 3000 rpm), the concentration of MRP and MUP in the extractants was determined as described for soil P fractionation, and the concentration of Fe and manganese (Mn) was determined by atomic absorption spectroscopy (AAS, PerkinElmer AAnalyst 400, Norwalk, CT, USA). The values of MRP and MUP in the NaOH-EDTA were used as a reference to select one soil of each P level to be analyzed by ^{31}P NMR

spectroscopy. The solutions were freeze-dried and then resuspended in 0.9 ml of a solution containing 1.0 M NaOH and 50 mM Na_2EDTA and 0.1 ml deuterium oxide and then analyzed (Turner, 2008). Liquid state ^{31}P NMR spectroscopy was carried out on a JEOL ECZR 600 MHz, using a 6 µs pulse (45°), a delay time of 2.0 s, an acquisition time of 0.4 s, and broadband proton decoupling (Turner, 2008). Approximately 25,000 scans were acquired for each sample. Spectra were plotted with a line broadening of 5 Hz and chemical shifts of signals were determined in parts per million (ppm) relative to the MDPA internal standard. Signals were assigned to P compounds based on Cade-Menun and Liu (2014), McLaren et al. (2017) and Celi et al. (2013). Peaks were calculated after integrating spectra, and the results were corrected for diester degradation products by subtracting α- and β-glycerophosphate and the mononucleotides from the total monoester area and adding them to the total diester area (Chen et al. 2021 and references therein).

4.2.4 Soil Organic Matter fractionation

The soil organic matter (SOM) density fractionation was carried out to identify three different fractions: free particulate organic matter (*f*POM), occluded particulate organic matter (oPOM) and mineral associated organic matter (MAOM). Separation of the three fractions was carried out as described by Cerli et al. (2012). The *f*POM was separated by floating, after suspending the soil in a 1.6 kg dm^{-3} sodium polytungstate solution. The remaining soil was dispersed by ultrasonication (Sonoplus HD 2200, Bandelin electronic GmbH & Co. KG, Berlin, Germany) to release occluded organic materials at a previously setup energy of 175 J mL^{-1} (Cerli et al., 2012). The samples were then vacuum filtered on a 0.7 µm GF/F filter placed on a Buckner funnel and the *o*POM fraction rinsed and recollected. The remaining soil was resuspended in deionized water, centrifuged at 10,000 rpm for 35 min and then repeatedly washed with deionized water to remove all ions entrapped in the residue. The residue containing the MAOM fraction was collected and dried in a ventilated oven at 40°C. Each fraction was then homogenized and sieved at 0.5 mm to determine the total carbon (C) and nitrogen (N) contents by dry combustion (UNICUBE, Elementar Analyses System GmbH, Langensbold, Germany). The amount of total P in each fraction was not determined because it was not possible to avoid the contamination of the three samples after suspending the soil in sodium polytungstate solution.

4.2.5 *Statistical analysis*

The statistical analyses were performed using the R version 4.1.1. Normality and data homoscedasticity were checked with Shapiro-Wilk and Levene tests, respectively. When necessary, data were transformed according to the data distribution. All the variables were tested for the analysis of variance (two-way ANOVA), followed by pair-wise post hoc analyses (Student-Newman-Keuls test) to determine the differences among the mean value at $p < 0.05$. The R packages *FactoMineR* and *factoextra* were used to compute the Principal Component Analysis (PCA) to investigate the relationship between relevant variables.

Matrices adopted for PCA were scaled and centered prior to performing the analysis and generating biplots. The number of principal components (PC) to consider was evaluated based on the eigenvalues and referring to the Kaiser-Guttman criteria. The *ggplot2* package was used to plot all the figures.

4.3 Results

4.3.1 Evolution of soil P pools with rice cultivation

As expected, the high-P soils resulted in higher amount of total Pi, followed by medium-P > low-P, and in all cases total Pi showed a slightly decrease after 60 days of rice cultivation. Considering the values reported in chapter 2, inorganic P measured by Olsen method resulted in the same trend with high-P > medium-P > low-P soils, albeit only high-P soils resulted in a significant decrease of inorganic Olsen-P after rice cultivation (Table 4.1). The distribution of Pi in the operationally-defined pools was influenced by the interaction between soil P level and the sampling time (p-value <0.05). In most of the cases, the predominant Pi pool was Fe-P, followed by res-P > exchange-P >> soluble-P. Although the soluble-P values were significantly lower than the other Pi pools, a variable amount of soluble-P was measured in all soils (high-P = 4.50 mg kg^{-1}, medium-P = 0.59 mg kg^{-1}, low-P = 0.32 mg kg^{-1}). By comparing the distribution of the Pi pools within the same P level during time, only high-P soils showed a decrease in soluble-P after rice cultivation, while all the soil P levels resulted in a general decrease in exchange-P. Medium-P and low-P soils showed an increase in Fe-P after rice cultivation, and the opposite was true in high-P soils. Conversely, res-P showed a decrease during time only in medium and low-P soils, while no significant differences were observed in high-P (Fig. 4.1a).

Organic P values were lower than total Pi, but also in this case total Po positively correlated with total soil P supply, as the highest values were related to high-P level, followed by medium-P and low-P, which were comparable. The total organic P suggests a decrease after rice cultivation in high P soil, however the large uncertainty in the obtained values attributed this difference to the random variability. The greatest amounts of organic P were measured in medium-P (3.69 ± 0.59 mg kg^{-1}) and low-P (2.30 ± 0.57 mg kg^{-1}) soils by Olsen method, which also resulted in a significant increase of Olsen-extractable Po after rice cultivation (medium-P = 7.66 ± 0.95 mg kg^{-1}; low-P = 5.51 ± 1.67 mg kg^{-1}). On the contrary, high-P soils resulted in lower organic P in Olsen extractant (1.42 ± 0.59 mg kg^{-1}), with a slight but not statistically significant increase after rice cultivation (Δ [P] = +2.48 mg kg^{-1}). Conversely to Pi, the highest distribution of Po was measured in the residual fraction, followed by Fe-P > exchange-P, while the organic soluble-P pool was not detected in any soils. Also in the case of Po a decrease in exchange-P was observed after 60 days of rice cultivation, matched by an increase of Fe-P, particularly evident in med- and low-P soils (Fig. 4.1b).

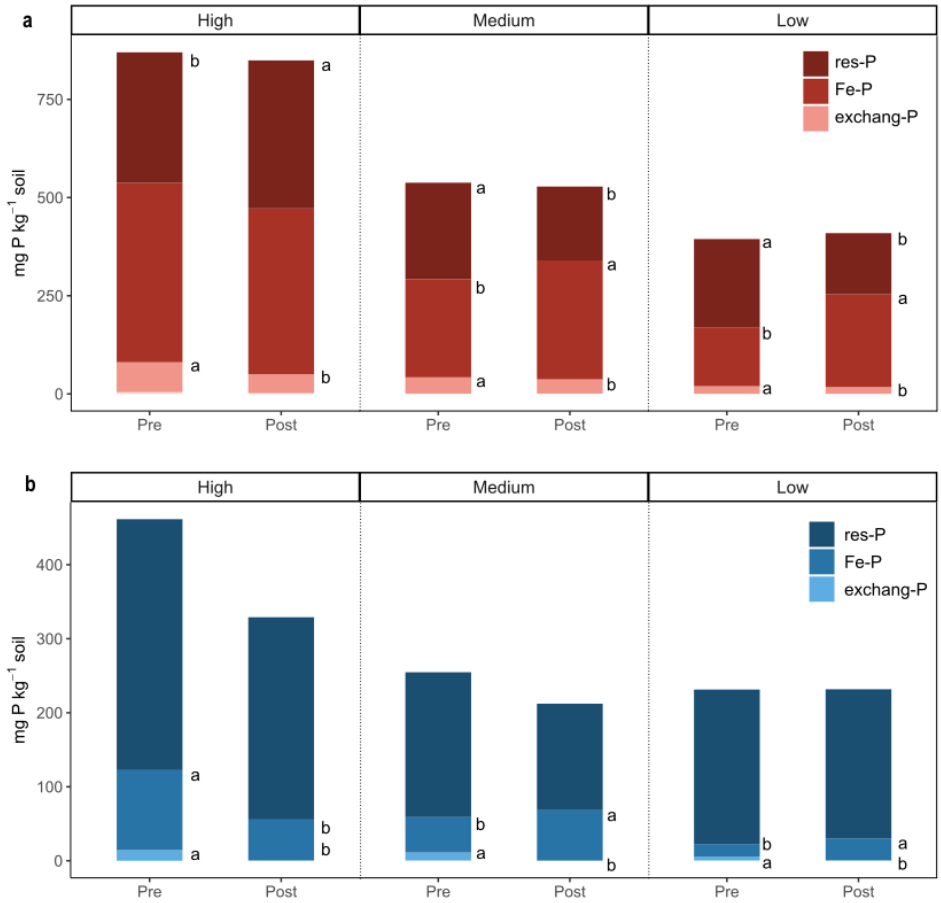

Figure 4.1 a) distribution of inorganic P (Pi) and b) organic P (Po) in the operationally-defined pools: soluble-P (0.1 M $CaCl_2$), exchangeable-P (anion exchanging resins), iron-P (acid ammonium oxalate), residual-P (sulfuric-perchloric digestion). In the high, medium, and low-P soil before (Pre) and after (Post) 60 days of rice cultivation under continuous flooding. Different letters above bars represent significant differences for the interaction P level x Time in the same P pool (p-value < 0.05). For the sake of graph readability, no error bars were reported.

4.3.2 Organic P forms under reducing conditions

NaOH-EDTA extraction recovered 42–74% of total P with significant differences among soil P levels. The highest P recovery was observed in high-P soil (74%), followed by medium-P (44%) and low-P (42%). Table 4.1 reports the values of Pi and Po measured in the NaOH-EDTA extractant in the three P levels and two sampling time. The values of Pi were significantly influenced by the P level (p-value < 0.01), and the highest values of Pi were observed in high-P soils. Conversely, the Po values were significantly lower than the Pi, but not significantly different among P levels. High P soils showed a slight increase in Po after rice cultivation, while the opposite was true in medium and low-P soils, despite the differences were not statistically significant. The values of Fe in the NaOH-EDTA extractants were significantly influenced by the P level (p-value < 0.05) and the sampling time (p-value < 0.01). In particular high-P soils resulted

in the highest Fe concentration, followed by medium- and low-P soils which in turn were comparable. As expected, the Fe concentrations were higher after rice cultivation, and such an effect was particularly significant in the soil with the lowest P supply. Conversely, Mn concentrations did not result in significant variations.

Table 4.1 Values of inorganic P, organic P, Fe and Mn in the 0.25 M NaOH – 50 mM EDTA extractants of high, medium low-P soils before (Pre) and after (Post) 60 days of rice cultivation under continuous flooding. Each value represents the average between four independent replicates. Lower case letters represent significant differences between sampling time, and upper case letters represent differences among soil P level according to the p-values reported in the table.

Soil P level	Time	Total					Olsen	NaOH-EDTA			
		P	C	N	C:N	C:P	P	Pi	Po	Fe	Mn
			mgkg^{-1}				mgkg^{-1}			mgkg^{-1}	
High											
	Pre	899	15000 a	2000 a	7.50 a	16.7 a	52.4 a	452	31.2	128	60.5
	Post	899	14600 b	2000 a	7.30 a	16.2 a	39.5 b	491	45.0	116	45.3
	average	899 A					45.9 A	472 A		122 A	
Medium											
	Pre	512	10100 a	1200 b	8.42 a	19.7 a	23.5 a	178	38.8	42.5 b	33.4 b
	Post	512	10100 a	1300 a	7.77 b	19.7 a	24.7 a	188	13.4	92.1 a	70.2 a
	average	512 A					24.1 B	183 B		67.3 B	
Low											
	Pre	377	10400 b	1300 b	8.00 a	27.6 b	12.7 a	145	21.8	60.3 b	52.4 a
	Post	377	11500 a	1500 a	7.67 b	30.5 a	12.6 a	155	16.0	82.4 a	34.6 b
	average	377 A					12.6 C	150 B		71.4 A	
p-value Soil P level		< 0.01	< 0.05	< 0.05	n.s.	< 0.05	< 0.05	<0.01	n.s	<0.05	n.s
p-value Sampling time		n.s.	< 0.05	< 0.05	< 0.05	n.s	n.s.	n.s	n.s	<0.01	n.s
p-value P level*time		n.s.	< 0.05	< 0.05	< 0.05	< 0.05	< 0.05	n.s	n.s	n.s	n.s

The ^{31}P NMR spectra acquired from 25 to -10 ppm were generally characterized by the presence of phosphates (6.6 - 6.2 ppm), monoesters (6.2 - 4.0 ppm), pyrophosphates (3.9 - 4.2 ppm), phosphonates (21.0 - 7.0 ppm), while the signals between 2.5 – 3.0 ppm range were scarcely present (Fig. 4.2). The spectra of the soils sampled after 60 days of rice cultivation under continuous flooding showed a lower signal to noise (S/N) ratio, possibly because of the higher concentration of paramagnetic ions (i.e. Fe or Mn).

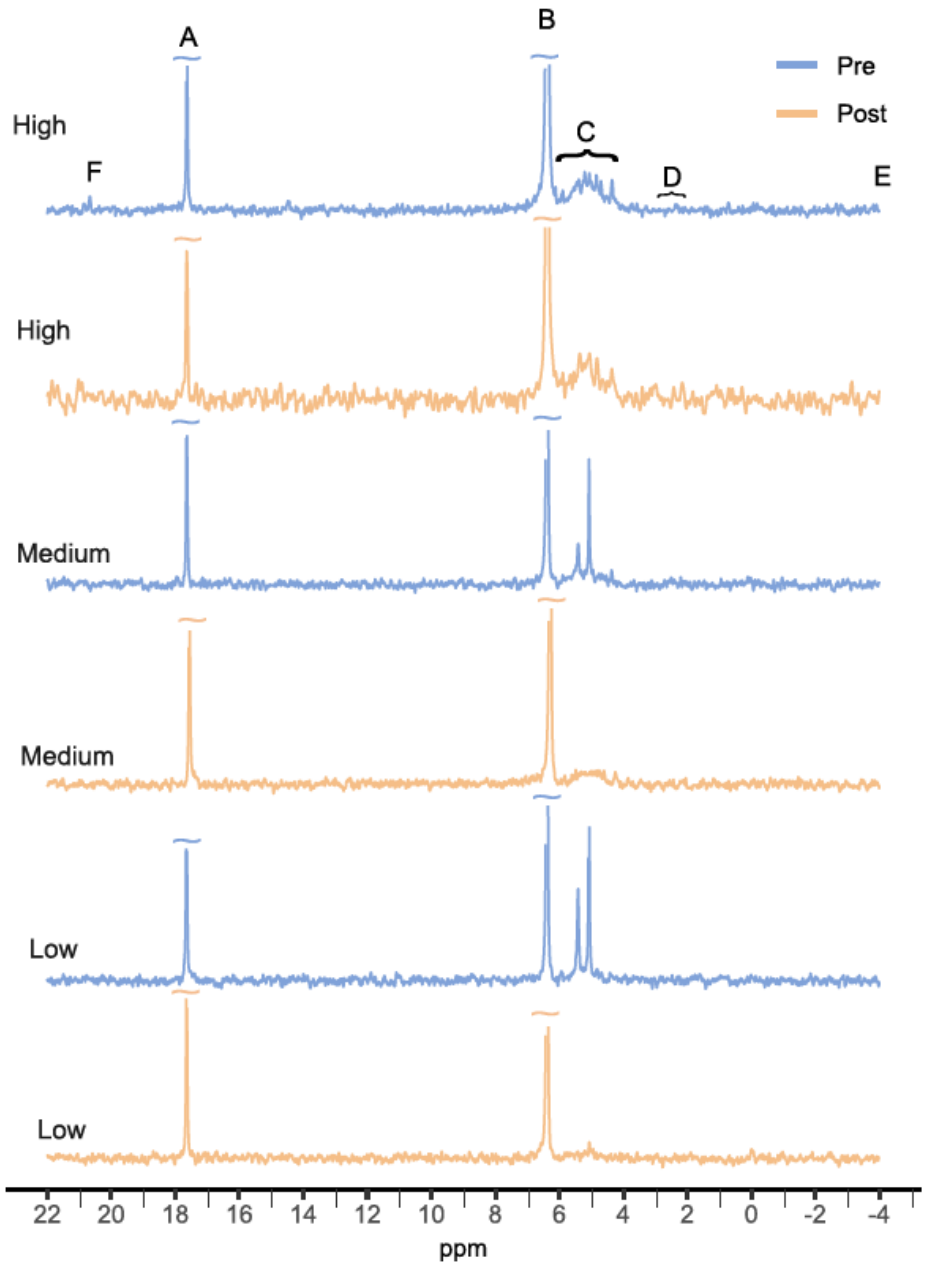

Figure 4.2 ^{31}P spectra of high-, medium-, and low-P soils before (Pre) and after (Post) days of rice cultivation extracted with 0.25 M NaOH 50 mM EDTA for 16 hours and a 1:20 soil:solution ratio. Number of scans= 50000. Spectra have been plotted with 5-Hz line broadening. (A) 17.63 ppm internal standard MDPA, (B) 6.6-6.2 ppm phosphates, (C) 6.2-4.0 ppm monoesters, (D) 2.5- -3.0 ppm diesters (E) -3.9- -4.2 ppm pyrophosphates, (F) 21.0-20.4 ppm phosphonates

In agreement with the Pi and Po values in NaOH-EDTA extractants, all the spectra showed a higher signal of Pi than Po. Among the P compounds detected by P-NMR, soil Pi accounted for 73.8 - 92.1 % of the P extracted by NaOH-EDTA, following a gradient from high- < medium- < low-P soils. Orthophosphate was the dominant compound, while pyrophosphate and polyphosphate were < 1.0% each of extracted P in most of the cases (Table 4.2). No significant variations of inorganic P forms were observed during rice cultivation, albeit pyrophosphates and phosphonates were not detected after rice cultivation in all soils (Table 4.2). Soil Po accounted for less than 10% of the P extracted by NaOH-EDTA in most of the cases, with the only exception in med- and low-P soil before rice cultivation, when Po accounted respectively for 31.1 and 49.9 % of the total P extracted by NaOH-EDTA (Table 4.2).

The monoester region showed the typical pattern characterized by the presence of different organic forms (Fig. 4.3). In high-P soils *myo*-inositol phosphate (*myo*-Ins6P) was clearly visible (6.1 – 5.2 – 4.9 – 4.7 ppm), as well as the signals at 4.4 ppm attributed to *scyllo*-inositol phosphate (*scyllo*-Ins6P). These signals were present both before and after rice cultivation. By contrast, in the medium-P and low-P soils, the spectral features of *myo* and *scyllo*-InsP6 were less pronounced while two intense signals at 5.6 - 5.3 ppm and 5.2 - 4.9 ppm appeared, attributed to β-glycerophosphates and mononucleotides, respectively. These signals showed a lower intensity in the soils sampled after rice cultivation. Monoesters were higher in high-P soil than in medium- and low-P soils. In medium-P soil α-, β-glycerophosphate and nucleotides content was 9.4 and 19 mg P kg^{-1} soil, respectively, while in low-P soil, 17 and 40 mg P kg^{-1} soil. Soil organic P accounted for less than 10% of the P extracted by NaOH-EDTA in most of the cases, with the only exception in med- and low-P soil before rice cultivation, when organic P accounted respectively for 31.1 and 49.9% of the total P extracted by NaOH-EDTA (Table 4.2). Moreover, different soil P levels resulted in a different distribution of organic P compounds, as in high-P soils the majority of organic P was orthophosphate monoesters, comprising around 5% of the extracted P after correction for diester degradation products. Considering the signals of nucleotides and β-glycerophosphates as a degradation products of RNA and phospholipids respectively, the signals related to those P compounds were attributed entirely orthophosphate diesters, which in turn contributed to the 18.0 and 13.8 % of the extracted P respectively in med- and low-P soils before rice cultivation (Table 4.2).

Table 4.2 Organic and inorganic P forms (expressed in mg P kg-1soil or as percentage of total P) determined by NaOH-EDTA extraction and solution 31P NMR spectroscopy in the soils with high, medium and low P supply, before (Pre) and after (Post) 60 days of rice cultivation under continuous flooding conditions.

Soil P level	Time	NaOH-EDTA P[a]	Organic P[b]	Organic P forms[c]		Inorganic P forms[c]		
				Monoesters	Diesters	Ortho-P	Pyro-P	Poly-P
		$mgkg^{-1}$ (%TP)[d]	$mgkg^{-1}$	$mgkg^{-1}$ (%NaH-EDTA P)		$mgkg^{-1}$ (%NaH-EDTA P)		
High								
	Pre	606 (67)	31.2	31.2 (5.1)	n.d.	445 (73)	3.63 (0.6)	3.63 (0.6)
	Post	665 (74)	45.0	45.0 (6.8)	n.d.	489 (74)	2.18 (0.3)	n.d.
Medium								
	Pre	216 (42)	67.4	38.8 (18)	28.6 (13.2)	176 (81)	1.45 (0.7)	n.d.
	Post	232 (45)	13.4	13.4 (5.8)	n.d.	186 (80)	1.09 (0.5)	n.d.
Low								
	Pre	158 (42)	78.7	21.8 (49)	56.9 (36.0)	145 (92)	0.00 (0.0)	n.d.
	Post	174 (46)	16.0	16.0 (6.2)	n.d.	152 (88)	2.90 (1.7)	n.d.

[a]Values in parentheses are the proportion (%) of the total soil phosphorus (Table 1)
[b]Sum of phosphate monoesters and diesters
[c]Values in parentheses are the proportion (%) of the P extracted in NaOH-EDTA
[d]TP is total P determined by $H_2SO_4/HClO_4$

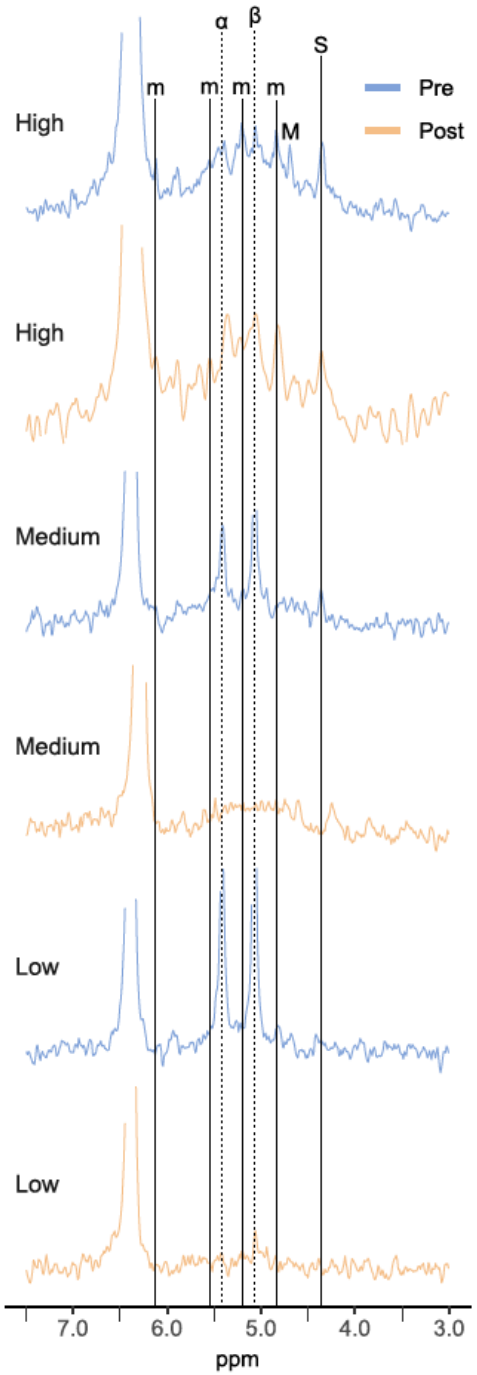

Figure 4.3 Zoom of ^{31}P spectra of High-, Medium- (Med), and Low-P soils before (Pre) and after (Post) days of rice cultivation represent the monoesters region (4-7 ppm) in ^{31}P spectra of the same soil. (S) scyllo IHP, (m) myo IHP, (M) mononucleotides, (β) β-glycerophosphates, (α) α-glycerophosphates

4.3.3 Enzymatic activity

The potential activity of Ac-PME was higher than that of Alk-PME, and only the former was significantly influenced by the sampling time (Fig. 4.4a). The highest values of Ac-PME were generally observed after rice cultivation, and the effect of rice cultivation on Ac-PME activity was greater in medium-P and low-P soils than high-P, albeit the differences were not significant. Conversely, the highest values of Alk-PME were observed before rice cultivation, and medium-P soils resulted in higher Alk-PME activity than high-P and low-P. Specific activity of Ac-PME and Alk-PME showed greater differences among the treatments (Fig. 4.4b), nevertheless only specific Ac-PME activity resulted in significant differences among soil P levels (p-value < 0.05), sampling time (p-value < 0.01) and the interaction of the two factors (p-value < 0.05). The highest values of Ac-PME were observed in low-P soil followed by medium-P and high-P. The latter did not show significant differences between before and after rice cultivation, while both medium-P and low-P soils displayed an increased Ac-PME activity after rice cultivation. Also in this case, the activity of Ac-PME was higher than Alk-PME in all treatments and statistically increased after cultivation in medium and low P soils. Conversely, Alk-PME activity was not affected by rice cultivation and only a slight decrease was observed after rice cultivation in low-P soils.

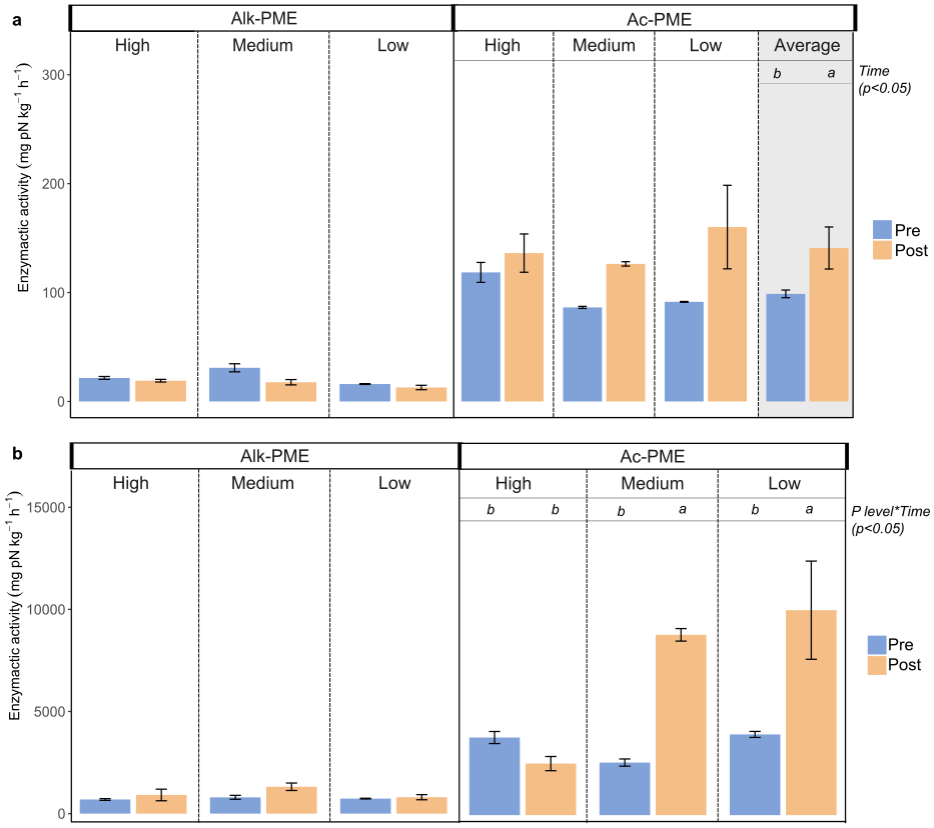

Figure 4.4 Enzymatic activity a), and specific enzymatic activity normalized to the amount of soil organic P b), of acid phosphatase and alkaline phosphatase in the high, medium and low-P soil before (Pre) and after (Post) 60 days of rice cultivation. Each value represents the average among four independent replicates, bars represent the standard errors. Bars with pattern represent the average among soil P levels, and uppercase letters represent differences between sampling time (p-value < 0.05). Lowercase letters with brackets represent differences among soil P levels (p-value < 0.05), and lowercase letters represent differences between sampling time within the same soil P level (p-value < 0.05)

4.3.4 Soil organic matter

In all soils, the OM distribution among the three density fractions showed a higher repartition in the mineral associated organic matter (MAOM). Low-P soils showed a higher proportion of C and N in *f*POM and oPOM compared to medium and high P soils, with an evident decrease after rice cultivation, albeit not statistically different. Also, the C/N of low P soils appeared different from medium and high P soils with lower values in all fractions (Fig. 4.5).

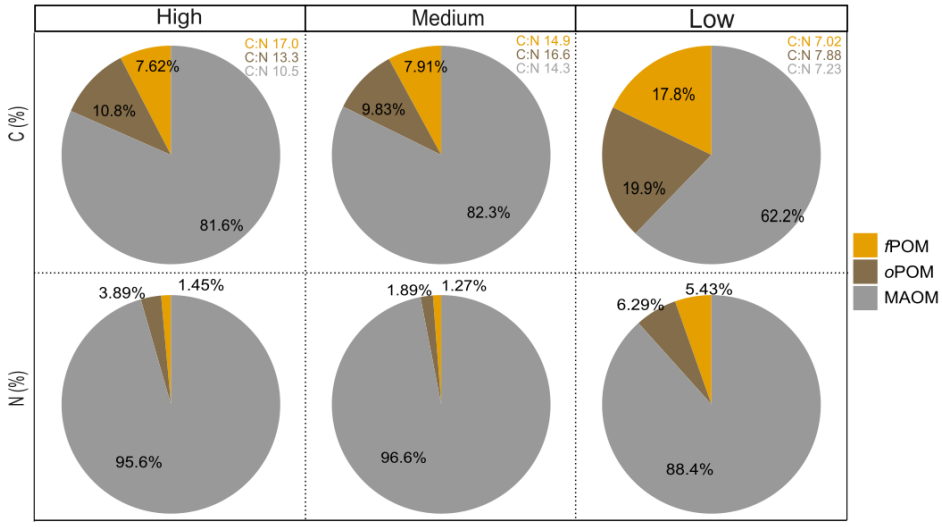

Figure 4.5 Percentage of carbon (C), and nitrogen (N) in free particulate organic matter (fPOM), occluded particulate organic matter (oPOM) and mineral associated organic matter (MAOM) for each fraction obtained in the density fractionation procedure, and values of C:N ratio for the same fraction before (Pre), and after (Post) rice cultivation.

4.3.3 Principal component analysis of the relevant variables

The first two principal components used to plot the PCA biplot explained the 67.5% of the variability in the dataset (Fig. 4.6). The disposition of the individuals in the biplot clearly indicates a difference based on the soil P levels, as well as the sampling time. In the first case the high-P soils were mostly associated to the exchangeable P in the soil, while medium and low-P soils were mostly related to the organic P forms (monoesters), and enzymatic activity. The P content in plant tissues (P_{plant}) positively correlated with the exchangeable P in soil. Noteworthy, a strong positive correlation was also observed with *f*POM and Ac-PME, especially in low and medium-P soils. Conversely, Alk-PME activity was negatively correlated with *f*POM. The activity of both enzymes was not correlated with the amount of MAOM nor with the soil monoester content.

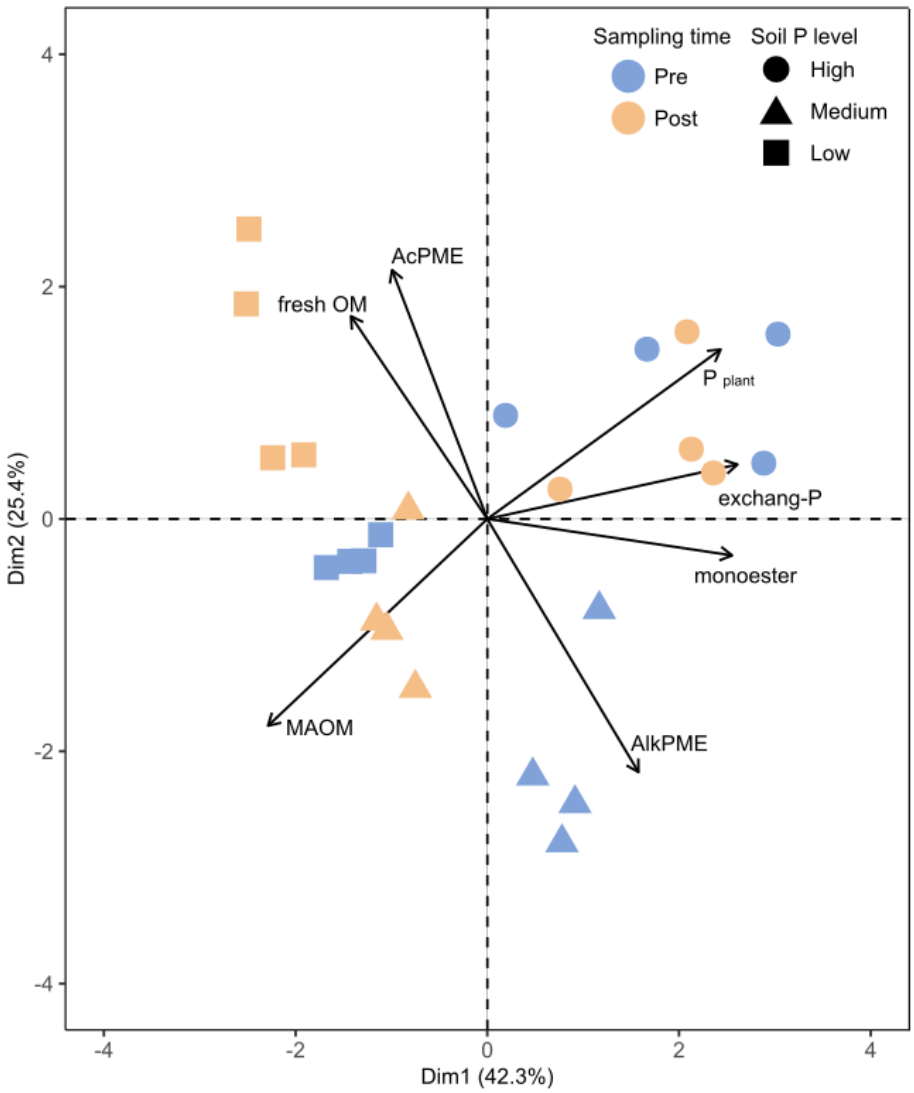

Figure 4.6 Principal component analysis of the relevant variables: acid and alkaline phosphatase soil activity, fresh and mineral associated organic matter (MAOM), P concentration in plant tissues (P plant), exchangeable soil P content, and amount of monoesters in soil as quantified by P-NMR. The different colors of the individuals represent sampling time before (Pre) and after (Post) 60 days of rice cultivation, while different shape represent different soil P levels.

4.4 Discussion

4.4.1 Organic P cycling under reducing conditions as affected by total P supply

The 60 days of rice cultivation under reducing conditions led to a pronounced decrease of exchangeable P with the concomitant increase of redox-sensitive P pools, while soluble-P pool remained quite constant. The exchangeable-P pool represents the amount of P that is displaced from the soil surfaces after the consumption of soluble P (Moody et al., 2013; Saggar et al., 1990). Such a process can possibly explain the apparently static behavior of soluble-P pool during rice cultivation, as the P depleted from the exchangeable-P pool can replace the P taken up by rice plants. However, this fraction appeared to feed also the redox-sensitive P pool, which increased in all soils after rice cultivation. Although the soils under reducing conditions experienced reductive dissolution of Fe (hydr)oxides with an expected increase of P in the soil solution (Ponnamperuma, 1972; Scalenghe et al., 2002; Wang et al., 2022a), co-precipitation processes may occur during soil flooding (Santoro et al., 2019; Zhang et al., 2003), especially when the reducing conditions are protracted (Heiberg et al., 2010; Refait et al., 2007). It is thus likely that the P_i promptly released by reductive dissolution in the first 7-14 days after soil flooding, as observed in chapter 2, was subsequently co-precipitated with the aqueous Fe(II), thus feeding the redox-sensitive P pool.

Soil organic P pools presented similar dynamics, although the differences resulted in a limited statistical significance. The slightly decrease of exchangeable P_o and the concomitant increase of redox-sensitive Po after rice cultivation confirm that also P_o forms are involved in the abiotic redox-driven processes and undergo more complex coprecipitation processes than P_i. Indeed, the composition of organic P forms in soil is a complex matter and it encompasses several families of chemical molecules (Cade-Menun, 2005; Turner et al., 2005), with a different involvement of adsorption, precipitation and physical entrapment mechanisms during coprecipitation (Santoro et al., 2019; Wang et al., 2017). This could affect the content and the chemical composition of the various P_o pools. We also noticed that the residual P_o was markedly higher than P_i. Considering that the residual P is generally defined as the amount of P that is not extracted from the soil via the extraction techniques used (Condron and Newman, 2011), the quantity of residual P depends on the fractionation scheme employed, and such a pronounced increase can be explained by the already reported poor capability of wet chemical extraction to address the complex dynamics which govern organic P in soils (McDowell et al., 2008; Turner et al., 2005).

The ^{31}P-NMR spectra clearly showed a variation in organic P forms related to total soil P supply. High-P soils were characterized by the prevalence of *myo*- and *scyllo*-Ins6P and a lower contribution of diesters. It can be inferred that high P soils experienced a progressive and selective accumulation of Ins6P during the decades of monocultural rice cropping characterizing the soils from NW Italy Po plain (Miniotti et al., 2016; Sodano et al., 2017; Zampieri et al., 2019), thanks to their greater affinity for Fe, emphasized by co-precipitation processes with respect to P_i and P-diesters (Santoro et al., 2019; Senn et al., 2015). Considering

the high relevance that Fe (hydr)oxides reductive dissolution has in the biogeochemical cycling of elements in paddy soils – demonstrated in Chapter 2 - the extent by which Ins6P is selectively accumulated over other organic compounds may be greater than what observed under aerobic conditions (Cade-Menun et al., 2015; Condron et al., 2015). Besides, the selective enrichment of Ins6P determined by abiotic stabilization through interaction with the mineral phase may be further corroborated by the larger amounts of MAOM observed in high-P soils. This material also showed a relatively high C:N ratio, suggesting that the chemical protection offered by mineral surfaces better preserved the organic compounds and slowdown their degradation (Cerli et al., 2012).
By contrast, ^{31}P-NMR spectra of medium- and low-P soils resulted in a different organic P speciation compared to what described for high-P soils, thus corroborating our first hypothesis that P speciation in soil is a function of soil total P supply. Moreover, the lower total P supply resulted in higher dynamicity of organic P forms during rice cultivation. Before rice cultivation, the spectra of medium- and low-P soils were indeed dominated by the signal of mononucleotides and β-glycerophosphates, likely related to the hydrolysis of RNA and phospholipids respectively with high pH NaOH-EDTA (Cade-Menun and Liu 2014; Colocho Hurtarte et al. 2020). The same signals were no more observed after 60 days of rice cultivation, thus suggesting that diesters might be more involved in organic P turnover at lower soil P supply than high P content. The presence of these organic P compounds was attributed to the burial of fresh plant material like leaves, husks and roots (Duersch et al. 2020), as also further corroborated by the lower C:N ratio which characterized SOM in med- and low-P soils. Moreover, these compounds are generally considered more labile than the recalcitrant Ins6P as they are weakly retained on the surfaces of Fe precipitates formed during coprecipitation processes (Santoro et al. 2019), possibly resulting in a greater availability for enzymatic hydrolysis, and thus explain their faster turnover at limited soil P availability.

4.4.2 Biotic processes controlling organic P availability

The results discussed in the in previous chapter of this thesis highlighted the important interplay between soil P pools and plant strategies to overcome P limitation and increase soil P availability. Hence, the decrease of exchangeable-P observed after rice cultivation can corroborate the role of exchangeable P pool in feeding the available one, continuously depleted by plants. As expected, orthophosphate is the most depleted form as the only one taken up by plants (Rose et al 2013), thus a selective enrichment of organic P forms is expected in the most labile pools (Kruse et al. 2015). However, this was observed only in high-P soil, and mainly attributed to a greater signal of *scyllo*-Ins6P, suggesting the intensification of microbial activity during rice growing, as *scyllo*-Ins6P is produced by microorganisms only (Liu et al., 2018). Conversely, medium- and low-P soils experienced a depletion of organic P forms during rice cultivation, with drastic losses of diesters. This highlighted an active utilization of organic P forms even under reducing conditions, by both plants and microorganisms (Wang

et al., 2022b; Rose et al., 2013). The specific enzymatic activity of Ac-PME was indeed greater in the soils with the lowest total P content with the ongoing of rice growth. In general Ac-PME activity was much higher than Alk-PME, as a consequence of soil pH (Eivazi and Tabatabai, 1977; Wu et al., 2021), which ranged between 5.9-6.9 in the twelve soils. The increase in Ac-PME activity observed after rice cultivation may be related to both microbial and root activity and may be emphasized by acidification strategies, particularly pronounced in the most P deficient soils, consistently to the results discussed in chapter 3. Conversely, the Alk-PME activity decreased after 60 days of rice cultivation, possibly due to the same pH changes which concurred to increase Ac-PME activity.

A positive correlation was observed between soil P monoester content and plant P uptake as well as between enzyme activity and the free particulate organic matter pool. It can be inferred that the latter, representing the fresh/undegraded plant residues, rich in labile substrates, may stimulate microorganisms to produce PME (Wu et al., 2021; Peng et al., 2021) but also other enzymes, such as phytases (Wu et al., 2021), that enhance OM decomposition and contribute to P release.

4.5 Conclusions

The studied soils, with a range of P supply, presented a distribution of P forms determined by the mechanisms governing inorganic and organic P cycling. Plants growing in high-P soils mostly utilized the inorganic P present in the soil solution, continuously fed by less labile P pools, with a limited involvement of organic P. Thus, high P soils experienced a progressive and selective accumulation of organic P, particularly Ins6P, likely occurring during the decades of monocultural rice cropping. By contrast, soils with low P supply showed a greater presence and faster turnover of β-glycerophosphates and mononucleotides, with the release of orthophosphate that contributes to feed the P pool available for plant uptake. These findings (Fig. 4.7) thus corroborated our hypothesis that organic P cycling in redox affected soils is driven by the alternance of reductive dissolution and coprecipitation processes, which in turn affect organic P fluxes from the less to the most labile P pools and viceversa, and their consequent utilization by plants. The total P supply controls these processes as in high P soils the processes are mostly governed by abiotic reactions, whereas in low P soils nutrient limitation leads the system to create a tighter cycle between organic P turnover and plant acquisition.

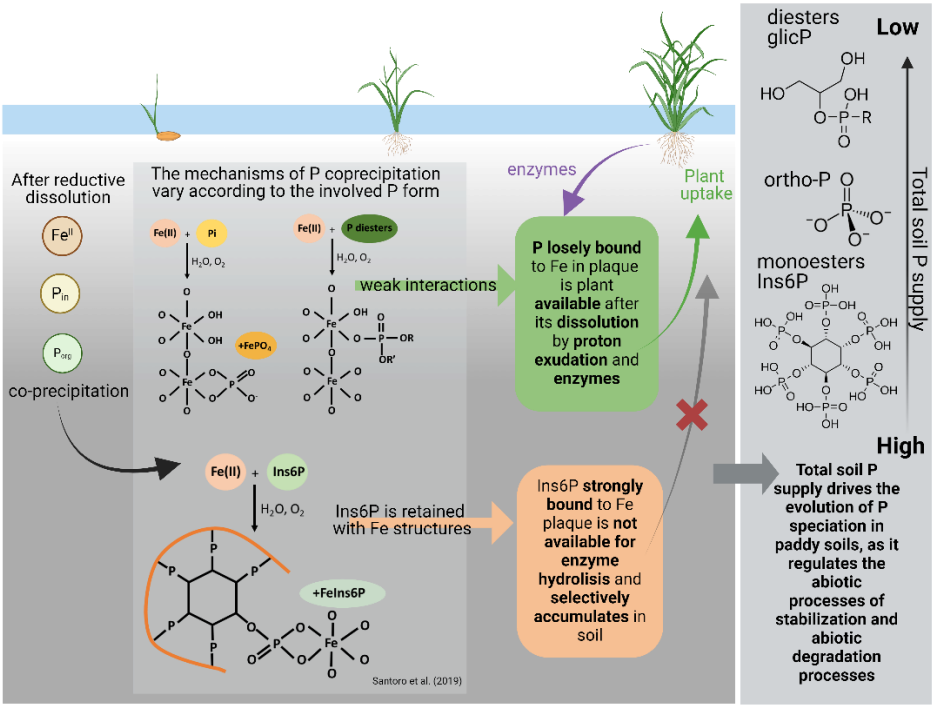

Figure 4.7 Summary of the results discussed in chapter 4, the mechanisms reported in the grey box are taken from Santoro et al. (2019).

CHAPTER 5

Root Fe plaque as a spatial-temporal dynamic P pool in rice grown under different water management

5.1 Introduction

The former chapter demonstrates that the kinetic of Fe precipitation occurring in flooded soils during rice cultivation leads to a selective enrichment of Ins6P over more labile organic P forms according to its higher affinity for Fe oxides and the total soil P supply which stimulates the utilization of labile organic P forms to plant uptake. However, the higher Eh of rhizosphere environment causes an hyperaccumulation of Fe oxides on the root surfaces (Khan et al., 2016a), thus the formation of root Fe plaque could result in a further enrichment of P forms in the oxic rhizosphere compared to the anoxic bulk soils. Besides, Fe plaque structural characteristics could represent a further driving force of the P selective enrichment. Indeed, although organic P forms are generally characterized by a faster and greater retention by Fe-precipitates compared to inorganic P, (Santoro et al., 2019), it was demonstrated that orthophosphate is preferentially retained by poorly crystalline Fe oxides (i.e. ferrihydrite), while Ins6P is mostly retained by more crystalline Fe oxides, like goethite (Celi et al., 2003; Prietzel et al., 2016). Based on these considerations, it could be hypothesized that the drivers of P speciation in the oxic rhizosphere differs from the anoxic bulk soil, and Fe plaque crystalline structure could represent the master variable controlling these processes.

The mineral composition of Fe plaque is generally recognized as a mixture of poorly crystalline oxides (i.e. ferrihydrite), and more crystalline minerals like goethite, lepidocrocite and small portions of siderite (Amaral et al., 2017a; Chen et al., 1980; Seyfferth et al., 2010b). The earlier stages of Fe plaque formation are characterized by the predominancy of poorly crystalline oxides, which in turn are transformed into more crystalline structures by the Fe(II)-catalyzed atom exchange (Boland et al., 2014; Hansel et al., 2005; Yee et al., 2006).

The introduction of water saving techniques in rice cultivation may cause a decreased Fe(II) release in porewater (Limmer et al., 2022; Miniotti et al., 2016), thus possibly explaining the limited crystallization observed in Fe plaque of rice grown under alternating wetting and drying irrigation (Linam et al., 2022). At the same time, a greater oxidation during Fe(II) oxidative precipitation led to faster formation of crystal nuclei, which are predicted to generate less crystalline structures (Chen and Thompson, 2018), further explaining the lower crystallization of root plaque.

Intermitted soil flooding may also cause a limited decrease of P release into solution (Scalenghe et al., 2012) possibly leading to an increase of solution P:Fe molar ratio. Such a factor is known to strongly impact both the mineral structures of Fe(III)-precipitates (Senn et al., 2015; Voegelin et al., 2013) and P retention mechanisms (Santoro et al., 2019). For instance, at P:Fe < 0.2 the Fe(III)

oxidative precipitation resulted in the formation of crystalline structures, followed by P sorption on these surfaces, while at higher P:Fe, Fe oxide crystallization is hindered by the rapid formation of Fe-phosphate nuclei with the consequent P retention via co-precipitation, which in turn resulted in a greater retention of Ins6P compared to inorganic phosphate (Santoro et al., 2019a; Senn et al., 2015; Voegelin et al., 2013b). Ultimately, P co-precipitation within Fe oxide structures resulted in a greater P release following their dissolution (Kraal et al., 2019), thus suggesting a possible implication to plant P uptake.

Based on these considerations, we hypothesized that the introduction of dry periods during rice cultivation could i) decrease Fe plaque crystallization according to the lower availability of Fe(II) in solution, and thus ii) change P forms and their retention mechanisms within the plaque. As a result of these modifications iii) P release from Fe plaque is a function of the interplaying processes controlled by plaque mineral composition, P retention mechanisms and plant effect on rhizospheric P cycling. We therefore aimed to investigate the effects of water management techniques on i) Fe plaque crystallization, ii) forms of P retained by these surfaces, and ultimately iii) the availability of P retained by plaque for rice plant uptake.

5.2 Material and methods

5.2.1 Mesocosms study design

The experiment was carried out at the Rice Research Center of the Ente Nazionale Risi (Castello d'Agogna, NW Italy) during the rice growing season 2022 (May-September). Rice seeds (*Oryza sativa L.* cv. Selenio) were germinated in a greenhouse and after 7 days transplanted into 1 m^3 mesocosms (Fig. 5.1), formerly filled with one of the twelve soils described in chapter 2, characterized by a low P supply (Table 2.3, soil LP d). The mesocosms were set up in a completely randomized split-plot design to test, in triplicates, three water management techniques and one level of P fertilization (plus-P, 46 kg P ha^{-1}) compared to a control without fertilization (no-P). The tested water management techniques were water seeding with i) continuous flooding (WFL), ii) alternating wetting and drying (AWD), and iii) dry seeding with delayed continuous flooding (DFL). The WFL mesocosms were maintained flooded until rice maturity, while AWD mesocosms were dried at the beginning of tillering (20 days after sowing - DAS) until the redox potential (Eh) reached values above +105 mV, then flooded again. The DFL mesocosms were flooded at the beginning of tillering (20 DAS), and then under continuous flooding until rice maturity. Flooded conditions were maintained throughout the experiment with municipally-treated drinking water or rainwater (water depth: 2–10 cm) until 1 week before harvesting, when the paddies were drained, as common farming practice.

Rhizon samplers (Rhizon MOM 19.21.21F, Rhizosphere, Wageningen, The Netherlands) were installed vertically in each mesocosm in the proximity of the root system, and the soil solution collected weekly and analyzed for P and Fe(II)

concentrations. Phosphate and aqueous Fe(II) concentrations in the soil solution were determined immediately after porewater sampling, by the Murphy and Riley and 1,10-orthophenanthroline colorimetric methods (Loeppert and Inskeep, 1996; Murphy and Riley, 1962), respectively. The molar ratio between P and Fe(II) was calculated using their molar concentration in the porewaters.

Figure 5.1 Pictures of the macrocosm experiment at a) 0 days after sowing (DAS), b) 30 DAS, c) 90 DAS, and d) harvesting (120 DAS).

5.2.2 Plant sampling and analysis

Plants were collected at tillering (30 DAS), mid stem elongation (60 DAS), heading (90 DAS) and harvesting (120 DAS) development stages. At each sampling time, after the determination of the dry biomass, P contents were determined in all plant parts (shoot, root, and panicle). The P concentration in plant tissues was determined on dry plant material (50 mg) after sulfuric-perchloric digestion and colorimetric quantification of P in the extracts using the malachite green method (Ohno and Zibilske, 1991). To characterize root Fe plaque one plant per treatment in each sampling time was dig from the soil, and the rhizosphere soils adherent to rice roots were removed by gently washing with deionized water. This process was repeated until no visible soil particles remained on the roots. The cleaned root system was bisected longitudinally creating two mirror images of the root system: one half was utilized for the wet chemical extraction, and the other half was utilized for intact Fe plaque spectroscopic analyses.

5.2.3 Fe plaque characterization

Wet chemical extraction

Following the procedure proposed by Yang et al. (2018), the first root sub-sample was shaken with 25 mL of a 0.2 M ammonium oxalate–0.14 M oxalic acid solution at pH 3.2 in a flask at 25 °C with a speed of 150 rpm for 2 h to extract amorphous Fe forms (AAO-Fe). Roots and flask after extraction of AAO-Fe were rinsed with deionized water and then 20 mL of 0.3 M sodium citrate, 2.5 mL of 1.0 M sodium bicarbonate solutions and 1.5 g of sodium dithionite salt were added. The samples were shaken at 150 rpm for 2 h to extract crystalline iron (hydr)oxides (DCB-Fe). The AAO- and DCB-Fe in the extracting solutions after filtration were determined by atomic absorption spectrometry (AAS, PerkinElmer AAnalyst 400, Norwalk, CT, USA).

Spectroscopic techniques

The second root sub-sample with intact Fe plaque was gently sonicated (20kHz applied for 2 h at 25°C) to physically remove Fe plaque without altering its mineral structures. After sonication, the suspension with dislodged Fe plaque was vacuum filtered through a 0.2 μm nitrocellulosic filter membrane. Once dry, the filters were utilized for Fe plaque characterization via spectroscopic techniques. Although the physical removal of Fe plaque did not result in the 100% collection of Fe plaque, this procedure was demonstrated to be able to capture the whole heterogeneity of rice root system without preferentially extracting a specific form of Fe plaque (Amaral et al., 2017). For this reason, we will hereafter refer to the filters as "Fe plaque". Total elemental composition was determined via x-ray fluorescence (Bruker S1 Titan 600 XRF). On the same samples Fourier-Transform Infrared spectra were collected in Attenuated Total Reflectance mode (ATR FT-IR) in the region from 400 cm^{-1} to 4000 cm^{-1} with a resolution of 4 cm^{-1}, using a Nexus 670 ThermoNicolet ATR FT-IR spectrometer. All the spectra were background subtracted during the acquisition. The final spectra were obtained after the baseline correction and the normalization by imposing the highest peak equal to 1, using OriginPro 2023 software. Powder X-ray diffraction (XRD) was performed by Bruker D8 XRD instrument equipped with Cu Kα radiation (λ = 1.5418 Å, 40 kV, 40 mA) and a high-resolution energy-dispersive 1D detector (LYNXEYE). Scans were acquired from 10° to 70° 2θ at a speed of 1° 2θ min^{-1}. Background subtraction was performed with Commander software (Bruker), and subsequently phase identification was carried out using DIFFRAC.EVA V7 software (Bruker).

P-k-edge XANES spectroscopy

On the intact Fe plaque deposited on the nitrocellulosic filter membrane, phosphorus K-edge X-ray absorption near edge structure (XANES) experiments were conducted at the National Synchrotron Light Source II (NSLS-II), Brookhaven, Upton, NY, United States. The 7-ID spectroscopy soft and tender 2 (7-ID-SST-2) beamline was equipped with a Si(111) monochromator.

Measurements were performed in partial electron yield (PEY) mode with a nominal resolution of 5.0 eV (2105 to 2135 eV; 2205 to 2350 eV) and 0.25 eV (2135 to 2205 eV). The PEY signal was normalized to the incident beam intensity of a clean gold grid to eliminate the effects of any incident beam fluctuations and optics absorption features. To minimize X-ray absorption by air, the sample compartment was under ultra-high vacuum, and multiple spectra were collected and averaged. The standards included in the LCF were: potassium dihydrogenphosphate (KH_2PO_4, Sigma-Aldrich - St. Louis, MO, USA) co-precipitated with ferrihydrite (inorganic P), inositol hexakisphosphate (sodium salt, Sigma-Aldrich - St. Louis, MO, USA) co-precipitated with ferrihydrite (organic P), and ammonium dihydrogenphosphate ($NH_4H_2PO_4$ - Sigma-Aldrich - St. Louis, MO, USA). Data analysis (background subtraction, normalization, and linear combination fitting) was performed using Athena software (Ravel and Newville, 2005), and following the protocol described by Werner and Prietzel (2015). Further details regarding standard synthesis, data normalization and linear combination fitting analysis are provided in the supplementary materials.

5.3 Results

5.3.1 Iron and phosphorus release into soil porewater

The temporal trends in porewater Fe(II) and P differed significantly according to water management (Fig. 5.2a), while they were less influenced by P fertilization. In all cases the Fe(II) porewater concentration reached a maximum within 25 days after flooding, hence at 25 DAS in WFL (1.30 mM) and AWD (1.53 mM) and at 45 DAS in DFL (1.50 mM). Subsequently, in both WFL and AWD the porewater Fe(II) release dropped until rice harvesting, with a more pronounced effect in the latter treatment. Conversely, in DFL a steady Fe(II) release during the whole rice cycle was observed. Despite not significant, in all the water treatments, no-P mesocosms showed a slightly lower Fe(II) release after the stem elongation phase (aprox 60 DAS). The porewater P concentration differed significantly among water management techniques and P fertilization. Generally, the trend of P release in porewater was similar to Fe(II) release, except for the DFL treatment. The maximum P release was observed at 20 DAS in WFL (0.12 mM) and AWD (0.09 mM), subsequently in WFL it remained stationary close to 1 mg L^{-1}, while in AWD a pronounced decrease was observed after 60 DAS (0.24 mg L^{-1}). Conversely, in DFL the P release in porewater was steady close to 0.25 mM during the whole growing season without specific temporal or treatment differences (Fig. 5.2b). The effect of P fertilization on P concentration was particularly evident at 20 DAS, with plus-P (0.10 mM) > no-P (0.02 mM), and then it declined resulting in no significant differences between the fertilization treatments.

The P:Fe molar ratio was significantly influenced by the interaction between sampling time and water management, and by the P fertilization treatments. During the first 14 days, no values were available in DFL, because of the delay in soil flooding, while in AWD and WFL the P:Fe molar ratios ranged from 0.04

to 0.44 (Fig. 5.2c). In all cases WFL showed slightly lower values than AWD, albeit the differences were not significant. At 21 DAS, in DFL the P:Fe molar ratio was 0.77, and significantly higher than WFL and AWD, which in turn were comparably close to 0.02. From 52 DAS, the values in AWD were close to 0.3, and always higher than WFL and DFL, which were respectively lower than 0.02, and higher than 0.03. However, the differences between the latter two were not statistically significant.

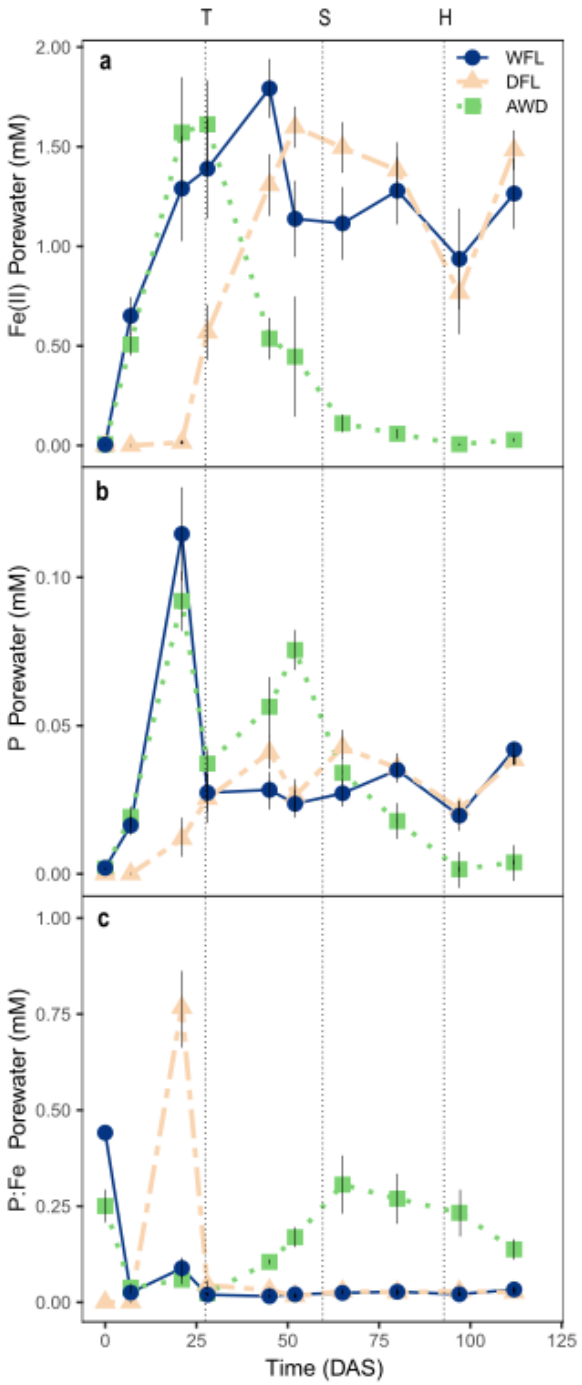

Figure 5.2a) reduced iron [Fe(II)], b) phosphorus (P), and c) P:Fe(II) molar ratio in the soil porewater solution during plant development mesocosms in alternating wetting and drying (AWD), delayed flooding (DFL) and continuous flooding (WFL) water management treatments. T: tillering; S: stem elongation; H: heading.

5.3.2 Plant development and P uptake

The application of water saving techniques did not result in significant difference in dry biomass, while a significant influence of P fertilization was observed particularly after stem elongation phase. In all the cases plus-P treatment resulted in an increase of shoot biomass, as well as in a decreased root to shoot ratio (Fig. 5.3a). The panicle dry biomass at heading was higher in plus-P treatment compared to no-P fertilization, albeit no significant differences were measured at harvesting in terms of rice yield. Indeed, the rice yield was entirely affected by the water management, with the highest yield (11 t ha^{-1}) related to DFL irrigation, followed by WFL (10 t ha^{-1}) and AWD (9.7 t ha^{-1}), which in turn resulted in the same yield level.

The plant P uptake during rice development was consistently higher in plus-P treatment compared to no-P treatment in all the sampling time. The effect of water management was instead different according to the interaction time*water treatment. In particular, in the early development stages, continuously flooded treatments resulted in higher P uptake (WFL = 15 mg; AWD = 13 mg), while after stem elongation DFL treatment resulted in the highest P uptake (Fig. 5.3b). Consistently, the straw P uptake measure at harvesting was DFL (20 kg ha^{-1}) ≥ (WFL 15 kg ha^{-1}) ≥ AWD (11 kg ha^{-1}) , and the amount of P offtake by seeds was DFL (24 kg ha^{-1}) ≥ (WFL 20 kg ha^{-1}) ≥ AWD (13 kg ha^{-1}).

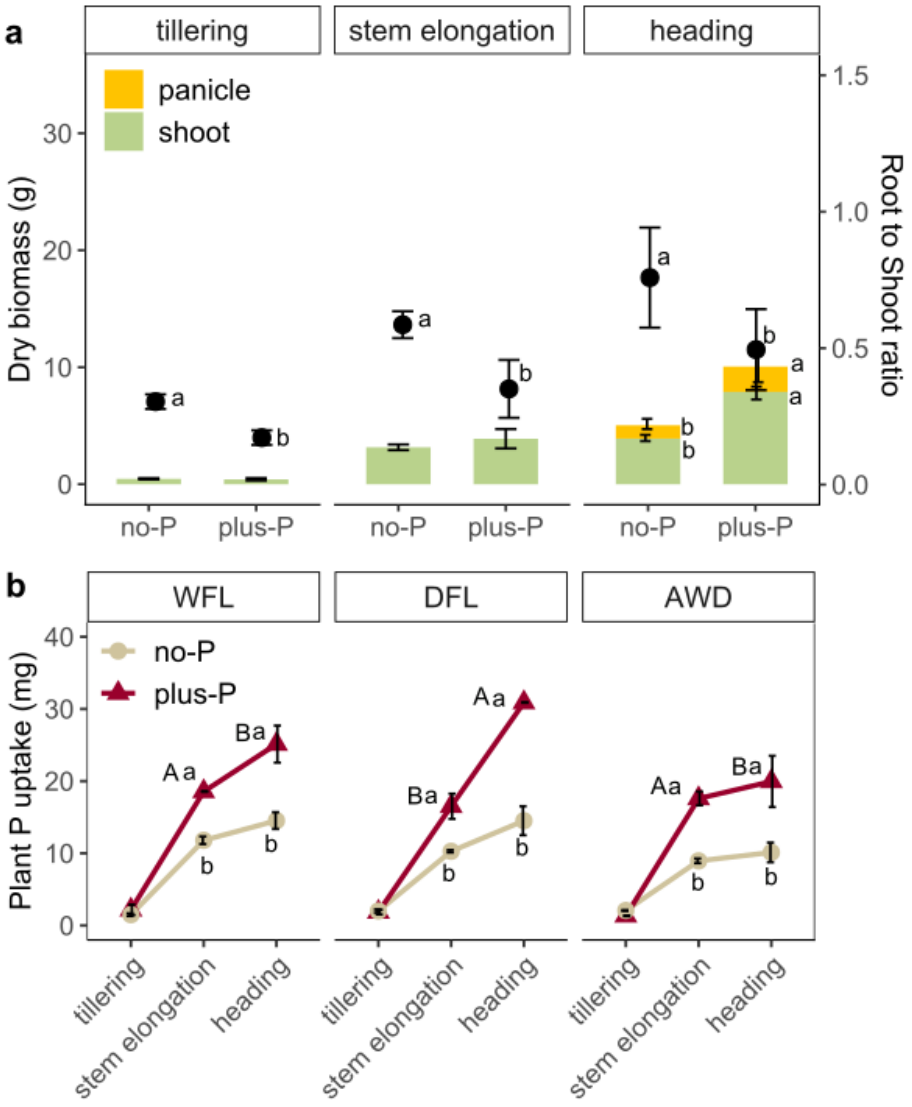

*Figure 5.3 a) average shoot and panicle dry biomass and root to shoot ratio of all water management un-fertilized (no-P) and fertilized rice plants (plus-P; 46 kg P ha^{-1}); b) P uptake of plant grown under continuous flooding (WFL), delayed flooding (DFL), and alternating wetting and drying (AWD) water management treatments, with (plus-P) or without (no-P) P fertilization; Upper case letters represent significant difference among water management, lower case letters represent statistically significant differences for the interaction time*P fertilization.*

5.3.3 Fe plaque composition and crystallization characteristics

Iron resulted the most abundant element in the plaque with an average deposit higher than 54%, followed by Si (21 %), Ca (14 %), P (10%), and other elements in lower percentage (Fig. 5.4). Total P was the fourth most abundant element in the plaque, and in all cases the highest P concentration was found at tillering compared to the other phenological stages, particularly in AWD. As expected, the highest values were generally associated to P fertilization, albeit the differences were only significant during the early development stages.

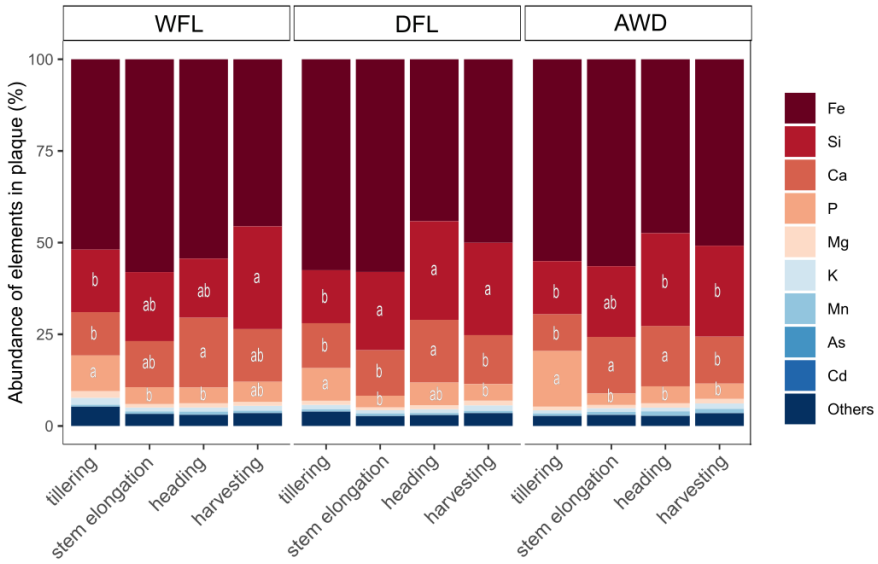

*Figure 5.4 Percentage abundance of element in Fe plaque of rice grown under continuous flooding (WFL), delayed flooding (DFL), and alternating wetting and drying (AWD) water management treatments, obtained by XRF survey. Different letters represent statistically significant differences among water management for the effect time*water management (p-value < 0.05). For the sake of graph readability standard errors are not reported.*

Wet chemical extraction resulted in all cases in the highest values of total Fe in root plaque (AAO-Fe + DCB-Fe) at tillering stage (30 mg Fe g^{-1} root), while the lowest one at stem-elongation stages (10 mg g^{-1} root). A sharpest increase was observed at heading stage, followed by a new decrease at harvesting (Fig. 5.5). During most of the growing period, the WFL and DFL were characterized by higher values of total Fe deposit than AWD, with the exemption of tillering stage when the DFL plants presented the lowest values. The wet chemical determination of Fe plaque composition showed that AAO-Fe was generally higher than DCB-Fe during most of the growing period, particularly in AWD; from stem elongation to harvesting time, the AAO-Fe in AWD (10 mg g^{-1} root) was indeed lower than WFL (13 mg g^{-1} root) and DFL (14 mg g^{-1} root), which in turn were comparable. Consistently, the DCB-Fe in root plaques was lower in the first development stages (tillering and stem-elongation), while the highest values

were observed at heading and harvesting, particularly in WFL (7 mg g^{-1} root) and DFL (8 mg g^{-1} root). At both development stages, the AWD treatment resulted in the lowest values of DCB-Fe (Fig. 5.5).

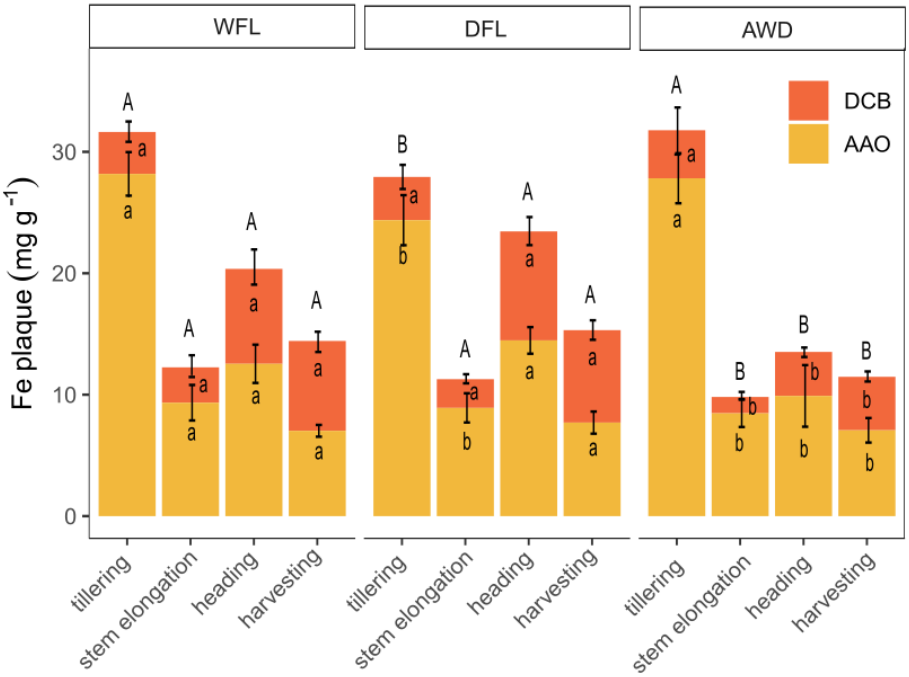

*Figure 5.5. Values of amorphous (AAO-Fe), crystalline (DCB-Fe), and total Fe in root plaques, during the development of rice plant grown under continuous flooding (WFL), delayed continuous flooding (DFL) and alternate wetting and drying (AWD). Upper-case letters represent statistical differences among water management in total Fe in plaque. Lower-case letters represent statistical differences for water management*development stage interaction*.

Consistently with wet chemical analyses, the X-ray diffraction patterns (Fig. 5.6) evidence the presence of 2-line ferrihydrite featured by two broad peaks at 60 and 36 2θ°, and goethite (25-19-12 2θ°). Interestingly the XRD patterns also display a broad peak at 30 2θ°, which could be attributed to both Fe precipitated with inorganic phosphate and/or Ins6P (Santoro et al., 2019). The other peaks were attributed to the presence of Si minerals, and soil contamination.

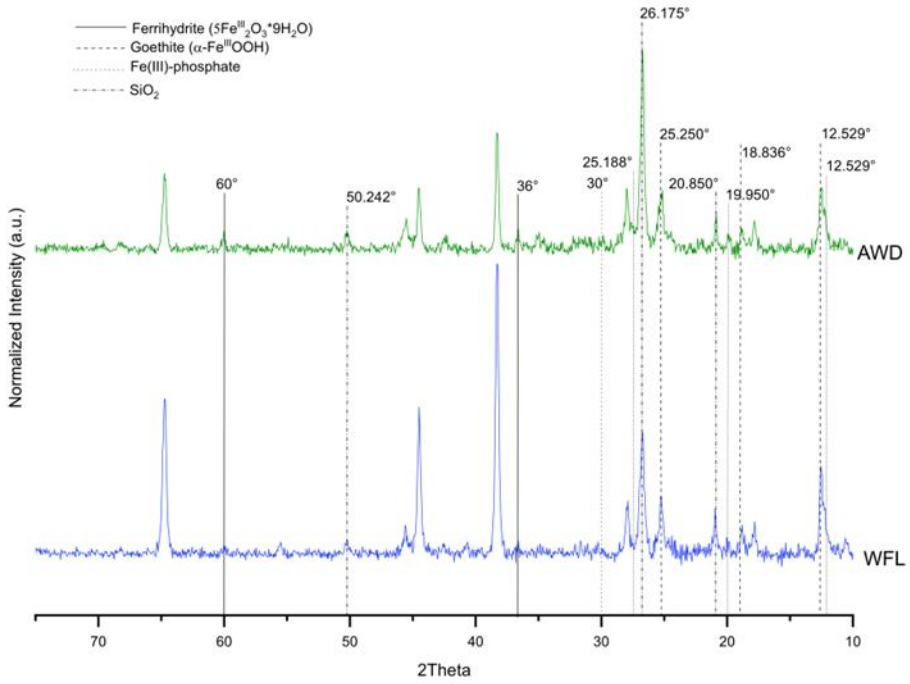

Figure 5.6 X-ray diffraction patterns of plaque from rice roots collected at 90 days after sowing under continuously flooded (WFL) and alternating wetting and drying (AWD) conditions.

5.3.4 Forms of P retained by plaque

The spectra of the synthesized standards showed distinctive features according to the P forms utilized to synthesize the materials (Fig. 5.7), as organic P showed a smaller white line (WL) intensity compared to inorganic P (Fe-P). Nonetheless the spectra of inorganic and organic P retained by ferrihydrite showed a particular pre-edge feature from 2148-2151 eV (Fig 5.7 enclosed box). In the case of Fe-P, this pre-edge feature can be considered a true pre-edge peak, while organic P had a small shoulder, in agreement with the results of Prietzel and co-authors (2016; 2018). The spectra of NH_4-P did not show the pre-edge feature, further supporting the hypothesis that this is attributed to the Fe-P interactions. Conversely, in this spectrum a specific post-edge pattern was observed. Further details regarding the main features of P-XANES spectra of standards and the implications for LCF analyses are given in Supplementary material (Section 5.3.2).

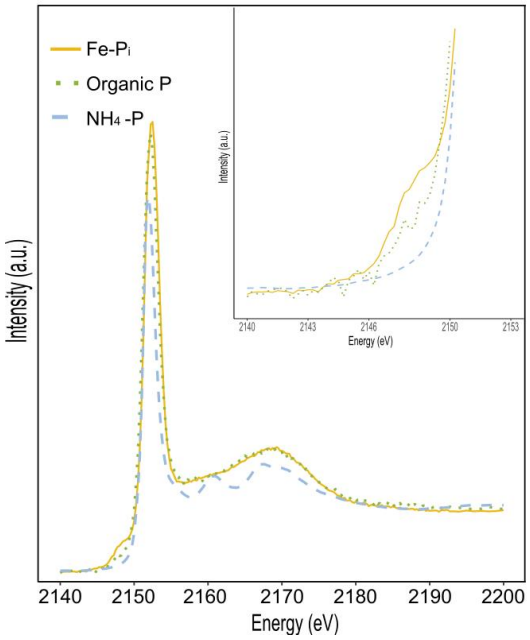

Figure 5.7 a) P-K-edge XANES spectra of orthophosphate co-precipitated with ferrihydrite (Fe-P), inositol hexakisphosphate co-precipitated with ferryhidrite (Organic P) , and ammonium phosphate (NH_4-P); enclosed box reports a close-up views of pre-edge regions.

The P K-edge XANES spectra of Fe plaque samples resulted in adequate signal to perform LCF fitting (Fig. S5.4, and Fig S5.5). The R factor values were slightly lower than those reported in literature for other P matrices (i.e. soil, slurry, etc), however the comparison between the spectra of the sample and the LCF showed that the latter closely resemble the former (Fig. 5.8). As further discussed in Supplementary material the R factor is not the only indicator of the quality of the fitting, and thus we concluded that the standards we selected for LCF are adequate to describe the P speciation of Fe plaque samples.

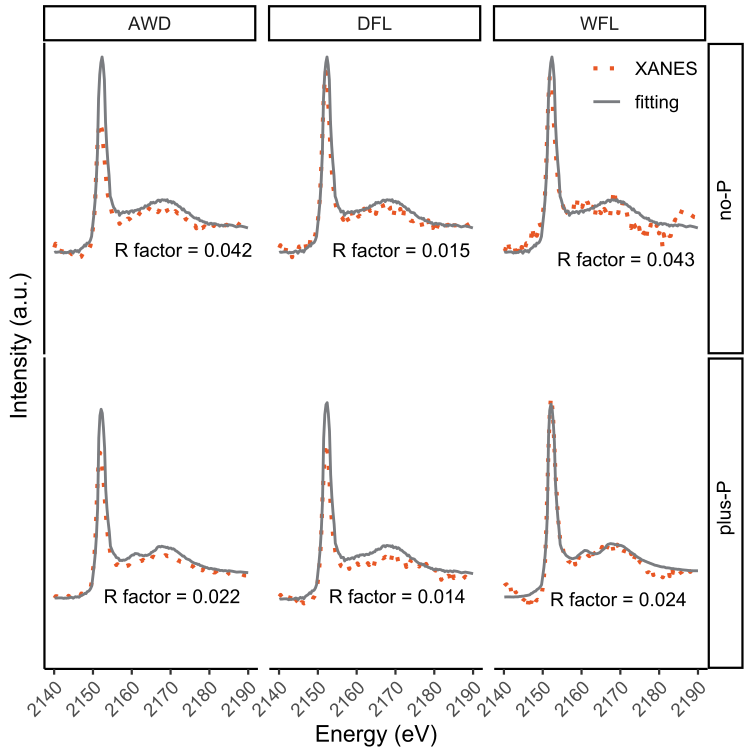

Figure 5.8. Comparison between P K-edge XANES spectra of Fe plaque of rice grown under alternating wetting and drying irrigation (AWD), delayed flooding (DFL), and continuous flooded soil (WFL), with 46 kg of P per ha of P fertilization (plus-P) or without P fertilization (no-P) and the relative spectra obtained by the weight of the standard included in the LCF (i.e. Fe-P_i, Organic P and NH_4-P).

The P forms present in the plaque were mostly influenced by P fertilization, followed by water management (Table 5.1). The P-XANES spectra of plaque collected after P fertilization resulted in greater amount of total P, which was mostly composed of inorganic P forms including the P fertilizer, while organic P forms were detected only in the latter development phases of DFL and AWD. The addition of P led to a distribution of the inorganic form between P-Fe and P-NH_4^+, with the former mostly retained in the early development stages and the latter progressively accumulating with plant growth. The depletion of inorganic P from plaque was particularly evident between tillering and stem elongation in all water treatments. In the subsequent phases, WFL presented the greatest amount of inorganic P while DFL and AWD showed the lowest inorganic P values and accumulation of organic P. Conversely, when no P fertilizer was supplied to the mesocosms, the amount of total P retained in the plaque was lower and characterized by a minor inorganic to organic P ratio. Indeed, inorganic P was mostly detected in the early development stages and represented only by P-Fe, while after stem elongation the majority of P in the plaque was attributed to organic P, especially in AWD.

Table 5.1 Linear combination fitting results presented as percentage of fitted compound and concentration of P forms determined in root plaque of plants grown under continuous flooding (WFL), delayed flooding (DFL), and alternating wetting and drying (AWD) with a P fertilization of 46 kg P ha^{-1} (plus-P), or with natural soil P supply (no-P).

Treatment			$Fe\text{-}P_i$	Organic P	NH_4-P	$Fe\text{-}P_i$	Organic P	NH_4-P
			%			mg P g^{-1} root		
WFL	no-P							
		tillering stem	100	0.00	0.00	5.01	0.00	0.00
		elongation	--	--	--	--	--	--
		heading	52.9	47.1	0.00	2.02	1.80	0.00
		harvesting	0.00	100	0.00	0.00	2.24	0.00
	plus-P							
		tillering stem	91.0	0.00	9.03	6.45	0.00	0.64
		elongation	43.4	56.6	0.00	1.31	1.71	0.00
		heading	73.3	0.00	26.7	3.86	0.00	1.41
		harvesting	30.6	0.00	69.4	1.40	0.00	3.17
DFL	no-P							
		tillering stem	97.1	2.90	0.00	5.54	0.17	0.00
		elongation	48.0	51.9	0.00	1.15	1.25	0.00
		heading	56.5	43.6	0.00	1.43	1.10	0.00
		harvesting	0.00	100	0.00	0.00	2.67	0.00
	plus-P							
		tillering stem	83.0	0.00	17.0	6.64	0.00	1.36
		elongation	53.3	15.3	31.4	2.00	0.58	1.18
		heading	34.0	0.00	66.0	1.80	0.00	3.49
		harvesting	0.00	75.0	25.0	0.00	2.96	0.99
AWD	no-P							
		tillering stem	100	0.00	0.00	5.89	0.00	0.00
		elongation	100	0.00	0.00	2.23	0.00	0.00
		heading	0.00	100	0.00	0.00	2.07	0.00
		harvesting	0.00	100	0.00	0.00	2.80	0.00
	plus-P							
		tillering stem	98.0	0.02	1.95	9.97	0.00	0.20
		elongation	80.6	10.2	9.2	3.98	0.50	0.45
		heading	54.2	17.6	28.2	2.05	0.67	1.07
		harvesting	0.00	40.2	59.9	0.00	1.86	2.78

FT-IR spectra of the plaque show significant differences with the water treatments but not with P fertilization. The most significant bands were in the 1400–400 cm^{-1} region and attributed to P-O stretching and bending modes. Particularly, in the spectra collected at stem elongation (Fig. 5.9a), the main P-O region was asymmetric and composed of two bands at 1030 and 1000 cm^{-1} attributed to νas(P-O) and νs(P-O), respectively (Santoro et al. 2019 and references therein). In the spectra of the plaque collected at rice heading, these bands remained similar in WFL and DFL, while in AWD the bands became more symmetric as the band at 1030 cm^{-1} was more intense and the one at 1000 cm^{-1} decreased (Fig. 5.9b).

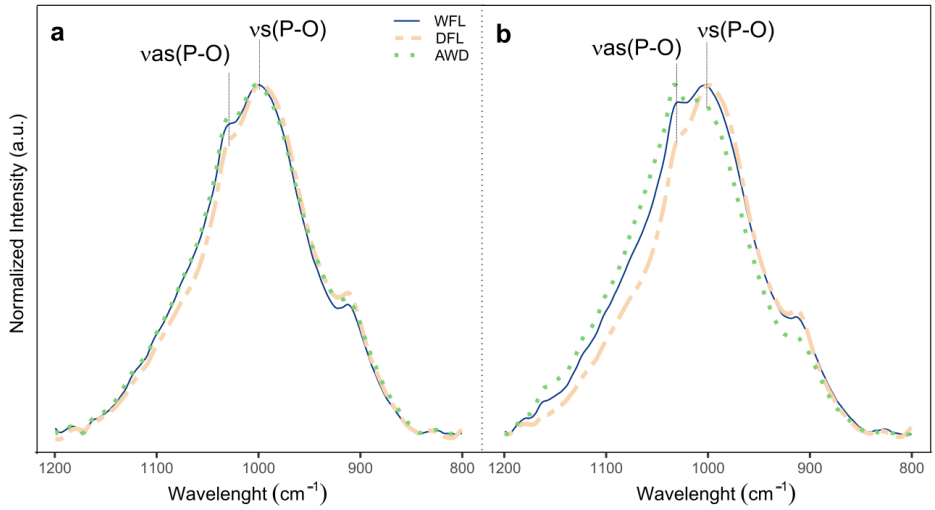

Figure 5.9. FT-IR spectra of Fe plaque collected at a) stem elongation, and b) heading of rice plant grown under continuous flooding (WFL), delayed continuous flooding (DFL) and alternate wetting and drying (AWD) in the 1200–800 cm^{-1} region.

5.3.5 Relationship among soil porewater composition, Fe plaque and plant P uptake

The aqueous Fe(II) concentration was significantly and positively correlated with the total and DCB-extractable Fe deposit on rice roots (r=0.26, $p < 0.05$), particularly in the latter stages of WFL and DFL irrigation (Fig. 5.10a). Notwithstanding the lack of correlation between the porewater P concentration and P deposit in plaque (r =0.21, $p > 0.05$), the latter was positively correlated with total Fe (Fig. 5.10b), and Ca content within the plaque (Fig. 5.10c). The AAO-extractable Fe only slightly correlated with P deposit in the plaque (r =0.17, p=0.07), and no correlation was observed with DCB-extractable Fe.

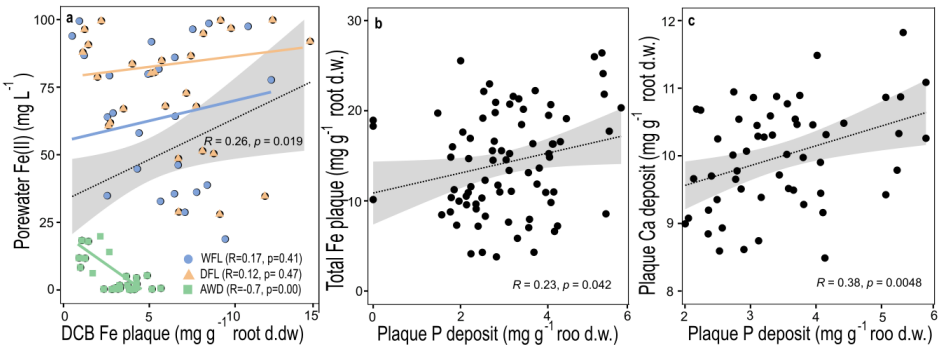

Figure 5.10. Correlations among reduced iron [Fe(II)] in porewater and dithionate (DCB) extractable Fe in plaque (a); total Fe in plaque and plaque P deposit (b); and total Ca in plaque and P deposit (c). The black line with confidence interval represents the correlation computed on the whole dataset, while the colored lines represent the correlation computed by continuous flooding (WFL), delayed continuous flooding (DFL) and alternate wetting and drying (AWD) treatment

Generally, the plant P uptake strongly correlated with the amount of P in plaque (r =0.77, p<0.05), while weaker correlations were observed with the P porewater concentration (r =0.15, p>0.05). Particularly, the best correlation between plant P uptake and P content in plaque was observed in AWD (r =0.48, p<0.05) and DFL (r =0.82, p<0.01), while in WFL plant P uptake was mostly related to porewater P concentration (r =0.47, p<0.05), rather than P retained in plaque (r =-0.19, p>0.05). In all cases, plant P uptake more positively correlated with AAO-extractable Fe than DCB-Fe in plaque, particularly at stem elongation and heading (r =0.21, p< 0.05), however a slightly positive correlation was observed at heading between P uptake and DCB-Fe in plaque (r =0.13, p<0.05).

5.4 Discussion

5.4.1 Porewater chemistry governs Fe plaque composition and recrystallization processes

The formation of root Fe plaque resulted from the oxidation of the aqueous Fe(II) concentration by the O_2 released from rice roots into the rhizosphere; as a consequence the formation of root Fe plaque was widely observed in rice cultivated under continuously flooded soils (Khan et al., 2016). The introduction of dry periods during rice cultivation decreased Fe(II) concentration into porewater and its fluxes to the roots, likely explaining the lower Fe plaque formation observed in AWD, and supported by the positive correlation between soil porewater Fe(II) concentration and total Fe plaque deposit on rice roots (Limmer et al., 2022; Linam et al., 2022; Zhou et al., 2018). In DFL, a lower Fe plaque deposit could be expected because the early development stages occurred under dry soil conditions, however after the instauration of reducing conditions the prompt activation of rhizospheric oxygenation mechanisms observed in Chapter 2 likely led to a fast plaque precipitation. Moreover, the high P concentration found in the porewater could have further contributed to increase Fe plaque deposit, as a faster Fe(II)-oxidation was observed at increasing P concentration in solution (Santoro et al., 2019; Voegelin et al., 2013).

In the subsequent growing phases the progressive increase of crystalline Fe phases in plaque could be attributed to the continuous supply of Fe(II) into the solution, ensured by the strongly reducing conditions we observed in WFL and DFL, which in turn may favor the evolution of plaque mineral phase via Fe atom exchange mechanism. Indeed, aqueous Fe(II) concentration is considered the master variable in catalyzing ferrihydrite recrystallization in soil (Boland et al., 2014; Grigg et al., 2022), as it regulates the process by which the aqueous Fe(II) is adsorbed onto Fe(III)-(hydr)oxides surfaces and oxidized to highly reactive structural Fe(III). The subsequent transfer of electrons to structural Fe(III) causes the release of Fe(II), and thus the recrystallization of the Fe(III) (oxyhydr)oxide phase (Boland et al., 2014; Handler et al., 2009; Hansel et al., 2005). Our results well corroborate this hypothesis because of the positive correlation between the aqueous Fe(II) concentration and DCB-extractable Fe in plaque observed in WFL and DFL treatments. On the other hand, the decreased Fe(II) concentration observed in the latter stages of AWD and its negative correlation with the DCB-extractable Fe within the plaque suggest that AWD decreased crystallization processes of root plaque. However, besides the limited aqueous Fe(II) availability, other factors can affect the recrystallization processes.
Despite AWD irrigation led to a slight decrease of porewater P concentrations, the P:Fe molar ratio of the solution was higher with respect to the continuously flooded treatments (WFL and DFL). Increased P:Fe molar ratios in solution during Fe(III) oxidative precipitation are reported to favor the formation of poorly crystalline minerals (Senn et al., 2015; Seyfferth, 2015; Voegelin et al., 2013). Particularly at P:Fe > 0.2 the formation of lepidocrocite is reported to be superseded by the formation of poorly crystalline ferrihydrite (Châtellier et al., 2013; Voegelin et al., 2013), which is in turn was hindered at P:Fe > 0.5 by the formation of amorphous Fe(III)-phosphate (Santoro et al., 2019; Senn et al., 2015). This can thus explain the lower Fe plaque crystallization observed in the phases characterized by greater P:Fe molar ratios in AWD. Moreover, the presence of Si and dissolved organic ligands was demonstrated to be highly effective during the stabilization of the Fe(III)-precipitates structures against the Fe(II)-catalyzed recrystallization (Jones et al., 2009; Schulz et al., 2022; ThomasArrigo et al., 2018).

5.4.2 Fe plaque crystallization regulates P retention by plaque

Phosphorus accumulation at the rhizosphere surfaces was firstly dependent on the amount of total Fe in the plaque, as deduced by the positive correlation reported between total Fe and P deposit. Consistently with former literature reports (Celi et al., 2020, 2003; Martin et al., 2004), the better correlation observed between P deposit and AAO-extractable Fe rather than DCB-extractable Fe suggests that poorly crystalline forms retained more P than the crystalline ones, corroborating our second hypothesis on the role of Fe mineral structure on P retention. However, from the deconvolution of P-XANES spectra it was not possible to quantify the amount of P retained by each type of Fe oxides, as further detailed in Supplementary Materials.

During the whole rice growing season the amount of P retained by plaque showed variations in terms of both quantity and forms. In the no-P treatments, inorganic P prevailed in the first phases of rice growth and was progressively replaced by organic P, which in turn could be related to the presence of different organic molecules, as discussed in supplementary materials. Conversely, in the plus-P treatments, organic P scarcely contributed to the amount retained in the plaque in WFL, whereas in DFL and AWD organic P was found in the plaque especially at last stages of growth. As discussed in chapter 4, in the no-P samples the more labile organic P forms (i.e. orthophosphate diesters, organic polyphosphate) were predominant over the recalcitrant forms (i.e. inositol phosphates). The limited P availability could have stimulated the release into solution of labile organic P forms, which, in turn, were promptly retained by Fe plaque, explaining the higher concentration of organic P measured in no-P compared to plus-P treatment.

In the soils where P was added, inorganic P bound to Fe increased at all phenological stages by 30% on average compared to no-P samples. In addition, a derived-P fertilizer form was surprisingly found on plaque surfaces, although the added ammonium phosphate is quite soluble and unlikely expected to precipitate as insoluble salt. However, considering the greater concentration of inorganic P measured in plus-P compared to no-P plaque, it is likely that the fertilizer was partly dissolved releasing orthophosphate and ammonium in the soil solution, and subsequently physically entrapped within the Fe plaque as ammonium phosphate, although further investigation is required to confirm this hypothesis.

Based on these considerations, the P present in the plaque seems to be retained by adsorption and precipitation mechanisms, combined with physical entrapment, as a function of P supply and water management. In support of this, FT-IR spectra of the plaque collected in WFL and AWD treatments at stem elongation stage revealed the presence of adsorbed P within the newly formed plaque structures, consistently with the solution P:Fe ratios. The P:Fe < 0.2 observed in WFL and AWD suggests that during the early development phases, when both treatments were maintained under the same flooded soil conditions, P was retained mainly by adsorption mechanisms on the newly formed poorly ordered Fe phases, as found by Santoro et al. (2019). Within the progress of rice growing season, the P-O stretching band became more symmetric in AWD compared to WFL, as observed in the FT-IR spectrum of plaque collected at heading stage, thus suggesting a greater presence of coprecipitated over adsorbed P in plaque. Indeed, according to the results of Santoro et al. (2019), the presence of co-precipitated P within Fe oxide structures led to a more symmetric intensity of the two main P-O stretching bands compared to the one typical of adsorbed-P. Such an effect was attributed to the presence of non-protonated phosphate ion within Fe(III)-phosphate precipitates, compared to the formation of P inner-sphere complexes during P adsorption within Fe oxides (Arai and Sparks 2001).

The delayed soil flooding provided by DFL caused an increased release of P into solution, leading to higher P:Fe ratios in the first rice development phases compared to water seeded treatments. However, this does not result in the dominance of co-precipitation mechanisms, as observed in FT-IR spectra of plaque collected at stem elongation. With rice growth, the continuous flooding

conditions in DFL ensured lower P:Fe ratios, matching those observed in WFL with the dominance of P adsorption mechanisms. These results corroborate our hypothesis that porewater chemistry controls not only the processes of Fe plaque formation and temporal transformations, but also the mechanisms of P retention likely contributing to the diversified role of plaque in P uptake.

5.4.3 Role of Fe plaque on P availability to rice plants grown under different water management techniques

The total Fe plaque deposit on rice root showed a variation during the rice growing cycle, which cannot be entirely related to the porewater Fe(II) kinetics. Indeed, the abiotic Fe(III) oxidative precipitation only partially explains the formation of Fe plaque, as the biotic microbially driven reactions (Maisch et al., 2019) and ability of rice plants to shape the rhizospheric environment discussed in chapter 3 should also be taken into account. In particular, the pronounced decrease of total Fe plaque observed at stem elongation could be explained by the highest P demand for plant P uptake reported in this growing phase (Wissuwa, 2005), because rice plants promoted the dissolution of Fe plaque to acquire P. These hypotheses are further supported by the strong positive correlation between P deposit in plaque and plant P uptake, especially evident in DFL and AWD. Although the same decrease of P concentration in plaque between tillering and stem elongation was observed also in WFL, the correlation between plant uptake and plaque P deposit was less evident in this treatment, which, in turn, resulted in a greatest dependency on porewater P concentration for plant P uptake.

These results suggested that the formation and subsequent structural evolution of Fe plaque strongly affects the P fluxes from the anaerobic/oxidizing bulk soil to plant uptake, and the mechanisms by which P is retained by those surfaces play a pivotal role in determining P availability for rice grown under different water saving techniques. Indeed, the presence of co-precipitated P rather than adsorbed P within ferrihydrite structures led to a faster and greater dissolution of Fe oxides. It is likely that the P co-precipitated within the Fe plaque could be dissolved immediately after its formation to meet the plant demand of P. As the plant strategies to acquire P can be very active in shaping the rhizospheric environment during the earlier growing phases - as demonstrated in chapter 3 and supported by Bhattacharyya et al. (2013) - the amount of P likely co-precipitated in the early formation of plaque with DFL could have favored plaque dissolution, explaining the greater P availability from plaque to plant, compared to the other treatments. However, the time resolution of the Fe plaque sampling could not be enough representative of the short term equilibria which govern the formation of Fe(III)-phosphate coprecipitates and their subsequent dissolution for plant P uptake. Conversely, the presence of co-precipitated P in the latter phases of AWD likely led to a lower P uptake compared to DFL, because of the temporal decoupling between plant demand and P release from Fe plaque, similarly to what discussed in Chapter 2. Indeed, the lower P:Fe molar ratio observed in the early development of AWD and the consequent P retention via adsorption led to a limited P release during the Fe plaque dissolution at stem elongation (Kraal et al.,

2019), while in the subsequent growing phases the lower crystallization of AWD plaque and the presence of co-precipitated P within its structures may have favored P release, available for plant uptake, in agreement with its positive correlation with P deposit into plaque.

Under continuously flooded conditions, the limited formation of Fe-phosphate coprecipitates into plaque possibly explained the negative correlation between plant uptake and plaque P deposit. Nonetheless, in this case the plant P demand is fulfilled by the porewater, which can be, in turn, re-supplied by P released from Fe plaque crystallization processes, as supported by the positive correlation between P uptake and DCB-extractable Fe in plaque. Indeed, the Fe(III)-precipitate aging - related to the formation of a more crystalline structure - was reported to favor P release, consequent to the decreased surface area and sorption capacity (Nenonen et al., 2023; Senn et al., 2017). The temporal differences in the correlation among plant P uptake, AAO-extractable and DCB-extractable Fe in plaque further support these hypotheses, as the former strongly correlated with plant uptake in the early development stages. Conversely, DCB-extractable Fe better correlated with plant uptake after heading, likely when the Fe(II)-catalyzed recrystallization may represent the dominant mechanism in Fe plaque evolution because of the high Fe(II) porewater concentration (Boland et al., 2014; Grigg et al., 2022).

Nevertheless, the release of P into solution can be further complicated by the re-adsorption of the released P (Wang et al., 2017), and by the interaction with other elements, present in the plaque structure, such as Ca (Nenonen et al., 2023; Senn et al., 2017). These re-adsorption processes resulted in a stronger retention of organic P forms (Wang et al., 2017), supporting the limited Ins6P release observed during ferrihydrite aging compared to orthophosphate (Chen et al., 2020; Senn et al., 2017). This could explain the selective enrichment of organic P forms over inorganic P we observed in plaque during time. In addition, organic P forms need to be hydrolyzed to inorganic P before becoming available to rice plants (Rose et al., 2013; Santoro et al., 2023). However, Fe oxides are known to retain the enzymes themselves, while inhibiting their activity (Giaveno et al., 2010; Tang et al., 2006), further contributing to the pronounced accumulation of organic P in plaque during time.

5.4 Conclusions

The dynamic evolution of root Fe plaque caused by both abiotic and biotic processes profoundly affects P cycling in paddy soils, and it might positively contribute to P availability for rice plants with the introduction of water-saving techniques. Indeed, the modification of porewater chemical composition after the instauration of dry conditions affects not only Fe plaque formation, but also its structural transformation, and subsequent release for plant uptake. The formation of poorly crystalline structures under AWD was related to the concomitant limited availability of aqueous Fe(II) for the transformation processes, and to the presence of phosphate nuclei within the plaque structure, as the high P:Fe molar ratio in the porewater likely contributes to the precipitation of Fe(III)-phosphate nuclei. Such a process might further hinder the crystallization of plaque during wet periods, but on the other hand it might have contributed to a greater P release from plant uptake compared to the P sorbed onto the crystalline plaque formed under continuous soil flooding. Besides, the dynamic evolution of plaque during the rice growing season also contributed to the processes of organic P cycling in paddy soils, and particularly to the stabilization of these P forms, likely because of the inhibitory effect of plaque surfaces against the processes of enzymatic hydrolysis and organic P release to plants.

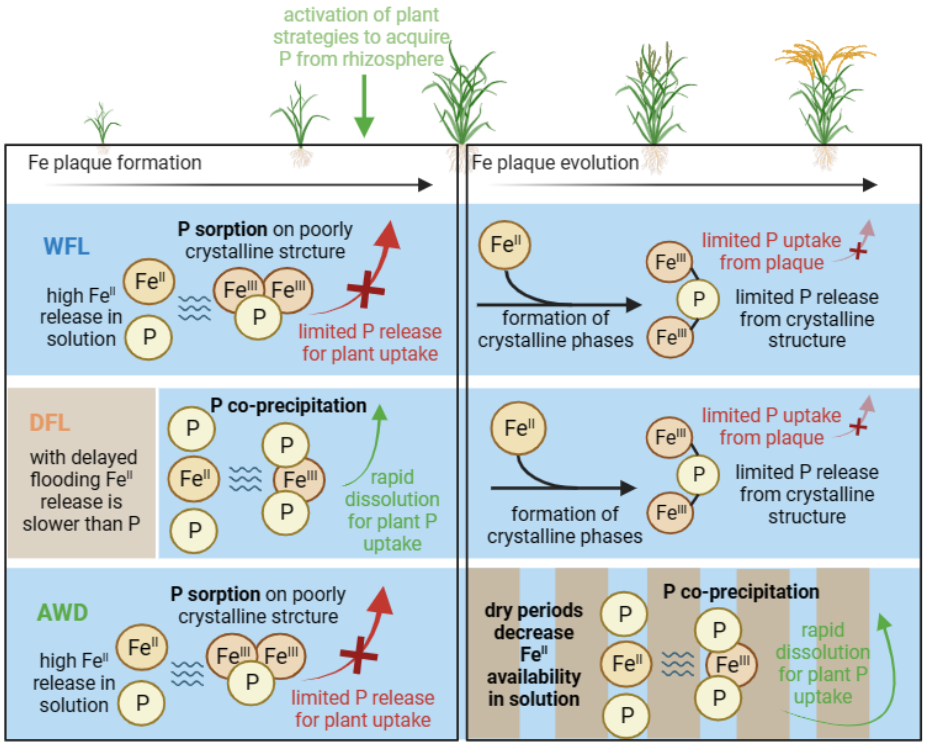

Figure 5.11 Comprehensive conceptual model of the results discussed in Chapter 5

CHAPTER 6

General discussion and conclusions

6.1 Improving the estimation of P availability in paddy soils by integrating inorganic and organic P cycling with rice plant responses

The first part of this thesis focused on the estimation of P availability in submerged paddy soils. The obtained results highlight the importance of considering the step-up redox gradient from the anoxic bulk soil to the oxidized rhizosphere during the evaluation of the processes driving P release for plant uptake. Indeed, the P released by the reductive dissolution in the anoxic bulk soil resulted only partly available to plant uptake because of the formation of Fe-P co-precipitates before the beginning of plant P demand from the solution phase. As a consequence, the chemical methods designed to estimate redox-sensitive P pool in soil (i.e. citrate-ascorbate, and/or oxalate) often over-estimated the actual soil P supply capacity because of a temporal decoupling between P release from reductive dissolution and plant P uptake. Consistently, the redox-sensitive P pool increased after rice cultivation while the easily desorbable P pool was depleted by plant uptake, therefore explaining the better representation of actual P availability given by anion exchanging resins. The interaction between Fe redox cycling and P were particularly effective in the retention of organic P forms - as Ins6P - because of the well acknowledged greater affinity of organic P during Fe(II) oxidative precipitation. Consequently, rice cultivation in submerged soils resulted in a selective enrichment of Ins6P, making this organic P form even more recalcitrant than what observed for aerobic soils.

Moving along the redox gradient from the bulk soil to the oxic rhizosphere, the reaction between the aqueous Fe(II) and the O_2 leaked from rice roots further complicates the availability of the redox-sensitive P pool. Indeed, the results suggest that the extent by which rice plants are capable to oxidize their rhizosphere may be considered a function of soil P supply, since rice plants grown in low-P soils resulted in a greater rhizosphere oxygenation gradient compared to the ones grown in high-P soils. Nonetheless, the greater Fe plaque deposit observed under P-limiting conditions did not match with a decreased P availability, likely because the proton exudation from P-starved roots triggered Fe plaque dissolution and the subsequent P release. The interplays between abiotic P stabilization during Fe(II) oxidative precipitation and plant responses also affect the cycling of organic P forms. Indeed, when P was scarcely available in soil, the organic P pool increased and was mostly composed of easily degradable forms, like diesters, characterized by a weak interaction during Fe(II) oxidative precipitation and therefore more easily hydrolysable and available to plants, as also supported by their prompt consumption during rice cultivation.

Considering the results obtained as a whole, we can conclude that P availability in submerged soils is determined by the interplays between the inorganic and organic P processes in the bulk soil and the capability of rice to shape its rhizospheric environment. Despite the role of the reductive dissolution of bulk

soil Fe (hydr)oxides in the release of P and Fe(II) into the solution, the following co-precipitation processes may mask the effective amount of P that can be available for plants, in particular after the formation of root Fe plaque. Moreover, co-precipitation processes are of primary importance in determining the selective accumulation of specific inorganic and organic P forms in submerged paddy soils. Indeed, P species characterized by a stronger affinity with Fe (hydr)oxides were stabilized against mineralization, while orthophosphate diesters were less retained by the surfaces, easily hydrolyzed by enzymes to inorganic P, becoming available for plant uptake. Thus, both abiotic and biotic processes promoted the selective retention of specific organic P forms as a function of soil total P supply. In soils with low P supply the plant adaptation mechanisms - including root development and O_2 release - are to be included among the major mechanisms governing P uptake in the complex environment of rice paddies, complemented by the progressive replenishment of labile organic pools to contribute to plant uptake.

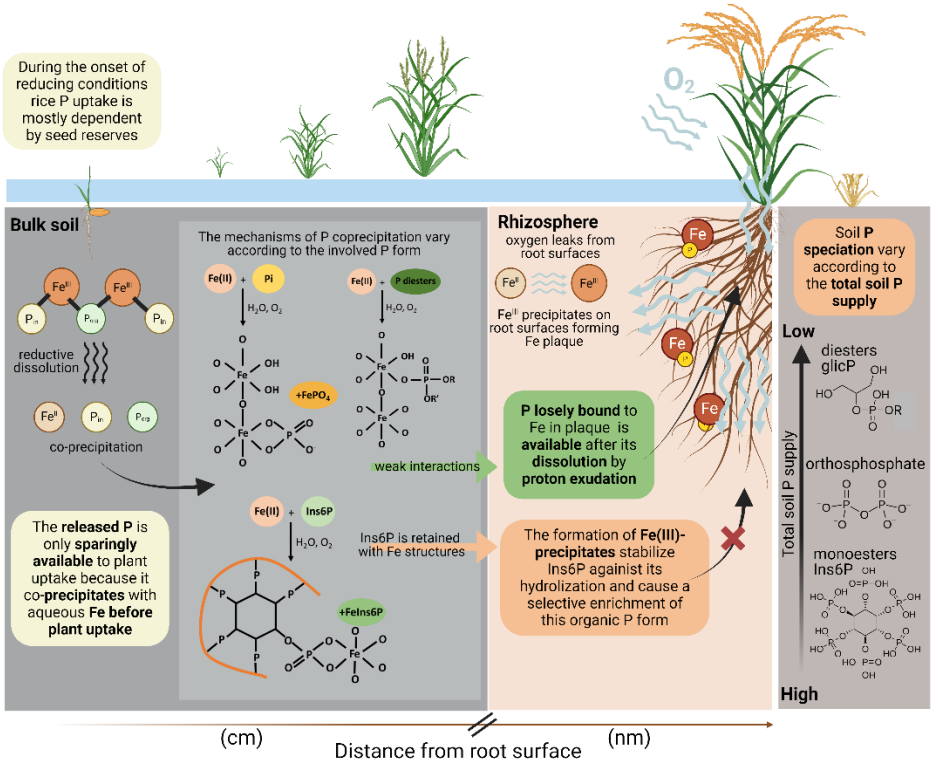

Figure 6.1 Conclusive conceptual summary of chapter 1-3. The P released by reductive dissolution is only limitedly available for plant uptake because of co-precipitation reactions with aqueous Fe. The extent and mechanisms of Fe-P co-precipitation also determine a stabilization of Ins6P, resulting in a selective enrichment of these organic P form. The activation of plant strategies to acquire P in the rhizosphere further contributes to the consumption of the P forms weakly retained during co-precipitation, leading to a different soil P speciation as a function of soil total P supply.

6.2 The implication of P fertilization and water regimes on P uptake from Fe plaque

One of the open questions in the literature is the role of Fe plaque in controlling P plant uptake. In this PhD thesis we found that Fe plaque formation and dissolution processes are affected by soil total P supply and changes during rice phenological stages. In general, we can infer that Fe plaque serves as a source of P if rice plants grown in limited P soils whereas it becomes a sink when soil P is sufficiently available in solution. During the early stages of plant growth, both Fe plaque formation and dissolution were influenced by root traits, which in turn were regulated by P availability. Phosphorus deficiency led not only to modifications in root morphology and traits that induced a faster and larger formation of Fe plaque, but also enhanced their subsequent dissolution through rhizosphere acidification. Consequently, the plaque-associated P could potentially serve as a nutrient source facilitating P uptake. On the other hand, in P rich soils, Fe plaque may serve as a P sink limiting plant uptake and growth to some extent, as plaque formation was not accompanied by a comparable dissolution. This study therefore contributes to further understanding the complex interactions between modifications in rice root traits and temporal Fe plaque dynamics on root surfaces as a function of P availability, which deeply shape nutrient cycling in the rhizosphere.

Finally, the effects of the application of innovative water management practices on Fe plaque formation, transformation and subsequent P release were investigated. The obtained results showed that the processes which govern Fe plaque mineral evolution varied according to water management during the rice growing season. Indeed, the high availability of aqueous Fe(II) observed in the early phases of continuous flooding led to the precipitation of poorly crystalline Fe (hydr)oxides followed by their transformation to more crystalline phases, likely due to the catalytic effect of aqueous Fe(II). These processes were in turn hindered by the lower Fe(II) concentration observed during the establishment of dry periods. Nonetheless, the adoption of water saving techniques during the rice growing season determined a greater P:Fe molar ratio in solution, further promoting the formation of amorphous Fe(III)-phosphate precipitates on the root surfaces. Besides the role of aqueous Fe(II) concentration, with the introduction of dry periods, the porewater chemistry became the master variable controlling Fe plaque formation and transformation. In particular, the porewater P:Fe molar ratio also controlled the P retention mechanisms as the P sorbed by the well-structured plaque formed in flooded soils resulted relatively less available to plants, therefore contributing to its accumulation at the rhizospheric level. Conversely, the Fe(III)-phosphate precipitated after the establishment of dry periods was more promptly dissolved during the re-wetting cycle, thus positively contributing to plant uptake. We can conclude that the different P concentration in the porewater caused by water management was compensated by the characteristics of Fe plaque and associated P forms, leading to unexpected comparable P contents in the rice plants, independently of the adopted water management.

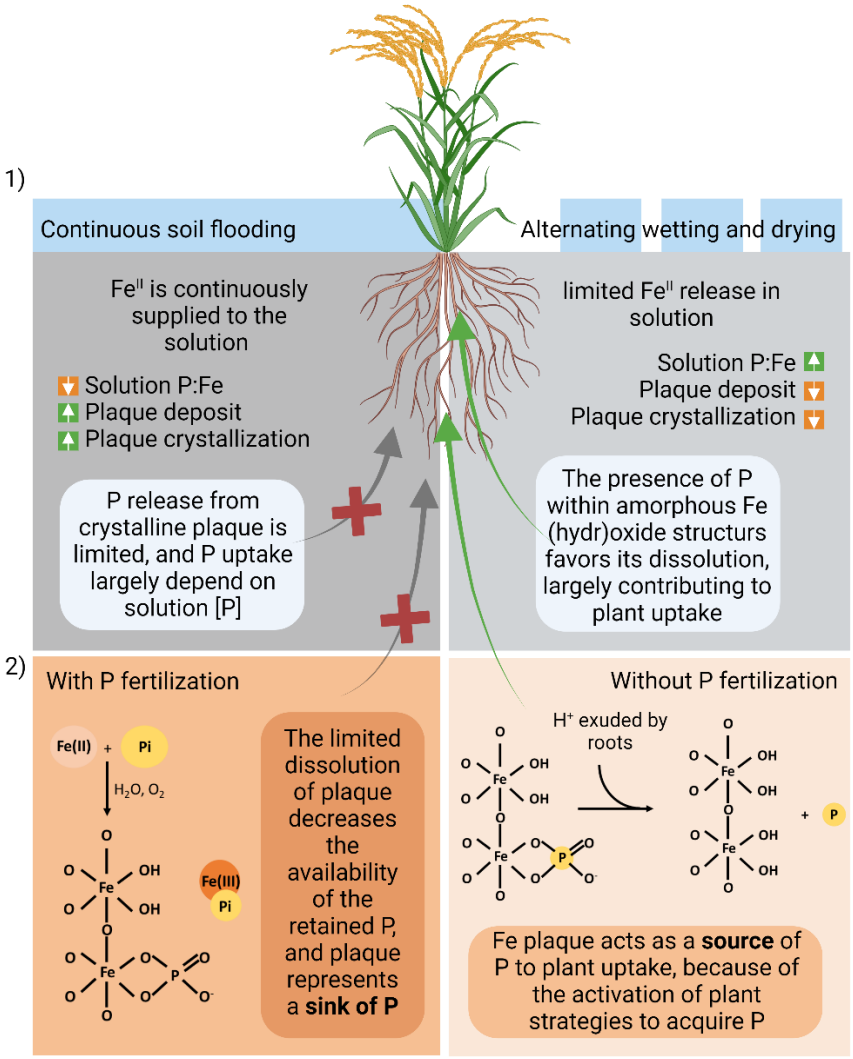

Figure 6.2 Conclusive conceptual summary of chapter 3-5. 1) Fe plaque surfaces do not contribute to P uptake in rice grown under continuous flooding, while the formation of amorphous Fe plaque observed under alternating wetting and drying conditions contributes to increase P release from plaque; 2) the P retained by plaque is particularly available at low soil P supply, because of the activation of plant strategy to overcome P limitation (i.e. proton exudation), thus further stressing the role of plants in shaping the rhizospheric environment.

6.2 General conclusions, environmental significance and future perspectives

This thesis significantly contributes to our understanding of P in paddy soils, particularly the mechanisms driving P availability to rice plants in these unique environments. In general, so far, anaerobic soils have been considered to exhibit higher P availability compared to aerobic soils. However, the investigation into the rhizospheric interaction mechanisms conducted in this study revealed that the relationship between P release into the solution from soil surfaces and plant uptake does not follow a linear pathway. The formation of Fe-P co-precipitates controlled by aqueous Fe(II) concentration and O_2 release by rice roots was identified as key factor that control the flux of P from the bulk soil to the oxic rhizosphere. Notwithstanding the crucial role of Fe(III)-precipitates in the retention of dissolved P, plants can access this sparingly available P forms throughout the adoption of several strategies such as modifications in root anatomy, exudation of protons and the activation of P root transporters. The presented results extend our understanding on the role of soil-plant interactions has on the regulation of the P fluxes from the reduced bulk soil to the plant. This, together with the identification of the most appropriate method to quantify the available P pool in rice temperate regions, and the investigation within a range of soil total P supply, may have important agronomic implications for the development of more sustainable P fertilization plans.

Undoubtedly, the current thesis has only focused on the soil-plant processes affecting rhizospheric Fe and P interactions and did not evaluate the role of microorganisms in shaping Fe redox cycling and P speciation in the rice rhizosphere. Further investigation should address the effects of Fe(II)-oxidizing bacteria on Fe plaque deposition, particularly when the abiotic Fe(II) oxidation is disadvantaged by the decreased rhizosphere pH. At the same time, also the activity of Fe(III)-reducing bacteria should be investigated regarding their role in Fe plaque dissolution matched with the release of the retained P. Up to present it remains unclear whether the activity of Fe(II)-oxidizing and/or Fe(III)-reducing bacteria might represent a further pathway of P utilization from Fe plaque by P-starved rice plants.

The results presented in this PhD thesis further underlined the pivotal role of soil total P content, which influences both abiotic and biotic processes occurring at the Fe plaque-root interface, highlighting the intricate interplays among total soil P supply, the plant ability to shape the rhizospheric environment, and the evolution of P speciation in flooded paddy soils. The greater retention of organic P forms during Fe(II) oxidative precipitation and their hampered hydrolysis in these coprecipitates resulted indeed in a selective enrichment of P monoesters with respect to the more labile P diesters.

Ultimately, in this PhD thesis we demonstrated that conversely to previous assumptions, the adoption of water-saving techniques did not lead to a reduction of P uptake by plants. The investigation into Fe plaque formation and temporal evolution revealed the pivotal role of the mineral structure and P retention mechanisms in controlling P release to plants. Indeed, unlike the decreased

plaque deposit associated with dry periods, a larger proportion of co-precipitated P was taken up by rice plant, guarantying a plant P content similar to traditional flooding. On the other hand, under continuously submerged conditions, the instauration of crystallization processes may have increased P retention by adsorption and reduced its release to plant. Although these studies evaluated the evolution of Fe plaque during the whole plant growth in controlled mesocosms, they need to be confirmed by larger scale field experiments to further support that the rhizospheric Fe-P processes can effectively contribute to guarantee a good P use efficiency with the introduction of water saving techniques. Besides, also in this case further investigations should consider the active role of microbial communities associated with the roots on rhizospheric Fe cycling and P speciation, which together with plant responses, may play an important role in controlling P availability to rice plants.

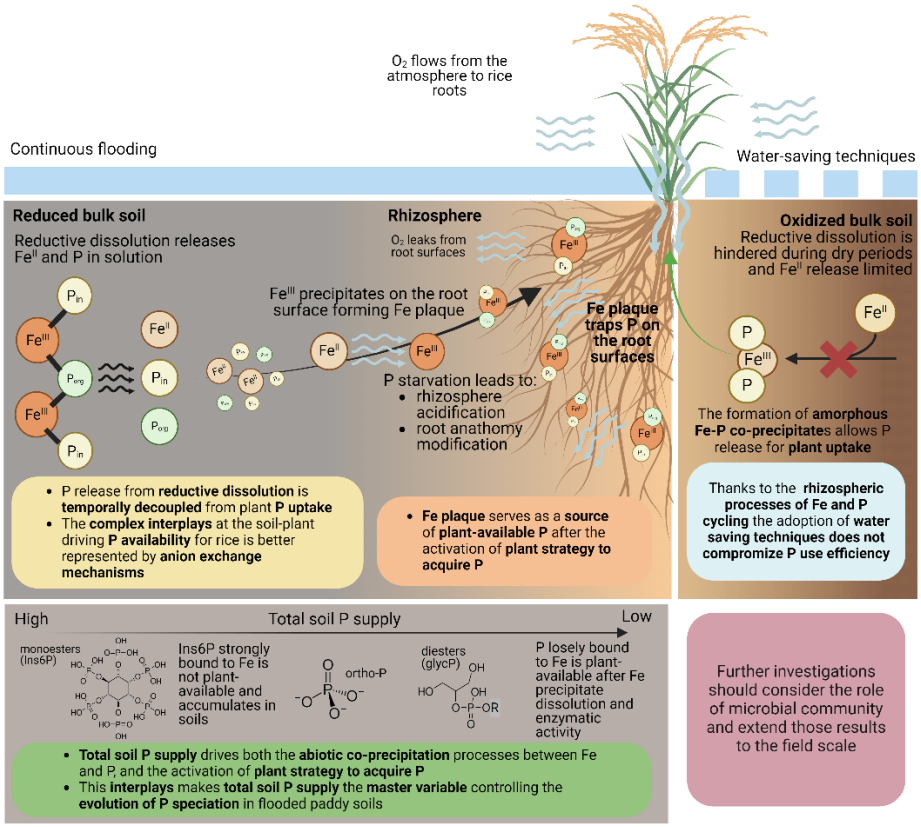

Figure 6.3 Conclusive conceptual model of the results discussed in this thesis. Phosphorus availability for rice plants grown in flooded soils is strongly driven by the mechanisms of Fe-P co-precipitation caused by the redox gradient from the reduced bulk soil to the oxidized rhizosphere (Chapter 1). The formation of root Fe plaque led to a source of plant-available P in the rhizosphere when the soil P supply is limited because of the activation of plant strategy to mobilize the nutrient (Chapter 2). The interplays between abiotic stabilization and plant mobilization mechanisms in turn drive the evolution of P speciation in flooded soil resulting in a selective enrichment of the more stable organic P forms in the soil with the highest total P supply (Chapter 4). Furthermore, the instauration of co-precipitation processes during Fe plaque formation guarantee plant P uptake without compromising water use efficiency with the introduction of water-saving irrigation (Chapter 5).

REFERENCES

Acosta-Motos, J.R., Rothwell, S.A., Massam, M.J., Albacete, A., Zhang, H., Dodd, I.C., 2020. Alternate wetting and drying irrigation increases water and phosphorus use efficiency independent of substrate phosphorus status of vegetative rice plants. Plant Physiol. Biochem. 155, 914–926. https://doi.org/10.1016/j.plaphy.2020.06.017

Ajmone-Marsan, F., Côté, D., Simard, R.R., 2006. Phosphorus Transformations under Reduction in Long-term Manured Soils. Plant Soil 282, 239–250. https://doi.org/10.1007/s11104-005-5929-6

Amaral, D.C., Lopes, G., Guilherme, L.R.G., Seyfferth, A.L., 2017a. A New Approach to Sampling Intact Fe Plaque Reveals Si-Induced Changes in Fe Mineral Composition and Shoot As in Rice. Environ. Sci. Technol. 51, 38–45. https://doi.org/10.1021/acs.est.6b03558

Amer, F., Bouldin, D.R., Black, C.A., Duke, F.R., 1955. Characterization of soil phosphorus by anion exchange resin adsorption and P32-equilibration. Plant Soil 6, 391–408. https://doi.org/10.1007/BF01343648

Arai, Y., Sparks, D.L., 2001. ATR–FTIR Spectroscopic Investigation on Phosphate Adsorption Mechanisms at the Ferrihydrite–Water Interface. J. Colloid Interface Sci. 241, 317–326. https://doi.org/10.1006/jcis.2001.7773

Ariani, M., Hanudin, E., Haryono, E., 2022. The effect of contrasting soil textures on the efficiency of alternate wetting-drying to reduce water use and global warming potential. Agric. Water Manag. 274, 107970. https://doi.org/10.1016/j.agwat.2022.107970

Armstrong, W., Armstrong, J., 2014. Plant Internal Oxygen Transport (Diffusion and Convection) and Measuring and Modelling Oxygen Gradients, in: Van Dongen, J.T., Licausi, F. (Eds.), Low-Oxygen Stress in Plants, Plant Cell Monographs. Springer Vienna, Vienna, pp. 267–297. https://doi.org/10.1007/978-3-7091-1254-0_14

Aulakh, M.S., Wassmann, R., Bueno, C., Kreuzwieser, J., Rennenberg, H., 2001. Characterization of Root Exudates at Different Growth Stages of Ten Rice (Oryza sativa L.) Cultivars. Plant Biol. 3, 139–148. https://doi.org/10.1055/s-2001-12905

Bacha, R.E., Hossner, L.R., 1977. Characteristics of Coatings formed on Rice Roots as Affected by Iron and Manganese Additions. Soil Sci. Soc. Am. J. 41, 931–935. https://doi.org/10.2136/sssaj1977.03615995004100050025x

Barber, D.A., Ebert, M., Evans, N.T.S., 1962. The Movement of 15 0 through Barley and Rice Plants. J. Exp. Bot. 13, 397–403. https://doi.org/10.1093/jxb/13.3.397

Barrow, N.J., Sen, A., Roy, N., Debnath, A., 2021. The soil phosphate fractionation fallacy. Plant Soil 459, 1–11. https://doi.org/10.1007/s11104-020-04476-6

Bedford, B.L., Bouldin, D.R., Beliveau, B.D., 1991. Net Oxygen and Carbon-Dioxide Balances in Solutions Bathing Roots of Wetland Plants. J. Ecol. 79, 943. https://doi.org/10.2307/2261090

Begg, C.B.M., Kirk, G.J.D., Mackenzie, A.F., Neue, H. -U., 1994. Root-induced iron oxidation and pH changes in the lowland rice rhizosphere. New Phytol. 128, 469–477. https://doi.org/10.1111/j.1469-8137.1994.tb02993.x

Bhattacharyya, P., Das, S., Adhya, T.K., 2013a. Root Exudates of Rice Cultivars Affect Rhizospheric Phosphorus Dynamics in Soils with Different Phosphorus Statuses. Commun. Soil Sci. Plant Anal. 44, 1643–1658. https://doi.org/10.1080/00103624.2013.769562

Birch, H.F., 1958. The effect of soil drying on humus decomposition and nitrogen availability. Plant Soil 10, 9–31. https://doi.org/10.1007/BF01343734

Blute, N.K., Brabander, D.J., Hemond, H.F., Sutton, S.R., Newville, M.G., Rivers, M.L., 2004. Arsenic Sequestration by Ferric Iron Plaque on Cattail Roots. Environ. Sci. Technol. 38, 6074–6077. https://doi.org/10.1021/es049448g

Boland, D.D., Collins, R.N., Miller, C.J., Glover, C.J., Waite, T.D., 2014. Effect of Solution and Solid-Phase Conditions on the Fe(II)-Accelerated Transformation of Ferrihydrite to Lepidocrocite and Goethite. Environ. Sci. Technol. 48, 5477–5485. https://doi.org/10.1021/es4043275

Borch, T., Kretzschmar, R., Kappler, A., Cappellen, P.V., Ginder-Vogel, M., Voegelin, A., Campbell, K., 2010. Biogeochemical Redox Processes and their Impact on Contaminant Dynamics. Environ. Sci. Technol. 44, 15–23. https://doi.org/10.1021/es9026248

Bouman, B.A.M., 2007. A conceptual framework for the improvement of crop water productivity at different spatial scales. Agric. Syst. 93, 43–60. https://doi.org/10.1016/j.agsy.2006.04.004

Briat, J.-F., Ravet, K., Arnaud, N., Duc, C., Boucherez, J., Touraine, B., Cellier, F., Gaymard, F., 2010. New insights into ferritin synthesis and function highlight a link between iron homeostasis and oxidative stress in plants. Ann. Bot. 105, 811–822. https://doi.org/10.1093/aob/mcp128

Cade-Menun, B., 2005. Characterizing phosphorus in environmental and agricultural samples by 31P nuclear magnetic resonance spectroscopy. Talanta 66, 359–371. https://doi.org/10.1016/j.talanta.2004.12.024

Cade-Menun, B., Liu, C.W., 2014. Solution Phosphorus-31 Nuclear Magnetic Resonance Spectroscopy of Soils from 2005 to 2013: A Review of Sample Preparation and Experimental Parameters. Soil Sci. Soc. Am. J. 78, 19–37. https://doi.org/10.2136/sssaj2013.05.0187dgs

Cade-Menun, B.J., He, Z., Zhang, H., Endale, D.M., Schomberg, H.H., Liu, C.W., 2015. Stratification of Phosphorus Forms from Long-Term Conservation Tillage and Poultry Litter Application. Soil Sci. Soc. Am. J. 79, 504–516. https://doi.org/10.2136/sssaj2014.08.0310

Cade-Menun, B.J., Preston, C.M., 1996. A COMPARISON OF SOIL EXTRACTION PROCEDURES FOR 31P NMR SPECTROSCOPY: Soil Sci. 161, 770–785. https://doi.org/10.1097/00010694-199611000-00006

Calvin, S., Furst, K.E., 2013. XAFS for everyone. CRC Press, Boca Raton.

Carrijo, D.R., Lundy, M.E., Linquist, B.A., 2017. Rice yields and water use under alternate wetting and drying irrigation: A meta-analysis. Field Crops Res. 203, 173–180. https://doi.org/10.1016/j.fcr.2016.12.002

Celi, L., De Luca, G., Barberis, E., 2003. Effects of interaction of organic and inorganic p with ferrihydrite and kaolinite-iron oxide systems on iron release. Soil Sci. 168, 479–488. https://doi.org/10.1097/01.ss.0000080333.10341.a4

Celi, L., Prati, M., Magnacca, G., Santoro, V., Martin, M., 2020. Role of crystalline iron oxides on stabilization of inositol phosphates in soil. Geoderma 374, 114442. https://doi.org/10.1016/j.geoderma.2020.114442

Celi, L., Said-Pullicino, D., Bol, R., Lang, F., Luster, J., 2022. Interconnecting soil organic matter with nitrogen and phosphorus cycling, in: Yang, Y., Keiluweit, M., Senesi, N., Xing, B. (Eds.), Multi-Scale Biogeochemical Processes in Soil Ecosystems. Wiley, pp. 51–77. https://doi.org/10.1002/9781119480419.ch3

Cerli, C., Celi, L., Kalbitz, K., Guggenberger, G., Kaiser, K., 2012. Separation of light and heavy organic matter fractions in soil — Testing for proper density cut-off and dispersion level. Geoderma 170, 403–416. https://doi.org/10.1016/j.geoderma.2011.10.009

Châtellier, X., Grybos, M., Abdelmoula, M., Kemner, K.M., Leppard, G.G., Mustin, C., West, M.M., Paktunc, D., 2013. Immobilization of P by oxidation of Fe(II) ions leading to nanoparticle formation and aggregation. Appl. Geochem. 35, 325–339. https://doi.org/10.1016/j.apgeochem.2013.04.019

Chen, A., Li, Y., Shang, J., Arai, Y., 2020. Ferrihydrite Transformation Impacted by Coprecipitation of Phytic Acid. Environ. Sci. Technol. 54, 8837–8847. https://doi.org/10.1021/acs.est.0c02465

Chen, C., Thompson, A., 2018. Ferrous Iron Oxidation under Varying pO 2 Levels: The Effect of Fe(III)/Al(III) Oxide Minerals and Organic Matter. Environ. Sci. Technol. 52, 597–606. https://doi.org/10.1021/acs.est.7b05102

Chen, C.C., Dixon, J.B., Turner, F.T., 1980. Iron Coatings on Rice Roots: Morphology and Models of Development. Soil Sci. Soc. Am. J. 44, 1113–1119. https://doi.org/10.2136/sssaj1980.03615995004400050046x

Colmer, T.D., 2003. Long-distance transport of gases in plants: a perspective on internal aeration and radial oxygen loss from roots: Gas transport in plants. Plant Cell Environ. 26, 17–36. https://doi.org/10.1046/j.1365-3040.2003.00846.x

Colocho Hurtarte, L.C., Santana Amorim, H.C., Kruse, J., Criginski Cezar, J., Klysubun, W., Prietzel, J., 2020. A Novel Approach for the Quantification of Different Inorganic and Organic Phosphorus Compounds in Environmental Samples by P L 2,3 -Edge X-ray Absorption Near-Edge Structure (XANES) Spectroscopy. Environ. Sci. Technol. 54, 2812–2820. https://doi.org/10.1021/acs.est.9b07018

Condron, L.M., Newman, S., 2011. Revisiting the fundamentals of phosphorus fractionation of sediments and soils. J. Soils Sediments 11, 830–840. https://doi.org/10.1007/s11368-011-0363-2

Condron, L.M., Turner, B.L., Cade-Menun, B.J., 2015. Chemistry and Dynamics of Soil Organic Phosphorus, in: Thomas Sims, J., Sharpley, A.N. (Eds.), Agronomy Monographs. American Society of Agronomy, Crop Science Society of America, and Soil Science Society of America, Madison, WI, USA, pp. 87–121. https://doi.org/10.2134/agronmonogr46.c4

Das, S., Tyagi, W., Rai, M., Yumnam, J.S., 2017. Understanding Fe 2+ toxicity and P deficiency tolerance in rice for enhancing productivity under acidic soils. Biotechnol. Genet. Eng. Rev. 33, 97–117. https://doi.org/10.1080/02648725.2017.1370888

Datta, A., Ullah, H., Ferdous, Z., 2017. Water Management in Rice, in: Chauhan, B.S., Jabran, K., Mahajan, G. (Eds.), Rice Production Worldwide. Springer International Publishing, Cham, pp. 255–277. https://doi.org/10.1007/978-3-319-47516-5_11

de Mello, J.W.V., Barrón, V., Torrent, J., 1998. Phosphorus and iron mobilization in flooded soils from brazil: Soil Sci. 163, 122–132. https://doi.org/10.1097/00010694-199802000-00006

Dobermann, A., Fairhurst, T., 2000. Rice: nutrient disorders & nutrient management, 1. ed. ed. Potash & Phosphate Institute [u.a.], Signapore.

Dodd, I.C., Puértolas, J., Huber, K., Pérez-Pérez, J.G., Wright, H.R., Blackwell, M.S.A., 2015. The importance of soil drying and re-wetting in crop phytohormonal and

nutritional responses to deficit irrigation. J. Exp. Bot. 66, 2239–2252. https://doi.org/10.1093/jxb/eru532
Duersch, B.G., Bhadha, J.H., Root, T.L., Louda, J.W., 2020. The role of rice (Oryza sativa L.) in sequestering phosphorus compounds and trace elements: Speciation and dynamics. Sci. Total Environ. 725, 138366. https://doi.org/10.1016/j.scitotenv.2020.138366
Dunn, B.W., Gaydon, D.S., 2011. Rice growth, yield and water productivity responses to irrigation scheduling prior to the delayed application of continuous flooding in south-east Australia. Agric. Water Manag. 98, 1799–1807. https://doi.org/10.1016/j.agwat.2011.07.004
Eivazi, F., Tabatabai, M.A., 1977. Phosphatases in soils. Soil Biol. Biochem. 9, 167–172. https://doi.org/10.1016/0038-0717(77)90070-0
Evans, D.E., 2004. Aerenchyma formation. New Phytol. 161, 35–49. https://doi.org/10.1046/j.1469-8137.2003.00907.x
Fang, W., Williams, P.N., Zhang, H., Yang, Y., Yin, D., Liu, Z., Sun, H., Luo, J., 2021. Combining Multiple High-Resolution In Situ Techniques to Understand Phosphorous Availability Around Rice Roots. Environ. Sci. Technol. acs.est.1c05358. https://doi.org/10.1021/acs.est.1c05358
Fang, W.-C., Wang, J.-W., Lin, C.C., Kao, C.H., 2001. Iron induction of lipid peroxidation and effects on antioxidative enzyme activities in rice leaves. Plant Growth Regul. 35, 75–80. https://doi.org/10.1023/A:1013879019368
Fischer, G., Tubiello, F.N., Van Velthuizen, H., Wiberg, D.A., 2007. Climate change impacts on irrigation water requirements: Effects of mitigation, 1990–2080. Technol. Forecast. Soc. Change 74, 1083–1107. https://doi.org/10.1016/j.techfore.2006.05.021
Frommer, J., Voegelin, A., Dittmar, J., Marcus, M.A., Kretzschmar, R., 2011. Biogeochemical processes and arsenic enrichment around rice roots in paddy soil: results from micro-focused X-ray spectroscopy. Eur. J. Soil Sci. 62, 305–317. https://doi.org/10.1111/j.1365-2389.2010.01328.x
Frossard, E., Condron, L.M., Oberson, A., Sinaj, S., Fardeau, J.C., 2000. Processes Governing Phosphorus Availability in Temperate Soils. J. Environ. Qual. 29, 15–23. https://doi.org/10.2134/jeq2000.00472425002900010003x
Fu, Y.Q., Yang, X.J., Shen, H., 2014. The physiological mechanism of enhanced oxidizing capacity of rice (Oryza sativa L.) roots induced by phosphorus deficiency. Acta Physiol. Plant. 36, 179–190. https://doi.org/10.1007/s11738-013-1398-3
Gatiboni, L.C., Condron, L.M., 2021. A rapid fractionation method for assessing key soil phosphorus parameters in agroecosystems. Geoderma 385, 114893. https://doi.org/10.1016/j.geoderma.2020.114893
George, T.S., Quiquampoix, H., Simpson, R.J., Richardson, A.E., 2007. Interactions between phytases and soil constituents: implications for the hydrolysis of inositol phosphates., in: Turner, B.L., Richardson, A.E., Mullaney, E.J. (Eds.), Inositol Phosphates: Linking Agriculture and the Environment. CABI, UK, pp. 221–241. https://doi.org/10.1079/9781845931520.0221
Giaveno, C., Celi, L., Richardson, A.E., Simpson, R.J., Barberis, E., 2010. Interaction of phytases with minerals and availability of substrate affect the hydrolysis of inositol phosphates. Soil Biol. Biochem. 42, 491–498. https://doi.org/10.1016/j.soilbio.2009.12.002

Gilardi, G.L.C., Mayer, A., Rienzner, M., Romani, M., Facchi, A., 2023. Effect of Alternate Wetting and Drying (AWD) and Other Irrigation Management Strategies on Water Resources in Rice-Producing Areas of Northern Italy. Water 15, 2150. https://doi.org/10.3390/w15122150

Goff, S.A., Ricke, D., Lan, T.-H., Presting, G., Wang, R., Dunn, M., Glazebrook, J., Sessions, A., Oeller, P., Varma, H., Hadley, D., Hutchison, D., Martin, C., Katagiri, F., Lange, B.M., Moughamer, T., Xia, Y., Budworth, P., Zhong, J., Miguel, T., Paszkowski, U., Zhang, S., Colbert, M., Sun, W., Chen, L., Cooper, B., Park, S., Wood, T.C., Mao, L., Quail, P., Wing, R., Dean, R., Yu, Y., Zharkikh, A., Shen, R., Sahasrabudhe, S., Thomas, A., Cannings, R., Gutin, A., Pruss, D., Reid, J., Tavtigian, S., Mitchell, J., Eldredge, G., Scholl, T., Miller, R.M., Bhatnagar, S., Adey, N., Rubano, T., Tusneem, N., Robinson, R., Feldhaus, J., Macalma, T., Oliphant, A., Briggs, S., 2002. A Draft Sequence of the Rice Genome (Oryza sativa L. ssp. japonica). Science 296, 92–100. https://doi.org/10.1126/science.1068275

Grigg, A.R.C., ThomasArrigo, L.K., Schulz, K., Rothwell, K.A., Kaegi, R., Kretzschmar, R., 2022. Ferrihydrite transformations in flooded paddy soils: rates, pathways, and product spatial distributions. Environ. Sci. Process. Impacts 24, 1867–1882. https://doi.org/10.1039/D2EM00290F

Gu, C., Margenot, A.J., 2021. Navigating limitations and opportunities of soil phosphorus fractionation. Plant Soil 459, 13–17. https://doi.org/10.1007/s11104-020-04552-x

Guedes, R.S., Fernandes, A.R., Alleoni, L.R.F., Kamogawa, M.Y., Colzato, M., Santos, S.R., 2015. Inorganic phosphorus fractions extracted by sodium dithionite-citrate-bicarbonate and determined using the malachite green method. Rev. Ciênc. Agrár. 58, 228–231. https://doi.org/10.4322/rca.1804

Handler, R.M., Beard, B.L., Johnson, C.M., Scherer, M.M., 2009. Atom Exchange between Aqueous Fe(II) and Goethite: An Fe Isotope Tracer Study. Environ. Sci. Technol. 43, 1102–1107. https://doi.org/10.1021/es802402m

Hansel, C.M., Benner, S.G., Fendorf, S., 2005. Competing Fe(II)-Induced Mineralization Pathways of Ferrihydrite. Environ. Sci. Technol. 39, 7147–7153. https://doi.org/10.1021/es050666z

Hansel, C.M., Fendorf, S., Sutton, S., Newville, M., 2001. Characterization of Fe Plaque and Associated Metals on the Roots of Mine-Waste Impacted Aquatic Plants. Environ. Sci. Technol. 35, 3863–3868. https://doi.org/10.1021/es0105459

Hayes, J.E., Richardson, A.E., Simpson, R.J., 1999. Phytase and acid phosphatase activities in extracts from roots of temperate pasture grass and legume seedlings. Funct. Plant Biol. 26, 801. https://doi.org/10.1071/PP99065

Hedley, M.J., Stewart, J.W.B., Chauhan, B.S., 1982. Changes in Inorganic and Organic Soil Phosphorus Fractions Induced by Cultivation Practices and by Laboratory Incubations. Soil Sci. Soc. Am. J. 46, 970–976. https://doi.org/10.2136/sssaj1982.03615995004600050017x

Heiberg, L., Pedersen, T.V., Jensen, H.S., Kjaergaard, C., Hansen, H.C.B., 2010. A Comparative Study of Phosphate Sorption in Lowland Soils under Oxic and Anoxic Conditions. J. Environ. Qual. 39, 734–743. https://doi.org/10.2134/jeq2009.0222

Hernández, J., Berger, A., Deambrosi, E., Lavecchia, A., 2013. Soil Phosphorus Tests for Flooded Rice Grown in Contrasting Soils and Cropping History. Commun. Soil Sci. Plant Anal. 44, 1193–1210. https://doi.org/10.1080/00103624.2012.756000

Hinkle, M.A.G., Wang, Z., Giammar, D.E., Catalano, J.G., 2015. Interaction of Fe(II) with phosphate and sulfate on iron oxide surfaces. Geochim. Cosmochim. Acta 158, 130–146. https://doi.org/10.1016/j.gca.2015.02.030

Hinsinger, P., 2001. Bioavailability of soil inorganic P in the rhizosphere as affected by root-induced chemical changes: a review. Plant Soil 237, 173–195. https://doi.org/10.1023/A:1013351617532

Hinsinger, P., Plassard, C., Tang, C., Jaillard, B., 2003. Origins of root-mediated pH changes in the rhizosphere and their responses to environmental constraints: A review. Plant Soil 248, 43–59. https://doi.org/10.1023/A:1022371130939

Hoffland, E., Wei, C., Wissuwa, M., 2006. Organic Anion Exudation by Lowland Rice (Oryza sativa L.) at Zinc and Phosphorus Deficiency. Plant Soil 283, 155–162. https://doi.org/10.1007/s11104-005-3937-1

Hossain, M.B., Jahiruddin, M., Loeppert, R.H., Panaullah, G.M., Islam, M.R., Duxbury, J.M., 2009. The effects of iron plaque and phosphorus on yield and arsenic accumulation in rice. Plant Soil 317, 167–176. https://doi.org/10.1007/s11104-008-9798-7

Huang, L.-Z., Zhang, X., Liu, R., Fang, L., 2022. The redox chemistry of phosphate complexed green rusts: Limited oxidative transformation and phosphate release. Chem. Eng. J. 429, 132417. https://doi.org/10.1016/j.cej.2021.132417

Jiaofeng, G., Yang, H., Peng, Z., Bohan, L., Hang, Z., 2022. Increasing phosphorus inhibits the retention and prevention of cadmium by iron plaque and promotes cadmium accumulation in rice plants. Chemosphere 307, 135642. https://doi.org/10.1016/j.chemosphere.2022.135642

Jørgensen, C., Jensen, H.S., Andersen, F.Ø., Egemose, S., Reitzel, K., 2011. Occurrence of orthophosphate monoesters in lake sediments: significance of myo- and scyllo-inositol hexakisphosphate. J. Environ. Monit. 13, 2328. https://doi.org/10.1039/c1em10202h

Julia, C.C., Rose, T.J., Pariasca-Tanaka, J., Jeong, K., Matsuda, T., Wissuwa, M., 2018. Phosphorus uptake commences at the earliest stages of seedling development in rice. J. Exp. Bot. 69, 5233–5240. https://doi.org/10.1093/jxb/ery267

Kappler, A., Bryce, C., Mansor, M., Lueder, U., Byrne, J.M., Swanner, E.D., 2021. An evolving view on biogeochemical cycling of iron. Nat. Rev. Microbiol. 19, 360–374. https://doi.org/10.1038/s41579-020-00502-7

Kato, Y., Okami, M., 2011. Root morphology, hydraulic conductivity and plant water relations of high-yielding rice grown under aerobic conditions. Ann. Bot. 108, 575–583. https://doi.org/10.1093/aob/mcr184

Khan, N., Seshadri, B., Bolan, N., Saint, C.P., Kirkham, M.B., Chowdhury, S., Yamaguchi, N., Lee, D.Y., Li, G., Kunhikrishnan, A., Qi, F., Karunanithi, R., Qiu, R., Zhu, Y.-G., Syu, C.H., 2016. Root Iron Plaque on Wetland Plants as a Dynamic Pool of Nutrients and Contaminants, in: Advances in Agronomy. Elsevier, pp. 1–96. https://doi.org/10.1016/bs.agron.2016.04.002

Kirk, G., 2004. The Biogeochemistry of Submerged Soils, 1st ed. Wiley. https://doi.org/10.1002/047086303X

Kirk, G.J.D., 2003. Rice root properties for internal aeration and efficient nutrient acquisition in submerged soil. New Phytol. 159, 185–194. https://doi.org/10.1046/j.1469-8137.2003.00793.x

Kirk, G.J.D., Santos, E.E., Santos, M.B., 1999. Phosphate solubilization by organic anion excretion from rice growing in aerobic soil: rates of excretion and decomposition,

effects on rhizosphere pH and effects on phosphate solubility and uptake. New Phytol. 142, 185–200. https://doi.org/10.1046/j.1469-8137.1999.00400.x

Kirk, G.J.D., Van Du, L., 1997. Changes in rice root architecture, porosity, and oxygen and proton release under phosphorus deficiency. New Phytol. 135, 191–200. https://doi.org/10.1046/j.1469-8137.1997.00640.x

Kögel-Knabner, I., Amelung, W., Cao, Z., Fiedler, S., Frenzel, P., Jahn, R., Kalbitz, K., Kölbl, A., Schloter, M., 2010. Biogeochemistry of paddy soils. Geoderma 157, 1–14. https://doi.org/10.1016/j.geoderma.2010.03.009

Kotula, L., Ranathunge, K., Schreiber, L., Steudle, E., 2009. Functional and chemical comparison of apoplastic barriers to radial oxygen loss in roots of rice (Oryza sativa L.) grown in aerated or deoxygenated solution. J. Exp. Bot. 60, 2155–2167. https://doi.org/10.1093/jxb/erp089

Kraal, P., Van Genuchten, C.M., Behrends, T., Rose, A.L., 2019. Sorption of phosphate and silicate alters dissolution kinetics of poorly crystalline iron (oxyhydr)oxide. Chemosphere 234, 690–701. https://doi.org/10.1016/j.chemosphere.2019.06.071

Kruse, J., Abraham, M., Amelung, W., Baum, C., Bol, R., Kühn, O., Lewandowski, H., Niederberger, J., Oelmann, Y., Rüger, C., Santner, J., Siebers, M., Siebers, N., Spohn, M., Vestergren, J., Vogts, A., Leinweber, P., 2015. Innovative methods in soil phosphorus research: A review. J. Plant Nutr. Soil Sci. 178, 43–88. https://doi.org/10.1002/jpln.201400327

Kuo, S., 1986. Concurrent Sorption of Phosphate and Zinc, Cadmium, or Calcium by a Hydrous Ferric Oxide. Soil Sci. Soc. Am. J. 50, 1412–1419. https://doi.org/10.2136/sssaj1986.03615995005000060008x

Kuzyakov, Y., Razavi, B.S., 2019. Rhizosphere size and shape: Temporal dynamics and spatial stationarity. Soil Biol. Biochem. 135, 343–360. https://doi.org/10.1016/j.soilbio.2019.05.011

Liang, Y., Zhu, Y.-G., Xia, Y., Li, Z., Ma, Y., 2006. Iron plaque enhances phosphorus uptake by rice (Oryza sativa) growing under varying phosphorus and iron concentrations. Ann. Appl. Biol. 149, 305–312. https://doi.org/10.1111/j.1744-7348.2006.00095.x

Limmer, M.A., Evans, A.E., Seyfferth, A.L., 2021. A New Method to Capture the Spatial and Temporal Heterogeneity of Aquatic Plant Iron Root Plaque In Situ. Environ. Sci. Technol. 55, 912–918. https://doi.org/10.1021/acs.est.0c02949

Limmer, M.A., Thomas, J., Seyfferth, A.L., 2022. The effect of silicon on the kinetics of rice root iron plaque formation. Plant Soil 477, 171–181. https://doi.org/10.1007/s11104-022-05414-4

Linam, F., Limmer, M.A., Tappero, R., Seyfferth, A.L., 2022. Rice husk and charred husk amendments increase porewater and plant Si but water management determines grain As and Cd concentration. Plant Soil 477, 135–152. https://doi.org/10.1007/s11104-022-05350-3

Liu, J., Cade-Menun, B.J., Yang, J., Hu, Y., Liu, C.W., Tremblay, J., LaForge, K., Schellenberg, M., Hamel, C., Bainard, L.D., 2018. Long-Term Land Use Affects Phosphorus Speciation and the Composition of Phosphorus Cycling Genes in Agricultural Soils. Front. Microbiol. 9, 1643. https://doi.org/10.3389/fmicb.2018.01643

Liu, J., Hu, Y., Yang, J., Abdi, D., Cade-Menun, B.J., 2015. Investigation of Soil Legacy Phosphorus Transformation in Long-Term Agricultural Fields Using Sequential

Fractionation, P K-edge XANES and Solution P NMR Spectroscopy. Environ. Sci. Technol. 49, 168–176. https://doi.org/10.1021/es504420n

Liu, J., Sui, P., Cade-Menun, B.J., Hu, Y., Yang, J., Huang, S., Ma, Y., 2019. Molecular-level understanding of phosphorus transformation with long-term phosphorus addition and depletion in an alkaline soil. Geoderma 353, 116–124. https://doi.org/10.1016/j.geoderma.2019.06.024

Liu, W.J., Zhu, Y.G., Hu, Y., Williams, P.N., Gault, A.G., Meharg, A.A., Charnock, J.M., Smith, F.A., 2006. Arsenic Sequestration in Iron Plaque, Its Accumulation and Speciation in Mature Rice Plants (Oryza Sativa L.). Environ. Sci. Technol. 40, 5730–5736. https://doi.org/10.1021/es060800v

Loeppert, R., Inskeep, W., 1996. Iron. In: Bigham JM (ed) Part 3 methods of soil analysis. Chemical Methods 639–664.

Lombi, E., Scheckel, K.G., Armstrong, R.D., Forrester, S., Cutler, J.N., Paterson, D., 2006. Speciation and Distribution of Phosphorus in a Fertilized Soil: A Synchrotron-Based Investigation. Soil Sci. Soc. Am. J. 70, 2038–2048. https://doi.org/10.2136/sssaj2006.0051

Lombi, E., Susini, J., 2009. Synchrotron-based techniques for plant and soil science: opportunities, challenges and future perspectives. Plant Soil 320, 1–35. https://doi.org/10.1007/s11104-008-9876-x

Lynch, J.P., 2007. Roots of the Second Green Revolution. Aust. J. Bot. 55, 493. https://doi.org/10.1071/BT06118

Lynch, J.P., Brown, K.M., 2008. Root strategies for phosphorus acquisition, in: White, P.J., Hammond, J.P. (Eds.), The Ecophysiology of Plant-Phosphorus Interactions, Plant Ecophysiology. Springer Netherlands, Dordrecht, pp. 83–116. https://doi.org/10.1007/978-1-4020-8435-5_5

Madurapperuma, W.S., Kumaragamage, D., 2008. Evaluation of Ammonium Bicarbonate–Diethylene Triamine Penta Acetic Acid as a Multinutrient Extractant for Acidic Lowland Rice Soils. Commun. Soil Sci. Plant Anal. 39, 1773–1790. https://doi.org/10.1080/00103620802073768

Maftoun, M., Ardekani, M.A.H., Karimian, N., Ronaghy, A.M., 2003. Evaluation of Phosphorus Availability for Paddy Rice Using Eight Chemical Soil Tests Under Oxidized and Reduced Soil Conditions. Commun. Soil Sci. Plant Anal. 34, 2115–2129. https://doi.org/10.1081/CSS-120024052

Magid, J., Tiessen, H., Condron, L.M., 1996. Dynamics of Organic Phosphorus in Soils under Natural and Agricultural Ecosystems, in: Humic Substances in Terrestrial Ecosystems. Elsevier, pp. 429–466. https://doi.org/10.1016/B978-044481516-3/50012-8

Maisch, M., Lueder, U., Kappler, A., Schmidt, C., 2019. Iron Lung: How Rice Roots Induce Iron Redox Changes in the Rhizosphere and Create Niches for Microaerophilic Fe(II)-Oxidizing Bacteria. Environ. Sci. Technol. Lett. 6, 600–605. https://doi.org/10.1021/acs.estlett.9b00403

Marschner, P., 2021. Processes in submerged soils – linking redox potential, soil organic matter turnover and plants to nutrient cycling. Plant Soil 464, 1–12. https://doi.org/10.1007/s11104-021-05040-6

Marschner, P., 2002. Mineral Nutrition of Higher Plants, in: Mineral Nutrition of Higher Plants. Elsevier, p. ii. https://doi.org/10.1016/B978-0-08-057187-4.50001-1

Martin, M., Celi, L., Barberis, E., 2004. Desorption and plant availability of myo-inositol hexaphosphate adsorbed on goethite. Soil Sci. 169, 115–124. https://doi.org/10.1097/01.ss.0000117787.98510.9d

McDowell, R.W., Condron, L.M., Stewart, I., 2008. An examination of potential extraction methods to assess plant-available organic phosphorus in soil. Biol. Fertil. Soils 44, 707–715. https://doi.org/10.1007/s00374-007-0253-3

McLaren, T.I., Smernik, R.J., Simpson, R.J., McLaughlin, M.J., McBeath, T.M., Guppy, C.N., Richardson, A.E., 2017. The chemical nature of organic phosphorus that accumulates in fertilized soils of a temperate pasture as determined by solution 31 P NMR spectroscopy. J. Plant Nutr. Soil Sci. 180, 27–38. https://doi.org/10.1002/jpln.201600076

Mekonnen, M.M., Hoekstra, A.Y., 2011. The green, blue and grey water footprint of crops and derived crop products. Hydrol. Earth Syst. Sci. 15, 1577–1600. https://doi.org/10.5194/hess-15-1577-2011

Mendelssohn, I.A., Kleiss, B.A., Wakeley, J.S., 1995. Factors controlling the formation of oxidized root channels: A review. Wetlands 15, 37–46. https://doi.org/10.1007/BF03160678

Mendelssohn, I.A., Postek, M.T., 1982. ELEMENTAL ANALYSIS OF DEPOSITS ON THE ROOTS OF SPARTINA ALTERNIFLORA LOISEL. Am. J. Bot. 69, 904–912. https://doi.org/10.1002/j.1537-2197.1982.tb13334.x

Ming, F., Mi, G., Zhang, F., Zhu, L., 2002. DIFFERENTIAL RESPONSE OF RICE PLANTS TO LOW-PHOSPHORUS STRESS AND ITS PHYSIOLOGICAL ADAPTIVE MECHANISM. J. Plant Nutr. 25, 1213–1224. https://doi.org/10.1081/PLN-120004383

Miniotti, E.F., Romani, M., Said-Pullicino, D., Facchi, A., Bertora, C., Peyron, M., Sacco, D., Bischetti, G.B., Lerda, C., Tenni, D., Gandolfi, C., Celi, L., 2016. Agro-environmental sustainability of different water management practices in temperate rice agro-ecosystems. Agric. Ecosyst. Environ. 222, 235–248. https://doi.org/10.1016/j.agee.2016.02.010

Moody, P.W., Speirs, S.D., Scott, B.J., Mason, S.D., 2013. Soil phosphorus tests I: What soil phosphorus pools and processes do they measure? Crop Pasture Sci. 64, 461. https://doi.org/10.1071/CP13112

Mori, A., Fukuda, T., Vejchasarn, P., Nestler, J., Pariasca-Tanaka, J., Wissuwa, M., 2016. The role of root size versus root efficiency in phosphorus acquisition in rice. J. Exp. Bot. 67, 1179–1189. https://doi.org/10.1093/jxb/erv557

Muller, P.Y., Janovjak, H., Miserez, A.R., Dobbie, Z., 2002. Processing of gene expression data generated by quantitative real-time RT-PCR. BioTechniques 32, 1372–1374, 1376, 1378–1379.

Munch, J.C., Ottow, J.C.G., 1980. Preferential reduction of amorphous to crystalline iron oxides by bacterial activity. Soil Science 129, 15–21.

Murphy, J., Riley, J.P., 1962. A modified single solution method for the determination of phosphate in natural waters. Anal. Chim. Acta 27, 31–36. https://doi.org/10.1016/S0003-2670(00)88444-5

Nannipieri, P., Giagnoni, L., Landi, L., Renella, G., 2011. Role of Phosphatase Enzymes in Soil, in: Bünemann, E., Oberson, A., Frossard, E. (Eds.), Phosphorus in Action, Soil Biology. Springer Berlin Heidelberg, Berlin, Heidelberg, pp. 215–243. https://doi.org/10.1007/978-3-642-15271-9_9

Narisetti, N., Henke, M., Seiler, C., Shi, R., Junker, A., Altmann, T., Gladilin, E., 2019. Semi-automated Root Image Analysis (saRIA). Sci. Rep. 9, 19674. https://doi.org/10.1038/s41598-019-55876-3

Nenonen, V.V., Kaegi, R., Hug, S.J., Göttlicher, J., Mangold, S., Winkel, L.H.E., Voegelin, A., 2023. Formation and transformation of Fe(III)- and Ca-precipitates in aqueous solutions and effects on phosphate retention over time. Geochim. Cosmochim. Acta S0016703723004350. https://doi.org/10.1016/j.gca.2023.09.004

Neto, A.P., Favarin, J.L., Hammond, J.P., Tezotto, T., Couto, H.T.Z., 2016. Analysis of Phosphorus Use Efficiency Traits in Coffea Genotypes Reveals Coffea arabica and Coffea canephora Have Contrasting Phosphorus Uptake and Utilization Efficiencies. Front. Plant Sci. 7. https://doi.org/10.3389/fpls.2016.00408

Ohno, T., Zibilske, L.M., 1991. Determination of Low Concentrations of Phosphorus in Soil Extracts Using Malachite Green. Soil Sci. Soc. Am. J. 55, 892–895. https://doi.org/10.2136/sssaj1991.03615995005500030046x

Olsen, S.R., Agriculture, U.S.D. of, 1954. Estimation of Available Phosphorus in Soils by Extraction with Sodium Bicarbonate, Circular (United States. Department of Agriculture). U.S. Department of Agriculture.

Parsons, C.T., Rezanezhad, F., O'Connell, D.W., Van Cappellen, P., 2017. Sediment phosphorus speciation and mobility under dynamic redox conditions. Biogeosciences 14, 3585–3602. https://doi.org/10.5194/bg-14-3585-2017

Pennisi, E., 2008. The Blue Revolution, Drop by Drop, Gene by Gene. Science 320, 171–173. https://doi.org/10.1126/science.320.5873.171

Pierzynski, G.M., 2000. Methods of phosphorus analysis for soils, sediments, residuals, and waters. North Carolina State University, North Carolina.

Plaxton, W.C., Tran, H.T., 2011. Metabolic Adaptations of Phosphate-Starved Plants. Plant Physiol. 156, 1006–1015. https://doi.org/10.1104/pp.111.175281

Ponnamperuma, F.N., 1972. The Chemistry of Submerged Soils, in: Advances in Agronomy. Elsevier, pp. 29–96. https://doi.org/10.1016/S0065-2113(08)60633-1

Prietzel, J., Harrington, G., Häusler, W., Heister, K., Werner, F., Klysubun, W., 2016. Reference spectra of important adsorbed organic and inorganic phosphate binding forms for soil P speciation using synchrotron-based K -edge XANES spectroscopy. J. Synchrotron Radiat. 23, 532–544. https://doi.org/10.1107/S1600577515023085

Prietzel, J., Klysubun, W., 2018. Phosphorus K -edge XANES spectroscopy has probably often underestimated iron oxyhydroxide-bound P in soils. J. Synchrotron Radiat. 25, 1736–1744. https://doi.org/10.1107/S1600577518013334

Pujol, V., Wissuwa, M., 2018. Contrasting development of lysigenous aerenchyma in two rice genotypes under phosphorus deficiency. BMC Res. Notes 11, 60. https://doi.org/10.1186/s13104-018-3179-y

Rabeharisoa, L., Razanakoto, O.R., Razafimanantsoa, M.-P., Rakotoson, T., Amery, F., Smolders, E., 2012. Larger bioavailability of soil phosphorus for irrigated rice compared with rainfed rice in Madagascar: results from a soil and plant survey: P use of rainfed and irrigated rice in Madagascar. Soil Use Manag. 28, 448–456. https://doi.org/10.1111/j.1475-2743.2012.00444.x

Raiesi, F., Beheshti, A., 2014. Soil specific enzyme activity shows more clearly soil responses to paddy rice cultivation than absolute enzyme activity in primary forests of northwest Iran. Appl. Soil Ecol. 75, 63–70. https://doi.org/10.1016/j.apsoil.2013.10.012

Ravel, B., Newville, M., 2005. ATHENA , ARTEMIS , HEPHAESTUS : data analysis for X-ray absorption spectroscopy using IFEFFIT. J. Synchrotron Radiat. 12, 537–541. https://doi.org/10.1107/S0909049505012719

Refait, Ph., Reffass, M., Landoulsi, J., Sabot, R., Jeannin, M., 2007. Role of phosphate species during the formation and transformation of the Fe(II–III) hydroxycarbonate green rust. Colloids Surf. Physicochem. Eng. Asp. 299, 29–37. https://doi.org/10.1016/j.colsurfa.2006.11.013

Reyes, I., Torrent, J., 1997. Citrate-Ascorbate as a Highly Selective Extractant for Poorly Crystalline Iron Oxides. Soil Sci. Soc. Am. J. 61, 1647–1654. https://doi.org/10.2136/sssaj1997.03615995006100060015x

Rose, T.J., Impa, S.M., Rose, M.T., Pariasca-Tanaka, J., Mori, A., Heuer, S., Johnson-Beebout, S.E., Wissuwa, M., 2013. Enhancing phosphorus and zinc acquisition efficiency in rice: a critical review of root traits and their potential utility in rice breeding. Ann. Bot. 112, 331–345. https://doi.org/10.1093/aob/mcs217

Rose, T.J., Wissuwa, M., 2012. Rethinking Internal Phosphorus Utilization Efficiency, in: Advances in Agronomy. Elsevier, pp. 185–217. https://doi.org/10.1016/B978-0-12-394277-7.00005-1

Saggar, S., Hedley, M.J., White, R.E., 1990. A simplified resin membrane technique for extracting phosphorus from soils. Fertil. Res. 24, 173–180. https://doi.org/10.1007/BF01073586

Sahrawat, K.L., 2005. Iron Toxicity in Wetland Rice and the Role of Other Nutrients. J. Plant Nutr. 27, 1471–1504. https://doi.org/10.1081/PLN-200025869

Santoro, V., Martin, M., Persson, P., Lerda, C., Said-Pullicino, D., Magnacca, G., Celi, L., 2019. Inorganic and organic P retention by coprecipitation during ferrous iron oxidation. Geoderma 348, 168–180. https://doi.org/10.1016/j.geoderma.2019.04.004

Santoro, V., Schiavon, M., Celi, L., 2023. Role of soil abiotic processes on phosphorus availability and plant responses with a focus on strigolactones in tomato plants. Plant Soil. https://doi.org/10.1007/s11104-023-06266-2

Santoro, V., Schiavon, M., Visentin, I., Constán-Aguilar, C., Cardinale, F., Celi, L., 2021. Strigolactones affect phosphorus acquisition strategies in tomato plants. Plant Cell Environ. 44, 3628–3642. https://doi.org/10.1111/pce.14169

Santoro, V., Schiavon, M., Visentin, I., Martin, M., Said-Pullicino, D., Cardinale, F., Celi, L., 2022. Tomato plant responses induced by sparingly available inorganic and organic phosphorus forms are modulated by strigolactones. Plant Soil 474, 355–372. https://doi.org/10.1007/s11104-022-05337-0

Scalenghe, R., Edwards, A.C., Ajmone Marsan, F., Barberis, E., 2002. The effect of reducing conditions on the solubility of phosphorus in a diverse range of European agricultural soils: Redox conditions and P solubility. Eur. J. Soil Sci. 53, 439–447. https://doi.org/10.1046/j.1365-2389.2002.00462.x

Scalenghe, R., Edwards, A.C., Barberis, E., Ajmone-Marsan, F., 2012. Are agricultural soils under a continental temperate climate susceptible to episodic reducing conditions and increased leaching of phosphorus? J. Environ. Manage. 97, 141–147. https://doi.org/10.1016/j.jenvman.2011.11.015

Schärer, M., De Grave, E., Semalulu, O., Sinaj, S., Vandenberghe, R.E., Frossard, E., 2009. Effect of redox conditions on phosphate exchangeability and iron forms in a soil amended with ferrous iron. Eur. J. Soil Sci. 60, 386–397. https://doi.org/10.1111/j.1365-2389.2009.01135.x

Schulz, K., Notini, L., Grigg, A.R.C., Kubeneck, L.J., Wisawapipat, W., ThomasArrigo, L.K., Kretzschmar, R., 2023. Contact with soil impacts ferrihydrite and lepidocrocite transformations during redox cycling in a paddy soil. Environ. Sci. Process. Impacts 25, 1945–1961. https://doi.org/10.1039/D3EM00314K

Schwertmann, U., Cornell, Rochelle M., Cornell, R. M., 2008. Iron Oxides in the Laboratory, 1st ed. Wiley, Hoboken.

Seck, P.A., Diagne, A., Mohanty, S., Wopereis, M.C.S., 2012. Crops that feed the world 7: Rice. Food Secur. 4, 7–24. https://doi.org/10.1007/s12571-012-0168-1

Senn, A.-C., Kaegi, R., Hug, S.J., Hering, J.G., Mangold, S., Voegelin, A., 2017. Effect of aging on the structure and phosphate retention of Fe(III)-precipitates formed by Fe(II) oxidation in water. Geochim. Cosmochim. Acta 202, 341–360. https://doi.org/10.1016/j.gca.2016.12.033

Senn, A.-C., Kaegi, R., Hug, S.J., Hering, J.G., Mangold, S., Voegelin, A., 2015. Composition and structure of Fe(III)-precipitates formed by Fe(II) oxidation in water at near-neutral pH: Interdependent effects of phosphate, silicate and Ca. Geochim. Cosmochim. Acta 162, 220–246. https://doi.org/10.1016/j.gca.2015.04.032

Seyfferth, A.L., 2015. Abiotic effects of dissolved oxyanions on iron plaque quantity and mineral composition in a simulated rhizosphere. Plant Soil 397, 43–61. https://doi.org/10.1007/s11104-015-2597-z

Seyfferth, A.L., Limmer, M.A., Tappero, R., 2021. A Method to Preserve Wetland Roots and Rhizospheres for Elemental Imaging. J. Vis. Exp. 62227. https://doi.org/10.3791/62227

Seyfferth, A.L., Webb, S.M., Andrews, J.C., Fendorf, S., 2010. Arsenic Localization, Speciation, and Co-Occurrence with Iron on Rice (Oryza sativa L.) Roots Having Variable Fe Coatings. Environ. Sci. Technol. 44, 8108–8113. https://doi.org/10.1021/es101139z

Shahandeh, H., Hossner, L.R., Turner, F.T., 1995. Evaluation of soil phosphorus tests for flooded rice soils under oxidized and reduced soil conditions. Commun. Soil Sci. Plant Anal. 26, 107–121. https://doi.org/10.1080/00103629509369284

Sodano, M., Lerda, C., Nisticò, R., Martin, M., Magnacca, G., Celi, L., Said-Pullicino, D., 2017. Dissolved organic carbon retention by coprecipitation during the oxidation of ferrous iron. Geoderma 307, 19–29. https://doi.org/10.1016/j.geoderma.2017.07.022

Soltanpour, P.N., Adams, F., Bennett, A.C., 1974. Soil Phosphorus Availability as Measured by Displaced Soil Solutions, Calcium-Chloride Extracts, Dilute-Acid Extracts, and Labile Phosphorus. Soil Sci. Soc. Am. J. 38, 225–228. https://doi.org/10.2136/sssaj1974.03615995003800020010x

Song, T., Xu, F., Yuan, W., Zhang, Y., Liu, T., Chen, M., Hu, Q., Tian, Y., Xu, W., Zhang, J., 2018. Comparison on physiological adaptation and phosphorus use efficiency of upland rice and lowland rice under alternate wetting and drying irrigation. Plant Growth Regul. 86, 195–210. https://doi.org/10.1007/s10725-018-0421-5

Tanaka, A., Loe, R., Navasero, S.A., 1966. Some mechanisms involved in the development of iron toxicity symptoms in the rice plant. Soil Sci. Plant Nutr. 12, 32–38. https://doi.org/10.1080/00380768.1966.10431951

Tang, J., Leung, A., Leung, C., Lim, B.L., 2006. Hydrolysis of precipitated phytate by three distinct families of phytases. Soil Biol. Biochem. 38, 1316–1324. https://doi.org/10.1016/j.soilbio.2005.08.021

Teo, Y.H., Beyrouty, C.A., Norman, R.J., Gbur, E.E., 1995. Nutrient uptake relationship to root characteristics of rice. Plant Soil 171, 297–302. https://doi.org/10.1007/BF00010285

Thompson, A., Chadwick, O.A., Rancourt, D.G., Chorover, J., 2006. Iron-oxide crystallinity increases during soil redox oscillations. Geochim. Cosmochim. Acta 70, 1710–1727. https://doi.org/10.1016/j.gca.2005.12.005

Trasar-Cepeda, C., Leirós, M.C., Gil-Sotres, F., 2008. Hydrolytic enzyme activities in agricultural and forest soils. Some implications for their use as indicators of soil quality. Soil Biol. Biochem. 40, 2146–2155. https://doi.org/10.1016/j.soilbio.2008.03.015

Turner, B.L., 2008. Soil organic phosphorus in tropical forests: an assessment of the NaOH–EDTA extraction procedure for quantitative analysis by solution 31 P NMR spectroscopy. Eur. J. Soil Sci. 59, 453–466. https://doi.org/10.1111/j.1365-2389.2007.00994.x

Turner, B.L., Frossard, E., Baldwin, D.S. (Eds.), 2005. Organic phosphorus in the environment. Presented at the Organic Phosphorus Workshop, CABI Pub, Wallingford, UK ; Cambridge, MA.

Vallino, M., Fiorilli, V., Bonfante, P., 2014. Rice flooding negatively impacts root branching and arbuscular mycorrhizal colonization, but not fungal viability. Plant Cell Environ. 37, 557–572. https://doi.org/10.1111/pce.12177

Vartapetian, B.B., Jackson, M.B., 1997. Plant Adaptations to Anaerobic Stress. Ann. Bot. 79, 3–20. https://doi.org/10.1093/oxfordjournals.aob.a010303

Voegelin, A., Senn, A.-C., Kaegi, R., Hug, S.J., Mangold, S., 2013. Dynamic Fe-precipitate formation induced by Fe(II) oxidation in aerated phosphate-containing water. Geochim. Cosmochim. Acta 117, 216–231. https://doi.org/10.1016/j.gca.2013.04.022

Wang, C., Thielemann, L., Dippold, M.A., Guggenberger, G., Kuzyakov, Y., Banfield, C.C., Ge, T., Guenther, S., Bork, P., Horn, M.A., Dorodnikov, M., 2022a. Microbial iron reduction compensates for phosphorus limitation in paddy soils. Sci. Total Environ. 837, 155810. https://doi.org/10.1016/j.scitotenv.2022.155810

Wang, C., Thielemann, L., Dippold, M.A., Guggenberger, G., Kuzyakov, Y., Banfield, C.C., Ge, T., Guenther, S., Bork, P., Horn, M.A., Dorodnikov, M., 2022b. Can the reductive dissolution of ferric iron in paddy soils compensate phosphorus limitation of rice plants and microorganisms? Soil Biol. Biochem. 168, 108653. https://doi.org/10.1016/j.soilbio.2022.108653

Wang, F., Rose, T., Jeong, K., Kretzschmar, T., Wissuwa, M., 2016. The knowns and unknowns of phosphorus loading into grains, and implications for phosphorus efficiency in cropping systems. J. Exp. Bot. 67, 1221–1229. https://doi.org/10.1093/jxb/erv517

Wang, X., Hu, Y., Tang, Y., Yang, P., Feng, X., Xu, W., Zhu, M., 2017. Phosphate and phytate adsorption and precipitation on ferrihydrite surfaces. Environ. Sci. Nano 4, 2193–2204. https://doi.org/10.1039/C7EN00705A

Wang, X., Shen, J., Liao, H., 2010. Acquisition or utilization, which is more critical for enhancing phosphorus efficiency in modern crops? Plant Sci. 179, 302–306. https://doi.org/10.1016/j.plantsci.2010.06.007

Wei, X., Zhu, Z., Wei, L., Wu, J., Ge, T., 2019. Biogeochemical cycles of key elements in the paddy-rice rhizosphere: Microbial mechanisms and coupling processes. Rhizosphere 10, 100145. https://doi.org/10.1016/j.rhisph.2019.100145

Weiss, J.V., Emerson, D., Megonigal, J.P., 2004. Geochemical control of microbial Fe(III) reduction potential in wetlands: comparison of the rhizosphere to non-rhizosphere soil. FEMS Microbiol. Ecol. 48, 89–100. https://doi.org/10.1016/j.femsec.2003.12.014

Weiss, J.V., Rentz, J.A., Plaia, T., Neubauer, S.C., Merrill-Floyd, M., Lilburn, T., Bradburne, C., Megonigal, J.P., Emerson, D., 2007. Characterization of Neutrophilic Fe(II)-Oxidizing Bacteria Isolated from the Rhizosphere of Wetland Plants and Description of Ferritrophicum radicicola gen. nov. sp. nov., and Sideroxydans paludicola sp. nov. Geomicrobiol. J. 24, 559–570. https://doi.org/10.1080/01490450701670152

Werner, F., Prietzel, J., 2015. Standard Protocol and Quality Assessment of Soil Phosphorus Speciation by P K -Edge XANES Spectroscopy. Environ. Sci. Technol. 49, 10521–10528. https://doi.org/10.1021/acs.est.5b03096

Winkler, P., Kaiser, K., Thompson, A., Kalbitz, K., Fiedler, S., Jahn, R., 2018. Contrasting evolution of iron phase composition in soils exposed to redox fluctuations. Geochim. Cosmochim. Acta 235, 89–102. https://doi.org/10.1016/j.gca.2018.05.019

Wissuwa, M., 2005. Combining a modelling with a genetic approach in establishing associations between genetic and physiological effects in relation to phosphorus uptake. Plant Soil 269, 57–68. https://doi.org/10.1007/s11104-004-2026-1

Wissuwa, M., 2003. How Do Plants Achieve Tolerance to Phosphorus Deficiency? Small Causes with Big Effects. Plant Physiol. 133, 1947–1958. https://doi.org/10.1104/pp.103.029306

Wolf, A.M., Baker, D.E., 1990. Colorimetric method for phosphorus measurement in ammonium oxalate soil extracts. Commun. Soil Sci. Plant Anal. 21, 2257–2263. https://doi.org/10.1080/00103629009368378

Wu, C., Ye, Z., Li, H., Wu, S., Deng, D., Zhu, Y., Wong, M., 2012. Do radial oxygen loss and external aeration affect iron plaque formation and arsenic accumulation and speciation in rice? J. Exp. Bot. 63, 2961–2970. https://doi.org/10.1093/jxb/ers017

Xu, F., Song, T., Wang, K., Xu, W., Chen, G., Xu, M., Zhang, Q., Liu, J., Zhu, Y., Rensing, C., Zhang, J., Yuan, W., 2020. Frequent alternate wetting and drying irrigation mitigates the effect of low phosphorus on rice grain yield in a 4-year field trial by increasing soil phosphorus release and rice root growth. Food Energy Secur. 9. https://doi.org/10.1002/fes3.206

Yamauchi, T., Nakazono, M., 2022. Mechanisms of lysigenous aerenchyma formation under abiotic stress. Trends Plant Sci. 27, 13–15. https://doi.org/10.1016/j.tplants.2021.10.012

Yamauchi, T., Shimamura, S., Nakazono, M., Mochizuki, T., 2013. Aerenchyma formation in crop species: A review. Field Crops Res. 152, 8–16. https://doi.org/10.1016/j.fcr.2012.12.008

Yamauchi, T., Tanaka, A., Mori, H., Takamure, I., Kato, K., Nakazono, M., 2016. Ethylene-dependent aerenchyma formation in adventitious roots is regulated differently in rice and maize: Ethylene-dependent aerenchyma formation in roots. Plant Cell Environ. 39, 2145–2157. https://doi.org/10.1111/pce.12766

Yang, X.-J., Xu, Z., Shen, H., 2018. Drying–submergence alternation enhanced crystalline ratio and varied surface properties of iron plaque on rice (Oryza sativa) roots. Environ. Sci. Pollut. Res. 25, 3571–3587. https://doi.org/10.1007/s11356-017-0509-x

Yee, N., Shaw, S., Benning, L.G., Nguyen, T.H., 2006. The rate of ferrihydrite transformation to goethite via the Fe(II) pathway. Am. Mineral. 91, 92–96. https://doi.org/10.2138/am.2006.1860

Yoshida, D., 1967. Effects of nutrient deficiencies on tne biosynthesis of nicotine in tobacco plants. Soil Sci. Plant Nutr. 13, 107–111. https://doi.org/10.1080/00380768.1967.10431983

Zampieri, M., Ceglar, A., Dentener, F., Dosio, A., Naumann, G., Van Den Berg, M., Toreti, A., 2019. When Will Current Climate Extremes Affecting Maize Production Become the Norm? Earths Future 7, 113–122. https://doi.org/10.1029/2018EF000995

Zampieri, Matteo, Ceglar, A., Manfron, G., Toreti, A., Duveiller, G., Romani, M., Rocca, C., Scoccimarro, E., Podrascanin, Z., Djurdjevic, V., 2019. Adaptation and sustainability of water management for rice agriculture in temperate regions: The Italian case-study. Land Degrad. Dev. 30, 2033–2047. https://doi.org/10.1002/ldr.3402

Zhang, X., Yao, H., Lei, X., Lian, Q., Roy, A., Doucet, D., Yan, H., Zappi, M.E., Gang, D.D., 2021. A comparative study for phosphate adsorption on amorphous FeOOH and goethite (α-FeOOH): An investigation of relationship between the surface chemistry and structure. Environ. Res. 199, 111223. https://doi.org/10.1016/j.envres.2021.111223

Zhang, X., Zhang, F., Mao, D., 1999. Effect of iron plaque outside roots on nutrient uptake by rice (Oryza sativa L.): Phosphorus uptake. Plant Soil 209, 187–192. https://doi.org/10.1023/A:1004505431879

Zhang, Y., Lin, X., Werner, W., 2004. Effects of aerobic conditions in the rhizosphere of rice on the dynamics and availability of phosphorus in a flooded soil – A model experiment. J. Plant Nutr. Soil Sci. 167, 66–71. https://doi.org/10.1002/jpln.200320349

Zhang, Y., Lin, X., Werner, W., 2003. The effect of soil flooding on the transformation of Fe oxides and the adsorption/desorption behavior of phosphate. J. Plant Nutr. Soil Sci. 166, 68–75. https://doi.org/10.1002/jpln.200390014

Zhou, H., Zhu, W., Yang, W.-T., Gu, J.-F., Gao, Z.-X., Chen, L.-W., Du, W.-Q., Zhang, P., Peng, P.-Q., Liao, B.-H., 2018. Cadmium uptake, accumulation, and remobilization in iron plaque and rice tissues at different growth stages. Ecotoxicol. Environ. Saf. 152, 91–97. https://doi.org/10.1016/j.ecoenv.2018.01.031

SUPPLEMENTARY MATERIAL

Chapter 5: Root Fe plaque as a spatial-temporal dynamic P pool in rice grown under different water management

5.2 Materials and Methods

5.2.1 P reference compounds synthesis and characterization

The standard materials were synthesized using a soluble Fe salt and three different P species. To obtain poorly crystalline coprecipitates we used a Fe(III)Cl_3 solution neutralized with a KOH solution (Schwertmann et al., 2008) with addition of potassium dihydrogenphosphate (KH_2PO_4), inositol hexakisphosphate (sodium salt), or β-glycerophosphate (sodium salt) at a P:Fe molar ratio of 0.3. The obtained Fe-P co-precipitates will be referred to as orthophosphate co-precipitated within ferrihydrite (Pi-fhy), inositol hexakiphosphate co-precipitated within ferrihydrite (Ins6P-fhy), and β-glycerophosphate coprecipitated within ferrihydrite (glycP-fhy). The same procedure was followed to synthesize more crystalline coprecipitates, using the method for goethite synthesis (Schwertmann et al., 2008). In this case, the solution P:Fe molar ratio was 0.1 in order not to interfere with crystallization of the coprecipitates (Senn *et al.*, 2015; Voegelin *et al.*, 2013). These minerals will be referred to as orthophosphate co-precipitated within goethite (Pi-goe), inositol hexakiphosphate co-precipitated within goethite (Ins6P-goe), and β-glycerophosphate coprecipitated within ferrihydrite (glycP-goe). Furthermore, a synthetic Fe plaque mixture was synthesized following the same procedure described for Pi-fhy, and by including in the solution 24 mM of Ca as $Ca(OH)_2$, 45 mM of Mg as $MgCl_2$, and 63 mM of Si as H_2SiO_3, according to previously reported Fe plaque composition (Limmer *et al.*, 2022). After the synthesis all the co-precipitates were tested for purity by XRD analysis. Ammonium phosphate (NH_4-P) in the form of $NH_4H_2PO_4$, calcium phosphate (Ca-P) in the form of $Ca(H_2PO_4)_2*H_2O$, and iron phosphate ($Fe_3PO_4*2H_2O$) were included in the analyses as reference compounds. All the chemicals were purchased from Sigma-Aldrich (St. Louis, MO, USA).

Phosphorus L_{2-3}-edge XANES spectroscopy

Phosphorus L_{2-3}-edge XANES measurement of standards were conducted at the 7-ID spectroscopy soft and tender 1 (7-ID-SST-1) beamline at the National Synchrotron Light Source II (NSLS-II), Brookhaven Upton NY United States. Spectra were collected in partial electron yield (PEY) mode due to sample charging. The PEY signal was normalized to the incident beam intensity of a clean gold grid to account for incident beam fluctuations and optics absorption features. The sample compartment was under ultra-high vacuum, and multiple spectra were collected and averaged for each sample. Data analysis was performed using Origin(Pro), Version 2023b, OriginLab Corporation, Northampton, MA, USA (Kruse et al., 2009; Colocho Hurtarte et al., 2020). In detail, after visual inspection for glitches, drifts, noise, and general quality, replicate spectra of the same sample were merged. Merged spectra were

background-corrected using a second order polynomial function between four points in the pre-edge and post-edge regions. Thereafter, each baseline-corrected spectrum was normalized to the highest intensity point across the spectrum.

Phosphorus K-edge XANES spectroscopy

Phosphorus K-edge X-ray absorption near edge structure (XANES) experiments were conducted at the 7-ID spectroscopy soft and tender 2 (7-ID-SST-2) beamline equipped with a Si(111) monochromator at the National Synchrotron Light Source II (NSLS-II) at Brookhaven National Laboratory. Measurements were performed in partial electron yield (PEY) mode with step sizes of 2 eV in the pre-edge region (2110-2135 eV), 0.3 eV in the edge region (2135-2185 eV), and 1 eV in the post-edge region (2185-2235 eV). The PEY signal was normalized to the incident beam intensity on a clean gold grid, and the sample compartment was under ultra-high vacuum. Duplicate spectra were collected and averaged for each sample. Data analysis (background subtraction, normalization, and linear combination fitting) was performed using Athena software (Ravel and Newville, 2005) following previous P-XANES protocols (Werner and Prietzel, 2015). Optimum baseline subtraction and edge-step normalization were identified by visual inspection in the energy range between -40 to -10 eV and +35 to +65 eV with respect to E0 which was at 2110 eV.

5.2.2 Standard mixtures

Various mixtures of the 6 standards were produced by mixing equal amounts of 2-3 standard compounds in an agate mortar and pestle. The mixtures were prepared according to P molar weight in order to test the power of P-XANES LCF to distinguish between different P species retained on the same Fe oxide (*e.g.*, Pi-fhy + Ins6P-fhy + glycP-fhy) and the same P species bound to different Fe oxides (*i.e.* ferrihydrite and goethite). In total, 6 standard mixtures were analyzed (Table S5.1). LCF was performed in the energy range 2140-2200 eV with several iterations of different standards: a) only the standards actually included in the mixture, b) all the P forms retained by ferrihydrite (Pi-fhy, Ins6P-fhy, and glycP-fhy), c) all the P forms retained by goethite (Pi-goe, Ins6P-goe), d) all the standards (Pi-fhy, Ins6P-fhy, glycP-fhy, Pi-goe, Ins6P-goe), e) all the standard excluding glycP-fhy.

Table S5.1 Summary of the mixture of standard used to validate the linear combination fitting (LCF) analysis. The symbol (-) is used when the standard was not included in the mixture.

Mix	Pi-fhy	Ins6P-fhy	glycP-fhy	Pi-goe	Ins6P-goe	glycP-goe
	weight (g)					
1	0.33	0.33	0.33	-	-	-
2	0.50	0.50	-	-	-	-
3	0.50	-	0.50	-	-	-
4	-	0.50	0.50	-	-	-
5	0.50	-	-	0.50	-	-
6	-	0.50	-	-	0.50	-

5.3 Results and Discussion

5.3.1 Phosphorus L_{2-3}-edge XANES spectra of reference materials

The L_{2-3}-edge XANES spectra of the different reference materials showed the spectral features described by Kruse *et al.*, 2009 for the NH_4-, Ca-, and Fe-P compounds (Fig. S5.1). This includes two peaks separated by 1 eV in the low-energy range, labeled respectively (a) and (b), due to the transition from spin-orbit split $2p_{2/3}$ and $2p_{1/2}$ electrons into the first unoccupied 3*s*-like antibonding state (Kruse *et al.*, 2009). A second peak 2 eV higher (c) is attributed to the presence of oxygen or metal ions from the $2p \rightarrow 3p$ forbidden transition due to 3*p*-3*d* overlapping state and crystal distortion (Bruun *et al.*, 2017). A broad and intense peak around 147 eV is further observed, labeled (d) and/or (f) owing to 2*p* to 3*d* transition, often called "shape resonance." The spectra of Ca-phosphate compounds generally present a shoulder (e) at the high-energy side of peak (c), likely attributed to the transition of P 2*p* to Ca 3*d* empty orbitals, and thus generally considered a distinguish feature of Ca-phosphate (Kruse *et al.*, 2009). Due to the specificity in feature (e), P L_{2-3}-edge XANES is generally capable of distinguishing between different Ca-phosphate compounds, while less information is available regarding different Fe-P forms (Zhu *et al.*, 2018; Kruse *et al.*, 2015). The shape and position of (f) peak in our L_{2-3}-edge XANES spectra of Ca-P standard corresponds well to those of $Ca(H_2PO_4)_2{*}H_2O$ described by Kruse *et al.*, 2009, as expected. Similarly, our NH_4-P compound spectrum was identical to previously reported $NH_4H_2PO_4$ spectra, albeit the differences among NH_4-P compounds more subtle than different Ca-P compounds (Kruse *et al.*, 2009). Our Fe-P standard showed different features than the NH_4-P and Ca-P spectra, notably the (b) peak was unresolved and a broad peak (a') appeared below peak (a). The (a') peak was formerly attributed to the transition of P 2*p* electrons into unoccupied states with a partial 3*d* character formed by hybridization of Fe(3*d*), O(2*p*) and P(3*p*) orbitals (Kruse *et al.*, 2009). This (a') peak was particularly pronounced in the spectra of synthetic Fe plaque, which mostly resembled those of Fe-P, even though Ca and other minor elements were included in the solution. The spectra of synthetic Fe plaque also showed a lower signal-to-noise ratio compared to the pure standards, likely due to the lower P concentration in the matrix and the potential of multiple P phases.

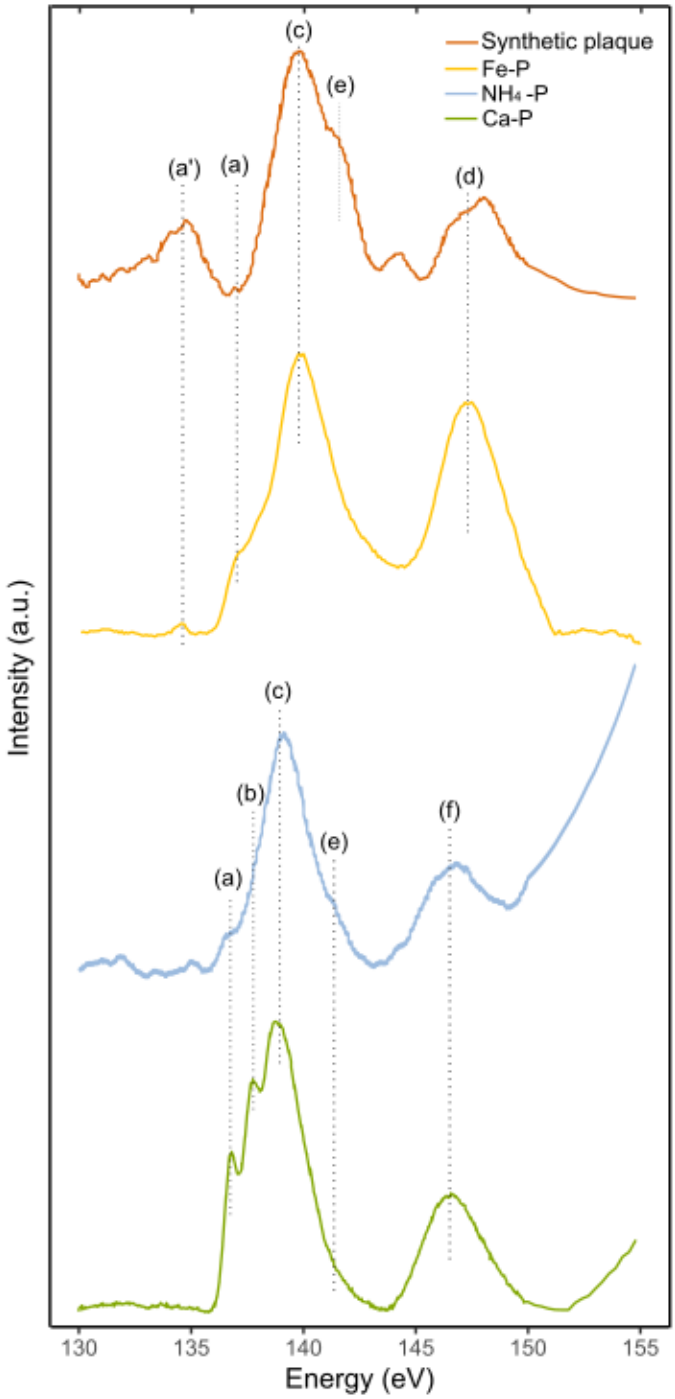

Figure S5.1. Stacked PEY P $L_{2\text{-}3}$-edge XANES spectra of calcium phosphate (Ca-P), ammonium phosphate (NH_4-P), iron phosphate (Fe-P), and synthetic Fe plaque.

5.3.2 Phosphorus K-edge spectra of P synthetic standard compounds

The spectra of the synthesized standards showed distinctive features according to the P forms utilized to synthesize the materials, while different Fe oxides resulted in limited spectral differences. Nonetheless all the organic P forms showed a smaller white line (WL) intensity compared to Pi, which was less evident on ferrihydrite (Fig. S5.2a) compared to goethite (Fig. S5.2b). These results are in agreement with Prietzel and co-authors (2016; 2018) who reported a larger WL intensity in the spectra of orthophosphate compared to other organic P forms (i.e. inositol hexakisphosphate and adenosin-triphosphate). Glycerophosphate seemed to inhibit goethite crystallization, as indicated by XRD spectra similar to glycP-fhy, and thus no P K-edge XANES spectrum is available for this standard (data not shown).

The spectra of all P forms retained by both ferrihydrite and goethite showed a particular pre-edge feature from 2148-2151 eV. In the case of Pi-fhy, glycP-fhy (Fig. S5.2a), and somewhat for Pi-goe (Fig. S5.2b), this pre-edge feature can be considered a true pre-edge peak, while Ins6P-fhy (Fig. S5.2a) had a small shoulder which was even smaller in Ins6P-goe (Fig. S5.2b). These pre-edge features in P L_{2-3}-edge XANES spectra of Fe-P compounds are attributed to the transition of P 1s electrons into Fe(4*p*) - O(2*p*) antibonding molecular orbitals, and the differences in pre-edge features are due to variation in P binding environments (Prietzel *et al.*, 2016*b*). Inner-sphere complexation via ligand exchange and surface precipitation are the most common mechanisms used to explain P retention by Fe oxides (Arai & Sparks, 2001), with the extent of each due to the solution P:Fe molar ratio and the P speciation (Châtellier *et al.*, 2013; Santoro *et al.*, 2019). P K-edge XANES spectra generally have a larger and narrower WL and a small pre-edge shoulder for inner-sphere complexation of P on Fe oxides, while surface precipitation produces a clear pre-edge peak and a smaller and wider WL (Khare *et al.*, 2007, 2005). Accordingly, the smaller WL observed in our adsorbed organic P species (i.e. Ins6P and glycP) compared to orthophosphate suggests that co-precipitation is more dominant for organic P species compared to orthophosphate (Santoro et al., 2019). However, the evaluation of the pre-edge feature shows the inverse, as the higher intensity of the pre-edge peak is observed in Pi-fhy compared to Ins6P-fhy, which suggests inner-sphere complexation is instead more important for organic P compared to orthophosphate (Khare *et al.*, 2007). Similar conflicting results were also obtained by Prietzel et al. (2016), who concluded that P-XANES spectra did not alter previous theory that P inner-sphere complexation dominates over surface precipitation. Regardless of the P retention mechanism, the evaluation of the P K-edge XANES spectra of the standard compounds included in this study resulted in markedly different WL intensity and pre-edge features, thus corroborating the findings of Prietzel et al. (2016; 2018) who suggested inclusion of multiple different Fe-bearing compounds as references for analyzing P speciation in soil samples.

The spectra of Ca-P and NH_4-P (Fig. S5.2c) did not show the pre-edge feature (Fig S5.2c), further supporting the hypothesis that this is attributed to the Fe-P interactions. Conversely, both Ca-P and NH_4-P spectra showed specific post-edge

features, whose shape and intensity can be related to different Ca-P compounds (Prietzel *et al.*, 2016). However, the K-edge XANES spectra of Ca-P and NH_4-P were not as diagnostic as the L_{2-3}-edge XANES spectra which seem to be better than K-edge XANES in distinguishing among different Ca-phosphate forms.

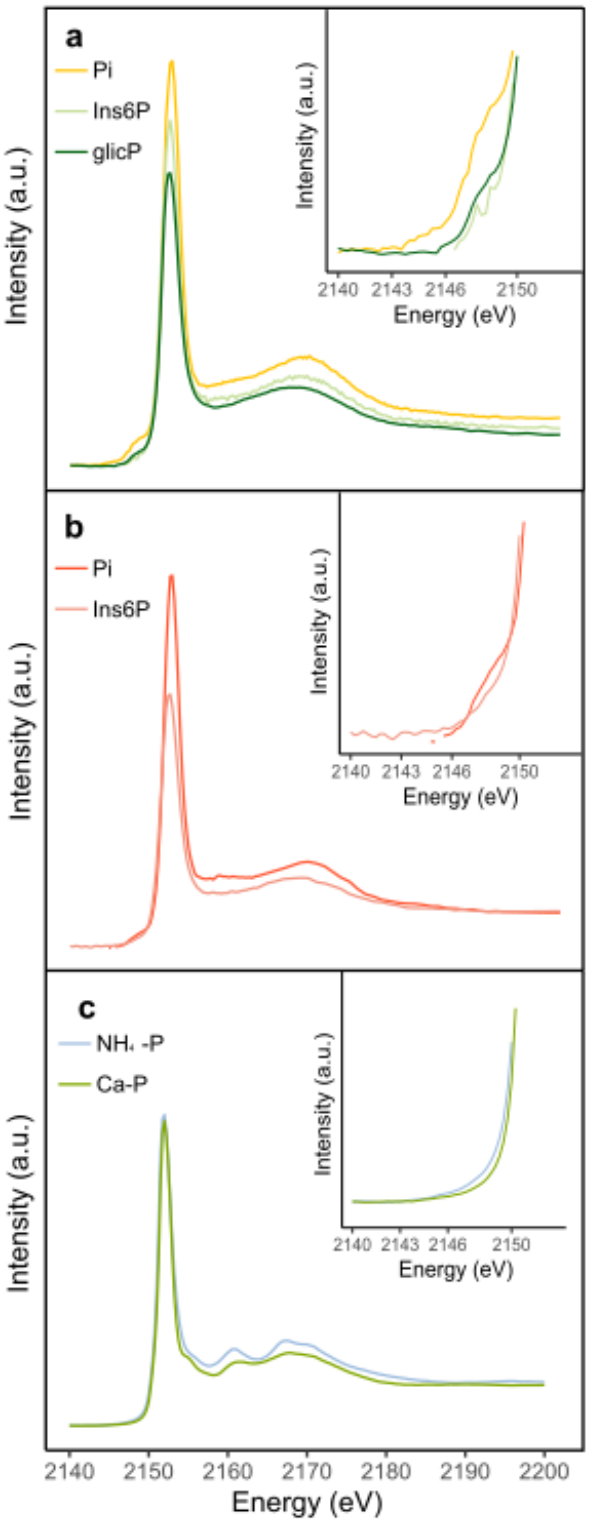

Figure S5.2. Phosphorus K-edge XANES spectra of a) orthophosphate (Pi), inositol hexakiphosphate (Ins6P), and glycerophosphate (glycP) co-precipitated with ferrihydrite, b) orthophosphate (Pi), and inositol hexakisphosphate (Ins6P), co-precipitated with goethite, and c) ammonium phosphate (NH_4-P) and calcium phosphate (Ca-P). Enclosed boxes represent close-up views of pre-edge regions.

5.3.3 Fe plaque chemistry and reference materials selection

The chemical composition of Fe plaque samples obtained from XRF survey was consistent to former literature reports (Limmer *et al.*, 2022). Table S5.2 reports the molar ratio among the main elements in plaque calculated from the concentration of the single element obtained from the XRF survey. In all cases plus-P treatment resulted in higher P:Fe and P:Ca molar ratios, suggesting that the P fertilizer may contribute to increase the amount of P retained by Fe plaque. Conversely, the different water management did not result in significant differences in any of the calculated molar ratio.

The P:Fe molar ratios measured in Fe plaque were comparable to those previously reported by Santoro *et al.* (2019) for the precipitates obtained by Fe(II) oxidation in the presence of P. Indeed, Fe plaque is formed by Fe(III) oxidative precipitation, and the P present in the solution is incorporated into the nanoparticles of the newly formed Fe(III)-precipitates resulting in surface poisoning and disruption of the overall structural order of the newly formed Fe oxides (Voegelin *et al.*, 2013; Châtellier *et al.*, 2013). Consequently, increasing solution P:Fe ratio progressively decreases the crystallinity of the end-products from lepidocrocite to ferrihydrite to Fe(III)-phosphate (Voegelin *et al.*, 2013; Senn *et al.*, 2015; Nenonen *et al.*, 2023). Formation of these short range ordered phases tends to increase P retention, and thus produces a greater P:Fe ratio of the end-products (Senn *et al.*, 2015; Santoro *et al.*, 2019). Considering the P:Fe molar ratio obtained by Santoro *et al.* (2019) it is likely that our Fe plaque is mainly composed of poorly crystalline ferrihydrite with incorporated P nuclei rather than amorphous Fe(III)-phosphate.

The Ca:Fe molar ratios were in all cases far lower than those previously reported in the literature (Senn *et al.*, 2015; Voegelin *et al.*, 2010). Such a difference could be attributed to the different concentration of Ca in the solution during the formation of Fe plaque. Indeed, the paddy porewater Ca concentration (Roberts *et al.*, 2011) was reported to be an order of magnitude lower than the Ca concentration measured during the synthesis of Fe(III)-precipitates in groundwater proposed by Senn *et al.* (2015) and Voegelin *et al.* (2010) where Ca decreased P coordination with Fe to allow Ca-O-P linkage formation during Fe(III) oxidative precipitation. Increasing solution Ca:Fe ratio inhibited P-O-Fe linkage, while higher solution Fe concentrations strongly coordinated P and hindered formation of Ca-phosphate (Voegelin *et al.*, 2010). The Ca:Fe ratios of our Fe plaque suggests that Ca-phosphate is not formed, however, it is likely that Ca is bridging the negatively charged phosphate-coordinated Fe(III)-monomers or oligomers (Voegelin *et al.*, 2010; Senn *et al.*, 2015; Nenonen *et al.*, 2023). In addition, the P:Ca molar ratios of our plaque samples do not support formation of pure Ca-phosphate phases. The P K-edge XANES spectral features of Fe(III)-Ca-phosphate electrostatic ternary complexes mostly resemble those of Fe(III)-phosphate rather than Ca-phosphate, especially at low Ca:Fe molar ratio (Voegelin *et al.*, 2010).

The Si:Fe molar ratios measured in plaque samples were far higher than those previously reported in the literature for Fe(III)-precipitates (Senn *et al.*, 2015; Voegelin *et al.*, 2013; Nenonen *et al.*, 2023). Nonetheless, the role of Si during Fe(III) oxidative precipitation was almost attributed to a distortion of the crystal nuclei and subsequent alteration of the Fe mineral structure rather than a direct effect on P retention. Furthermore, we cannot completely exclude the contamination of the Fe plaque samples with very small soil particles, thus possibly explaining the high Si concentrations measured in the samples. For these reasons we consider a Si:Fe molar ratios formely reported in the literature for Fe plaque samples from Seyfferth (2015) and Limmer *et al.* (2022) instead of our Si:Fe molar ratios for standard selection and synthesis.
Considering that XRF analysis is not able to distinguish between inorganic and organic P forms, and the overall P:Fe:Ca molar ratios calculated for Fe plaque samples, the reference materials included in the LCF exercises were Pi-fhy, Ins6P-fhy, glycP-fhy, Pi-goe, Ins6P-goe, glycP-goe, and NH_4-P. The latter reference was included to test whether the P fertilizer can be directly retained by Fe plaque, as proposed by Lombi *et al.*, 2006 for soil samples.

Table S5.2. Molar ratio among P:Fe:Ca:Si of the Fe plaque of rice grown under continuous flooded soil (WFL) or alternating wetting and drying irrigation (AWD), with 46 kg of P per ha of P fertilization (plus-P) or without P fertilization (no-P). The molar ratios were calculated according to the concentration obtained from the XRF analysis.

Water management	P fertilization	Molar ratios			
		P:Fe	P:Ca	Ca:Fe	Si:Fe
AWD					
	plus-P	0.23 ± 0.10	0.56 ± 0.23	0.41 ± 0.01	1.0 ± 0.04
	no-P	0.11 ± 0.07	0.34 ± 0.04	0.32 ± 0.17	0.92 ± 0.37
WFL					
	plus-P	0.20 ± 0.08	0.49 ± 0.01	0.39 ± 0.16	0.97 ± 0.30
	no-P	0.14 ± 0.05	0.35 ± 0.03	0.40 ± 0.11	1.2 ± 0.32

5.3.4 Linear combination fitting of P K-edge XANES of standard mixtures

All of the standard mixture samples produced high quality P K-edge XANES spectra for LCF with selected reference materials. The results of LCF conducted using only the known standards for each mixture (Table S5.3, Fit a) showed that the percentage of glycP-fhy was slightly overestimated at the cost of other P forms when all the P forms were included in the same mixture (Mix 1), and that the Fe mineral (ferrihydrite or goethite) binding P could not be distinguished (Mixes 5 and 6). LCF using only P forms coprecipitated with ferrihydrite (Table S5.3, Fit b) resulted in a similar quality of fits, with glycP-fhy again being overestimated, this time at the expense of Ins6P-fhy. LCF using only Pi-goe and Ins6P-goe as standards (Table S5.3, Fit c) resulted in the correct estimation of the amount of inorganic and organic P in the mixtures, considering organic P as the sum of Ins6P and glycP. When glycP-fhy was included in the mixture (Mix 1, Mix 3, Mix 4) the LCF erroneously identified it as Ins6P-goe, resulting in an

overestimation of the latter organic P form. Regarding inorganic P, when Pi-fhy was included in the mixture (Mix 1, Mix 2, Mix 3, Mix 5) the LCF overestimated Pi-goe at the expense of Pi-fhy, and Ins6P-goe at the expense of Ins6P-fhy (Mix 2, Mix 4). Including all standards in the LCF (Table S5.3, Fit d) resulted in overestimations of glycP-fhy at the expense of Ins6P-fhy, but overall a generally correct computation of the proportion of inorganic and organic (Ins6P + glycP) P. The amounts of Pi and Po in the mixtures were very accurate, though the model could not distinguish between ferrihydrite and goethite (consistent overestimation of goethite), or between glycP and Ins6P. Removing glycP from the standards resulted in the most accurate LCF (Table S5.3, Fit e).

The fitting results support the results of Kruse et al., (2009) who suggested that the LCF of P K-edge XANES spectra are able to distinguish between inorganic and organic P species, but not between different organic P species. This is likely because the P K-edge XANES spectral features of glycP and Ins6P are very similar. P L-edge XANES showed greater differentiation of P species but its application in natural samples like soil samples is still limited by the high P concentration required to obtain results suitable for LCF (Colocho Hurtarte *et al.*, 2020; Kruse *et al.*, 2009). Furthermore, the study of Prietzel and Klysubun, (2018) demonstrated the capability of P K-edge XANES LCF procedure to differentiate between Ins6P-fhy and free Ins6P, and between Ins6P-goe and free Ins6P, however they did not test the capability of the procedure to correctly identify these P forms in a complex mixture. Our results show that the identification of the same P form retained by different Fe oxides in the same mixture is not accurate when based on P K-edge XANES linear combination fitting, as Pi and Ins6P were overestimated on goethite at the expense of ferrihydrite. This also indicates that the pre-edge feature is more useful in the identification of different P forms rather that different Fe oxides, corroborating the hypothesis that the differences observed in this feature are mostly related to the different binding environment of specific P forms rather than P retention mechanisms.

Table S5.3 Comparison among the theoretical composition of the mixtures of standards and the results obtained by linear combination fitting by the inclusion of only the standards actually included in the mixture (Fit a),all the P forms retained by ferrihydrite (Fit b), all the P forms retained by goethite (Fit c), all the standards (Fit d), all the standard excluding glycP-fhy (Fit e). Pi-fhy = orthophosphate coprecipitated with ferrihydrite; Ins6P-fhy = inositol hexakiphosphate coprecipitated with ferrihydrite; glycP-fhy = glycerophosphate coprecipitated with ferrihydrite; Pi-goe = orthophosphate coprecipitated with goethite; Ins6P-goe = inositol hexakiphosphate coprecipitated with goethite.

Mixture		Pi-fhy	Ins6P-fhy	glycP-fhy	Pi-goe	Ins6P-goe	*R factor*
		weight (g)					
1	Theoretical	0.33	0.33	0.33	-	-	-
	Fit a)	0.18	0.33	0.49	ni	ni	0.002
	Fit b)	0.17	0.33	0.49	ni	ni	0.002
	Fit c)	ni	ni	ni	0.30	0.70	0.002
	Fit d)	0.20	0.03	0.46	0.02	0.29	0.001
	Fig e)	0.37	0.06	ni	0.03	0.53	0.001
2	Theoretical	0.5	0.5	-	-	-	-
	Fit a)	0.57	0.43	ni	ni	ni	0.003
	Fit b)	0.30	0.23	0.48	ni	ni	0.003
	Fit c)	ni	ni	ni	0.47	0.53	0.003
	Fit d)	0.13	0.13	0.47	0.15	0.13	0.002
	Fig e)	0.24	0.23	ni	0.28	0.24	0.002
3	Theoretical	0.5	-	0.5	-	-	-
	Fit a)	0.5	ni	0.5	ni	ni	0.008
	Fit b)	0.30	0.19	0.51	ni	ni	0.005
	Fit c)	ni	ni	ni	0.51	0.49	0.003
	Fit d)	0.09	0.00	0.49	0.20	0.23	0.003
	Fig e)	0.10	0.00	ni	0.44	0.45	0.003
4	Theoretical	-	0.5	0.5	-	-	-
	Fit a)	ni	0.5	0.5	ni	ni	0.004
	Fit b)	0.01	0.50	0.50	ni	ni	0.004
	Fit c)	ni	ni	ni	0.21	0.79	0.004
	Fit d)	0.00	0.17	0.46	0.02	0.36	0.003
	Fig e)	0.00	0.18	ni	0.06	0.76	0.003
5	Theoretical	0.5	-	-	0.5	-	-
	Fit a)	0.0	ni	ni	1.0	ni	0.007
	Fit b)	0.50	0.00	0.50	ni	ni	0.016
	Fit c)	ni	ni	ni	1.00	0.00	0.008
	Fit d)	0.18	0.00	0.50	0.32	0.00	0.009
	Fig e)	0.22	0.00	ni	0.78	0.00	0.008
6	Theoretical	-	0.5	-	-	0.5	-
	Fit a)	ni	0.2	ni	ni	0.8	0.030
	Fit b)	0.00	0.50	0.50	ni	ni	0.040
	Fit c)	ni	ni	ni	0.19	0.81	0.042
	Fit d)	0.00	0.21	0.47	0.00	0.32	0.033
	Fig e)	0.00	0.33	ni	0.00	0.68	0.032

The inclusion of Pi-fhy, Ins6P, and the P fertilizer as standards for the LCF of the mixtures pointed to satisfactory results (Fig. S5.3a). P fertilizer was seldom included in the LCF, and then only in Mix 3 and Mix 6 where it is included as <5% of the total. These small loadings in LCF are not reliable and should be confirmed with other methods or excluded from the reported P speciation results (Werner & Prietzel, 2015). The proportions of inorganic and organic P forms was always correctly estimated if we consider the amount of P attributed to Ins6P-fhy as the sum of Ins6P-fhy and glycP-fhy.
The values of R factors reported in Table S5.3 and Fig. S5.3b, are in line with the values generally reported in literature (Prietzel *et al.*, 2016; Prietzel & Klysubun, 2018; Werner & Prietzel, 2015), thus suggesting a good estimation from the fitting. However, Werner and Prietzel (2015) suggested a more careful evaluation of the fitting quality based on the visual inspection of the results, as the R factor information from some irrelevant spectral regions.

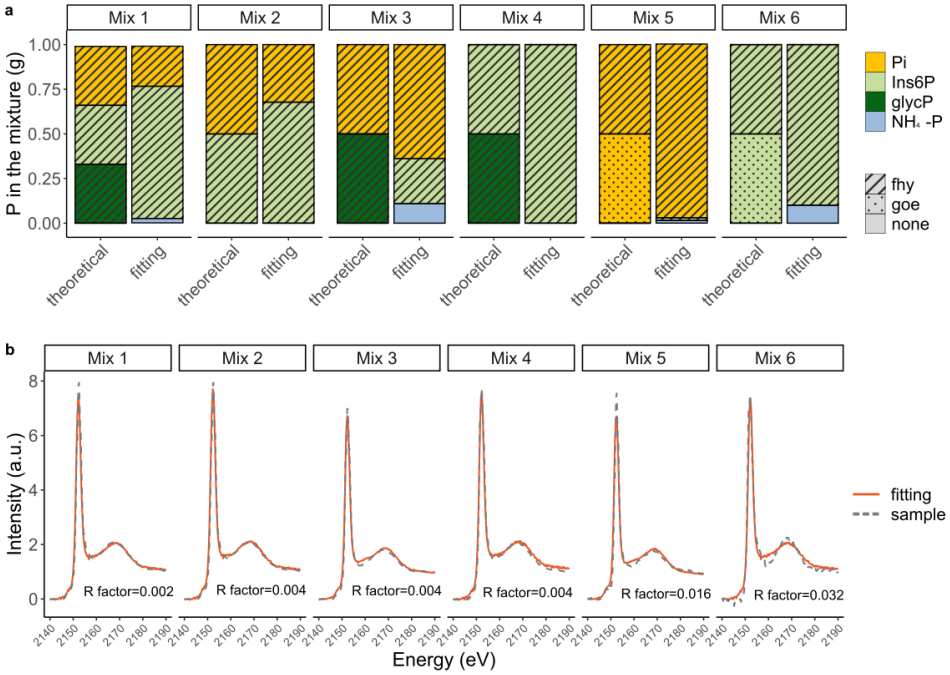

Figure S5.3 a) phosphorus speciation of standard mixtures of orthophosphate co-precipitated with ferrihydrite (Pi-fhy), inositol hexakisphosphate co-precipitated with ferrihydrite (Ins6P-fhy), glycerophosphate co-precipitated with ferrihydrite (glycP-fhy), orthophosphate co-precipitated with goethite (Pi-goe), and inositol hexakisphosphate co-precipitated with goethite (Ins6P-goe). (Mix 1-4) without Pi-goe and Ins6P-goe, (Mix 2, 5-6) without glycP-fhy,, (Mix 3,5) without Ins6P-fhy, calculated by linear combination fitting; and b) comparison between P K-edge XANES spectra of the mixture and the relative spectra obtained by the weight of the standard included in the LCF.

5.3.5 Linear Combination Fitting of P K-edge XANES of Fe plaque samples

Unlike the P L_{2-3}-edge XANES, the P K-edge XANES spectra of our Fe plaque samples had adequate signal to perform LCF fitting (Fig. S5.4 and S5.5). Sample charging and low P concentrations are likely the limiting factor here, as P concentrations of 3 mg g^{-1} are generally considered the lower limit for P L_{2-3}-edge XANES spectroscopy (Colocho Hurtarte *et al.*, 2020). According to the Fe plaque chemistry, and the results obtained from LCF of standard mixtures, the LCF model of Fe plaque samples included Pi-fhy, Ins6P-fhy and the NH_4-P fertilizer as standards. The quality of the fitting was lower for samples compared to standard mixtures. As discussed in the previous section, the R factor is not the only indicator of the quality of the fitting, however, the comparison between the spectra of the sample and the LCF showed that the latter closely resemble the former. These findings suggests that the standards we selected for LCF are adequate to describe the P speciation of Fe plaque samples, but the P concentrations in the samples represent the real limitations in the application of P L_{2-3}- and/or K-edge XANES spectroscopy on Fe plaque or soil samples.

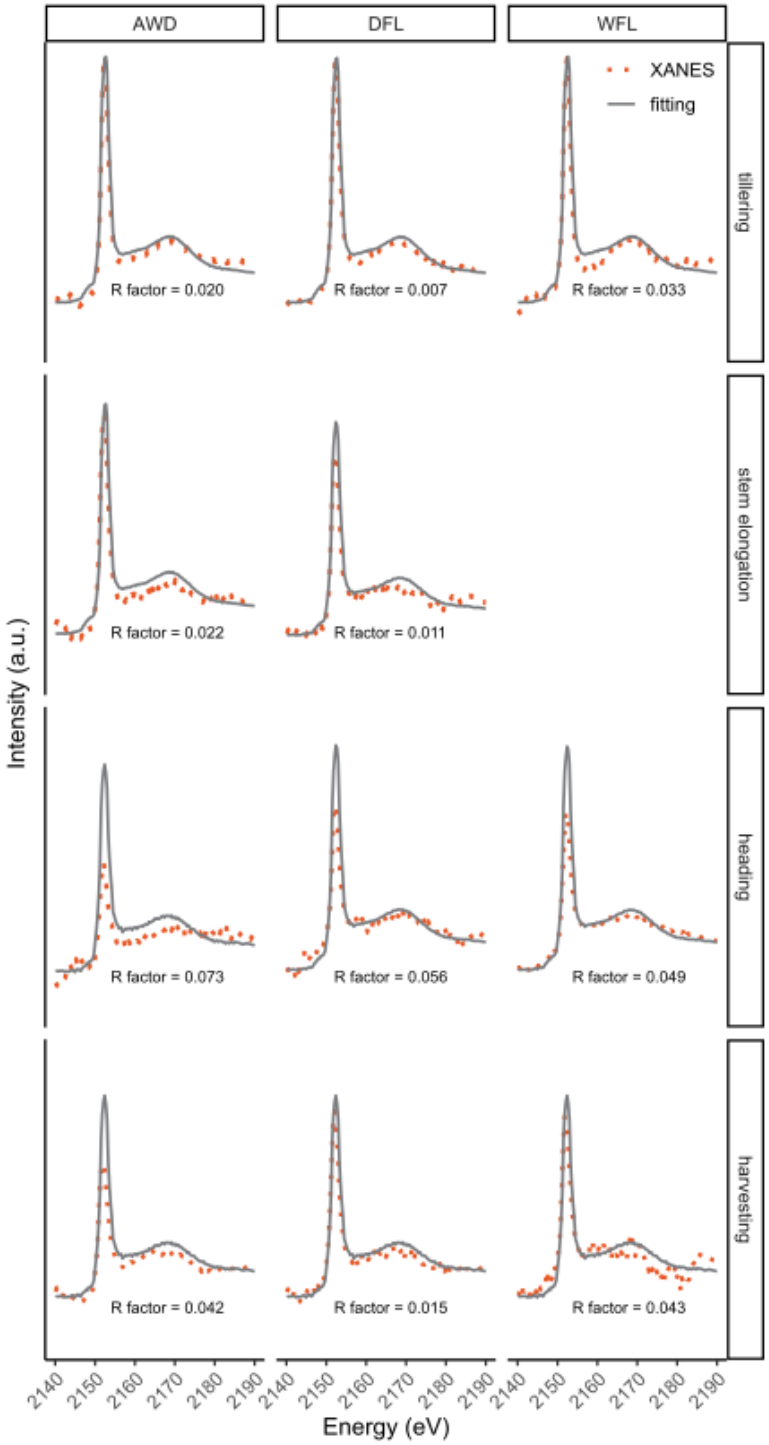

Figure S5.4. Comparison between P K-edge XANES spectra of Fe plaque of rice grown under alternating wetting and drying irrigation (AWD), delayed flooding (DFL), and continuous flooded soil (WFL), without P fertilization during the main development stages, and the relative spectra obtained by the weight of the standard included in the LCF (i.e. Pi-fhy, Ins6P-fhy, and NH_4-P).

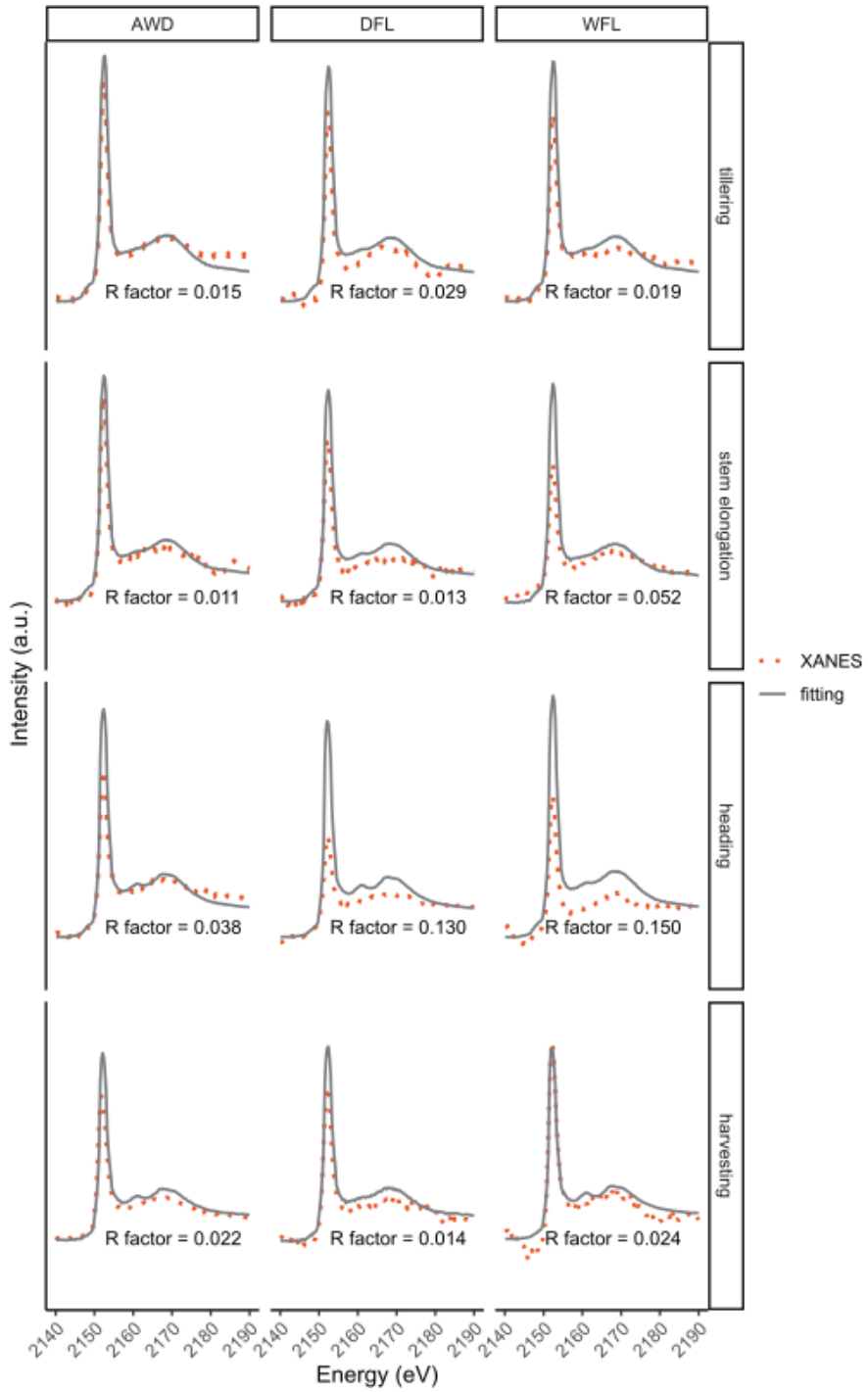

Figure S5.4. Comparison between P K-edge XANES spectra of Fe plaque of rice grown under alternating wetting and drying irrigation (AWD), delayed flooding (DFL), and continuous flooded soil (WFL), with 46 kg ha^{-1} of P fertilization during the main development stages, and the relative spectra obtained by the weight of the standard included in the LCF (i.e. Pi-fhy, Ins6P-fhy, and NH_4-P).